Editorial Board

CONTENTS

G.O.Nikolaenko, O.S.Vodoriz, *cand. phys.-math. Sciences*
E.I. Rogacheva *doc. phys.-math. Sciences, Professor*
Tavrina T.V., *cand. phys.-math. Sciences, Associate Professor*
Lisachuk G.V. *doc. tehn. Sciences, Professor*

National Technical University "Kharkiv Polytechnic Institute"
2 Kyrpychova Str., Kharkiv, 61002, Ukraine

THERMAL CONDUCTIVITY OF $PbSe_{1-x}Te_x$
($x = 0 – 0.04$) SOLID SOLUTIONS

The dependence of lattice thermal conductivity λ_L of pressed samples of $PbSe_{1-x}Te_x$ solid solutions on the composition ($x = 0 – 0.04$) at a temperature of 325 K is obtained. The $\lambda_L(x)$ curve shows a maximum near $x = 0.0075$. Measurement of the temperature dependence of λ_L in the range of 150-600 K showed that a concentration anomaly in the same range of compositions is also observed on the composition dependence of power factor β in the temperature dependence of λ_L . The non-monotonic character of the $\lambda L(x)$ and $\beta(x)$ dependences is associated with critical phenomena accompanying the transition of the percolation type from dilute to concentrated solid solutions. In the study and practical application of $PbSe_{1-x}Te_x$ solid solutions, it is necessary to take into account the non-monotonic nature of the change in thermal conductivity with composition. Bibl. 15, Fig. 3.
Key words: *$PbSe_{1-x}Te_x$ solid solutions, thermal conductivity, composition, temperature, percolation.*

Introduction

Semiconducting isovalent and isostructural substitutional $PbSe_{1-x}Te_x$ solid solutions are promising medium-temperature thermoelectric (TE) materials [1, 2]. Since the efficiency of using TE materials is determined by the figure of merit *ZT* ($ZT = S^2\sigma T / \lambda$, where *S* is the Seebeck coefficient, σ is the electrical conductivity, λ is the total thermal conductivity, and *T* is the absolute temperature), one of the ways to increase *ZT* is to decrease λ. The thermal conductivity of a semiconductor includes two main components - lattice (λ_L) and electronic (λe), which reflect the distribution of the heat flux in the substance by phonons and conduction electrons [1,2]. Enhancing phonon scattering and, therefore, decreasing λ_L without negatively affecting the electronic properties (*S*, σ) remains an urgent problem of TE materials science [1-3].

Experimentally, the thermal conductivity of polycrystalline $PbSe_{1-x}Te_x$ solid solutions was studied in many works [4-6], where the main attention was paid to the compositions from the side of *PbTe*. Thus, in [4, 5], the total λ decreased with an increase in the Se content to $x \sim 0.5$, and then increased again. It was shown in [6] that λ_L also decreases with an increase in the Se content

to $x = 0.25$, which, according to the authors, is due to phonon scattering because of local deformation caused by the difference in the masses of Te and Se atoms. The theoretical calculation of λ_L carried out by the authors of [7] showed that at room temperature at $x = 0.5$, a maximum decrease in λ_L by ~ 30 % is observed in comparison with λ_L of *PbTe* and *PbSe* compounds.

Earlier, in a number of works reviewed in [8], anomalies were found in the isotherms of properties, including thermal conductivity, in solid solutions based on IV-VI compounds at a low content of the second component (~ 0.5-1.5 at.%). According to the assumption of the authors of these works, the concentration anomalies are associated with the presence of phase transitions of the percolation type in going from dilute to concentrated solid solutions.

An anomalous area of thermal conductivity growth on the dependence of $\lambda(x)$ at room temperature was also observed by the authors [9] in the *PbSe$_{1-x}$Te$_x$* solid solution from the side of *PbTe* in the range of $x = 0.9925$ - 0.9875. It was of interest to find out whether a similar effect will be manifested in the same *PbSe$_{1-x}$Te$_x$* solid solutions only by *PbSe*. Therefore, in [10] a study of the concentration dependences of the microhardness *H, S, σ* of cast and extruded polycrystalline samples of *PbSe$_{1-x}$Te$_x$* ($x = 0$ - 0.045) solid solutions at room temperature and near $x = 0.01$ revealed areas of abnormal decrease in *H* and *S* and growth of *σ*. However, the thermal properties of these samples were unstudied.

This work is devoted to the study of the effect of composition and temperature on the thermal conductivity of solid solutions based on lead selenide in the *PbSe$_{1-x}$Te$_x$* system ($x = 0$ - 0.04).

Experimental

Polycrystalline *PbSe$_{1-x}$Te$_x$* samples ($x = 0, 0.0025, 0.005, 0.01, 0.0125, 0.015, 0.0175, 0.035, 0.04$) were synthesized by alloying the initial elements in evacuated quartz ampoules at a temperature of 1380 K, followed by homogenizing annealing at a temperature of 870 K for 240 hours. All samples had *p*-type conductivity. To measure the thermal conductivity, hot-pressed cylindrical specimens with a diameter of 15 mm and a height of 5.5 mm (pressing temperature 650 K, pressure 0.4 GPa, holding time under load 10 s) were prepared from cast ingots, followed by annealing at 720 K for 250 h.

Thermal conductivity was measured in the temperature range of 150-600 K on a VT-λ-400 device using a dynamic calorimeter in a monotonic heating mode. Three measurements of λ were carried out for each sample. The relative measurement error did not exceed 5%. The lattice component of thermal conductivity λ_L was separated from the total thermal conductivity by subtracting the electronic component λ_e which was calculated according to the Wiedemann-Franz law $\lambda_e = L\sigma T$ (for a degenerate semiconductor the Lorentz number $L = \pi^2 k^2/3e = 2.45 \cdot 10^{-8}$ W·Ohm·K^{-2} [11]. The electric conductivity σ was measured by the four-probe method with an accuracy of 5 %.

Discussion of results

Fig. 1 shows a dependence of lattice thermal conductivity on the composition of *PbSe₁₋ₓTeₓ* solid solution at a temperature of 325 K. It is seen that with a general tendency to decrease λ_L with increasing *Te* content on the dependence $\lambda_L(x)$ a maximum is observed near $x = 0.0075$, which indicates a decrease in phonon scattering and an increase in the propagation velocity of elementary excitations near $x = 0.0075$.

In this regard, it was of interest to find out what the nature of the concentration dependence of the power factor in the temperature dependence of λ_L will be. Therefore, the total thermal conductivity λ of the samples under study was measured in the temperature range 150-600 K. Fig. 2 shows the temperature dependences $\lambda(T)$ of some PbSe₁₋ₓTeₓ ($x = 0$, 0.0025, 0.005, 0.0175) samples. The rest of the samples had a similar character of the dependences $\lambda(T)$. From Fig. 2 it can be seen that in the investigated temperature range the values of λ decrease, which is typical for phonon-phonon scattering and is consistent with the dependences $\lambda(T)$ given in [4 – 6].

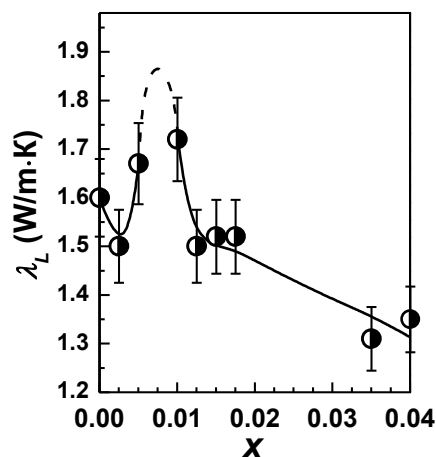*Fig. 1. Dependence of lattice thermal conductivity λ_L of PbSe₁₋ₓTeₓ solid solution*

on the composition x at a temperature of 325 K
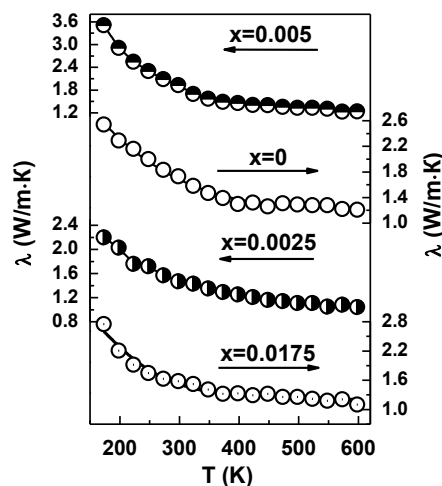
Fig. 2. Temperature dependences of total thermal conductivity λ of PbSe₁₋ₓTeₓ solid solution

Our estimated calculation of the electronic component of thermal conductivity showed that for *PbSe* polycrystal at room temperature $\lambda_e = 1 \cdot 10^{-2}$ W/(m·K), $\lambda_L/\lambda = 99.4\%$, and for *PbSe₁₋ₓTeₓ* solid solution the value $\lambda_e = (0.5 - 1.4) \cdot 10^{-2}$ W/(m·K), $\lambda_L/\lambda = (99.2 - 99.8)\%$. Thus, in PbSe and in the *PbSe₁₋ₓTeₓ* solid solution on its basis, the main contribution to the thermal conductivity is made by λ_L. Based on this, it can be assumed that the experimental values of λ obtained in this work practically coincide with the values of the lattice thermal conductivity.

It is known that at temperatures above the Debye temperature Θ_D (for *PbSe* $\Theta_D = 138$ K) λ_L of semiconductors with a rise in temperature decreases according to the law $\lambda_L \sim T^{-1}$ [11,12]. Assuming the power character of the temperature dependence λ_L ($\lambda_L \sim T^\beta$), the power factor β was estimated for the studied samples (Fig. 3). As is evident from Fig. 3, after a decrease in β upon the introduction of the first portion of the impurity ($x = 0.0025$), one can observe a sharp increase in the power factor at $x = 0.005$, when β reaches an almost theoretical value ($\beta = -1.05 \pm 0.05$). Besides, a subsequent sharp decrease to $\beta = -0.5 \pm 0.05$ is observed, which indicates the presence of some transformations in the crystal, which significantly change the processes of heat transfer and phonon scattering. The subsequent increase in β and the constancy of λ_L in the range $x = 0.0125 - 0.0175$ indicate the complex nature of these transformations, which may be accompanied by ordering processes. It was interesting to compare the values of β obtained by other authors with the results of this work. A numerical estimate of the power factor β for a number of experimental dependences $\lambda_L(T)$ for *PbSe* polycrystals given in [5, 6, 13] showed that the values of β are $\beta = -(0.7 - 0.9)$. The deviation of β values for pure *PbSe* from the theoretical value is obviously due to the presence of grain boundaries, nonstoichiometry defects and other imperfections in polycrystals.

Fig. 3. Dependence of the power factor β in the temperature dependence of lattice thermal conductivity λ_L on the composition of the PbSe₁₋ₓTeₓ solid solution

The anomalous growth of λ_L near $x = 0.0075$ can be described, as was done in [9], within the problem of the spheres of percolation theory [14, 15]. In this model, each introduced substitut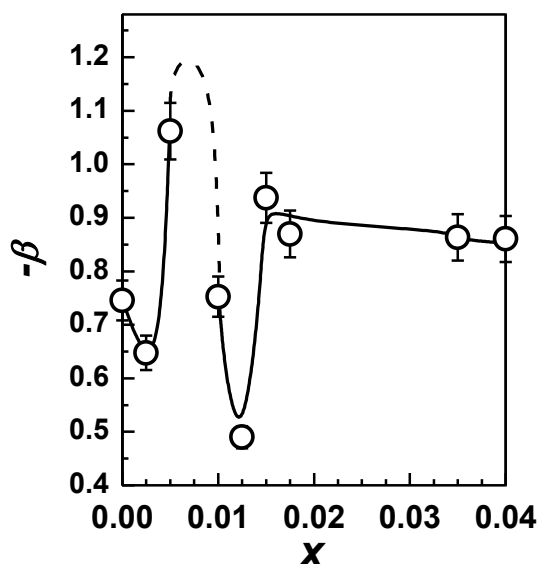ional atom (in this case the Te atom), represented as a sphere, causes a field of static deformation with radius R_0 and excitation of the phonon spectrum in the crystal. When a certain critical concentration x_c of substitutional atoms (percolation threshold) is reached, a chain of interconnected atoms is formed that permeates the entire crystal (an infinite cluster). When the first portions of *Te* are introduced into the *PbSe* lattice, the crystal structure becomes disordered, which is manifested in a decrease in thermal conductivity at $x = 0.0025$. A further increase in the *Te* concentration leads to the fact that the deformation fields of neighboring substitutional atoms begin to overlap, which causes a decrease in local elastic lattice stresses, an increase in the rate of propagation of thermal oscillations of the crystal lattice and, consequently, an increase in thermal conductivity. Within the framework of the problem of the percolation theory spheres, using the assumption of the short-range nature of the deformation interaction, the critical concentration can be determined from the condition $4/3 N_c (2R_0)^3 \approx 2.7$, where N_c is the average number of centers of spheres with radius R_0 per unit volume [15]. Assuming that the critical concentration with the maximum value λ_L corresponds to $x_c = 0.0075$, we obtained $R_0 = 1.39 a_0$ (where a_0 is the unit cell parameter of *PbSe*). A further increase in the concentration of *Te* causes new crystal deformations in the solid solution, and hence a decrease in λ_L at $x > 0.015$. With a high probability, as noted above, such a percolation transition is accompanied by ordering processes.

Thus, we associate the anomalous growth of $\lambda_L(x)$ in the *PbSe₁₋ₓTeₓ* solid solution near $x = 0.0075$ with the manifestation of critical phenomena accompanying the transition of the percolation type from dilute solid solutions to concentrated ones. The presence of such a growth region of $\lambda_L(x)$ should be taken into account when developing materials based on *PbSe*, therefore, an increase in thermal conductivity can lead to a decrease in the value of *ZT*. The results of the work once again confirm the assumption, grounded in [8], about the universal nature of such concentration anomalies.

Conclusions

The composition dependences of lattice thermal conductivity λ_L of pressed samples of *PbSe₁₋ₓTeₓ* ($x = 0 – 0.04$) solid solutions at a temperature of 325 K and a power factor β in the temperature dependence of λ_L. On the dependences $\lambda_L(x)$ and $\beta(x)$ near $x = 0.0075$, clear maxima were observed, the presence of which indicated the existence of transformations in the lattice subsystem of the crystal, leading to an increase in the rate of phonon propagation and changes in their scattering processes. The non-monotonic nature of the dependences $\lambda_L(x)$ and $\beta(x)$ is associated with the manifestation of critical phenomena that accompany the phase transition of the percolation type, which occurs during the transition from dilute to concentrated solid solutions. The results of this work, as well as our previous data on the study of *PbSe₁₋ₓTeₓ* solid solutions, show that when interpreting the results, optimizing the TE properties and practical application of

these materials, it is necessary to take into account the concentration anomalies of thermal conductivity in a certain range of compositions near the initial components *PbTe* and *PbSe*.

References

1. Rowe D.M. (1995). *CRC Handbook of Thermoelectrics*. Boca Raton, London, New York, Washington: CRC Press.

2. Anatychuk L.I. (1979). *Termoelementy i termoelektricheskiie ustroistva. Spravochnik [Thermoelements and thermoelectric devices. Reference book].* Kyiv: Naukova dumka [in Russian].

3. Ren Z., Lan Y., Zhang Q. (2017). *Advanced thermoelectrics: Materials, contacts, devices, and systems*. Boca Raton: CRC Press Taylor & Francis Group.

4. Pei Y., Shi X., LaLonde A., Wang H., Chen L., Snyder G.J. (2011). Convergence of electronic bands for high performance bulk thermoelectrics. *Nature Letter*, 473, 66-69.

5. Basu R., Bhattacharya Sh., Bhatt R., Singh A., Aswal D. K., Gupta Sh. K. (2013). Improved thermoelectric properties of Se-doped n-type PbTe$_{1-x}$Se$_x$ ($0 \leq x \leq 1$). *Journal of Electronic Materials*, 42(7), 2292-2296.

6. Li J.Q., Li S.P., Wang Q.B., Wang L., Liu F.S., Ao W.Q. (2011). Synthesis and thermoelectric properties of the PbSe$_{1-x}$Te$_x$ alloys. *Journal of Alloys and Compounds*, 509, 4516-4519.

7. Tian Zh., Garg J., Esfarjani K., Shiga T., Shiomi J., Chen G. (2012). Phonon conduction in PbSe, PbTe, and PbTe$_{1-x}$Se$_x$ from first-principles calculations. *Phys. Rev. B*, 85, 184303.

8. Rogacheva E.I., Nashchekina O.N., Dresselhaus M.S. (2005). Thermal conductivity isotherm anomalies in semiconductor solid solutions based on IV-VI compounds. *J. Thermoelectricity*, 4, 82-90.

9. Rogacheva E.I., Vodorez O.S., Nashchekina O.N., Dresselhaus M.S. (2014). Concentration anomalies of the thermal conductivity in PbTe–PbSe semiconductor solid solutions. *Phys. St. Sol. B*, 251, 1231-1238.

10. Vodoriz O.S., Tavrina T.V., Nikolaenko G.O., Rogachova O.I. (2020). Mechanical and thermoelectric properties of PbSe$_{1-x}$Te$_x$ semiconductor solid solutions (x = 0 – 0.04). *Metallofiz. Noveishie Tekhnol.*, 42(4), 487-495 (in Ukrainian).

11. Tritt T.M. (2004). *Thermal conductivity: theory, properties, and applications*. New York: Kluwer Academic, Plenum Publishers.

12. Berman R. (1976). *Thermal conduction in solids*. Oxford: Clarendon Press.

13. Pei Y.-L., Liu Y. (2012). Electrical and thermal transport properties of Pb-based chalcogenides: PbTe, PbSe and PbS. *J. Alloys and Compounds*, 514, 40-44.

14. Tarasevich Yu.Yu. (2002). *Percoliatsiia: teoriia, prilozheniia, algoritmy [Percolation: theory, applications, algoriythms].* Moscow: Editorial URSS [in Russian].

15. Stauffer D., Aharony A. (1992). *Introduction to percolation theory. Wasington, DC: Taylor & Francis.*

Ніколаєнко Г.О., Водоріз О.С.,

Рогачова О.І., *докт. фіз.-мат. наук, професор*

Тавріна Т.В. *канд. фіз.-мат. наук, доцент*

Лісачук Г.В. *канд. фіз.-мат. наук, професор*

Національний технічний університет
«Харківський політехнічний інститут»,
вул. Кирпичова, 2, Харків, 61002, Україна

ТЕПЛОПРОВІДНІСТЬ ТВЕРДИХ РОЗЧИНІВ
PbSe$_{1-x}$Te$_x$ (x = 0 – 0.04)

Одержано залежність граткової теплопровідності λ$_L$ пресованих зразків твердих розчинів PbSe$_{1-x}$Te$_x$ від складу (x = 0 – 0.04) за температури 325 К. На кривій λ$_L$(x) виявлено максимум поблизу x = 0.0075. Вимірювання температурної залежності λ$_L$ в інтервалі 150 - 600 К показало, що концентраційна аномалія в цьому ж інтервалі складів спостерігається і на залежності степеневого коефіцієнта β у температурній залежності λ$_L$ від складу. Немонотонний характер залежностей λ$_L$(x) і β(x) пов'язується з критичними явищами, що супроводжують перехід перколяційного типу від розведених до концентрованих твердих розчинів. При дослідженні і практичному застосуванні твердих розчинів PbSe$_{1-x}$Te$_x$ необхідно враховувати немонотонний характер зміни теплопровідності зі складом. Бібл. 15, рис. 3.

Ключові слова: тверді розчини *PbSe$_{1-x}$Te$_x$*, теплопровідність, склад, температура, перколяція.

Николаенко Г.А., Водориз А.С.,

Рогачева Е.И., *докт. физ.-мат. наук, профессор*

Таврина Т.В., *канд. физ.-мат. наук, доцент*

Лисачук Г.В., докт. *техн. наук, професор*

Национальный технический университет

«Харьковский политехнический институт»,

ул. Кирпичева, 2, Харьков, 61002, Украина

ТЕПЛОПРОВОДНОСТЬ ТВЕРДЫХ РАСТВОРОВ
PbSe$_{1-x}$Te$_x$ (*x* = 0 - 0.04)

Получена зависимость решеточной теплопроводности λ$_L$ прессованных образцов твердых растворов PbSe$_{1-x}$Te$_x$ от состава (x = 0 - 0.04) при температуре 325 K. На кривой λ$_L$(X) выявлен максимум вблизи x = 0.0075. Измерение температурной зависимости λ$_L$ в интервале 150 - 600 K показало, что концентрационная аномалия в этом же интервале составов наблюдается и на зависимости степенного коэффициента β в температурной зависимости λ$_L$ от состава. Немонотонный характер зависимостей λ$_L$(x) и β(x)связывается с критическими явлениями, сопровождающими переход перколяционного типа от разбавленных к концентрированным твердым растворам. При исследовании и практическом применении твердых растворов PbSe$_{1-x}$Te$_x$ необходимо учитывать немонотонный характер изменения теплопроводности с составом. Библ. 15, рис. 3.

Ключевые слова: твердые растворы *PbSe$_{1-x}$Te$_x$*, теплопроводность, состав, температура, перколяции.

References

1. Rowe D.M. (1995). *CRC Handbook of Thermoelectrics*. Boca Raton, London, New York, Washington: CRC Press.

2. Anatychuk L.I. (1979). *Termoelementy i termoelektricheskiie ustroistva. Spravochnik [Thermoelements and thermoelectric devices. Reference book].* Kyiv: Naukova dumka [in Russian].

3. Ren Z., Lan Y., Zhang Q. (2017). *Advanced thermoelectrics: Materials, contacts, devices, and systems*. Boca Raton: CRC Press Taylor & Francis Group.

4. Pei Y., Shi X., LaLonde A., Wang H., Chen L., Snyder G.J. (2011). Convergence of electronic bands for high performance bulk thermoelectrics. *Nature Letter*, 473, 66-69.

5. Basu R., Bhattacharya Sh., Bhatt R., Singh A., Aswal D. K., Gupta Sh. K. (2013). Improved thermoelectric properties of Se-doped n-type PbTe$_{1-x}$Se$_x$ ($0 \leq x \leq 1$). *Journal of Electronic Materials*, 42(7), 2292-2296.

6. Li J.Q., Li S.P., Wang Q.B., Wang L., Liu F.S., Ao W.Q. (2011). Synthesis and thermoelectric properties of the PbSe$_{1-x}$Te$_x$ alloys. *Journal of Alloys and Compounds*, 509, 4516-4519.

7. Tian Zh., Garg J., Esfarjani K., Shiga T., Shiomi J., Chen G. (2012). Phonon conduction in PbSe, PbTe, and PbTe$_{1-x}$Se$_x$ from first-principles calculations. *Phys. Rev. B*, 85, 184303.

8. Rogacheva E.I., Nashchekina O.N., Dresselhaus M.S. (2005). Thermal conductivity isotherm anomalies in semiconductor solid solutions based on IV-VI compounds. *J. Thermoelectricity*, 4, 82-90.

9. Rogacheva E.I., Vodorez O.S., Nashchekina O.N., Dresselhaus M.S. (2014). Concentration anomalies of the thermal conductivity in PbTe–PbSe semiconductor solid solutions. *Phys. St. Sol. B*, 251, 1231-1238.

10. Vodoriz O.S., Tavrina T.V., Nikolaenko G.O., Rogachova O.I. (2020). Mechanical and thermoelectric properties of PbSe$_{1-x}$Te$_x$ semiconductor solid solutions (x = 0 – 0.04). *Metallofiz. Noveishie Tekhnol*., 42(4), 487-495 (in Ukrainian).

11. Tritt T.M. (2004). *Thermal conductivity: theory, properties, and applications*. New York: Kluwer Academic, Plenum Publishers.

12. Berman R. (1976). *Thermal conduction in solids*. Oxford: Clarendon Press.

13. Pei Y.-L., Liu Y. (2012). Electrical and thermal transport properties of Pb-based chalcogenides: PbTe, PbSe and PbS. *J. Alloys and Compounds*, 514, 40-44.

14. Tarasevich Yu.Yu. (2002). *Percoliatsiia: teoriia, prilozheniia, algoritmy [Percolation: theory, applications, algoriythms]*. Moscow: Editorial URSS [in Russian].

15. Stauffer D., Aharony A. (1992). *Introduction to percolation theory. Wasington, DC: Taylor & Francis*.

Submitted 06.08.2020

E.I. Rogacheva, *doc. phys. - math. Sciences, Professor*

K.V. Novak, D.S. Orlova

O.N. Nashchekina, *cand. phys. - math. Sciences, Assistant Professort*

A.Yu. Sipatov, *doc. phys. - math. Sciences, Professor*

G.V. Lisachuk, *doc. techn. Sciences, Professor*

National Technical University "Kharkiv Polytechnic Institute"

2 Kyrpychova Str., Kharkiv, 61002, Ukraine

SIZE EFFECTS AND THERMOELECTRIC PROPERTIES OF $BI_{0.98}SB_{0.02}$ THIN FILMS

The room-temperature dependences of thermoelectric properties (the Seebeck coefficient S, the electrical conductivity σ, the Hall coefficient RH, and the thermoelectric power factor P = S2·σ) on the thickness (d = 5 - 250 nm) of the Bi$_{0.98}$Sb$_{0.02}$ solid solution thin films grown on mica substrates by thermal evaporation in vacuum from a single source were obtained. It is shown that the monotonic component of the σ(d) dependence is well described within the framework of the Fuchs-Sondheimer theory for the classical size effect. The presence of an oscillating component in the d-dependences of σ, S, RH and S2·σ is attributed to the manifestation of the quantum size effect, and the experimentally determined period of quantum oscillations Δd = 45 ± 5 nm is in good agreement with the Δd value calculated theoretically within the framework of the model of an infinitely deep potential well. Bibl. 77, Fig. 1.

Key words: *Bi$_{0.98}$Sb$_{0.02}$* solid solution, thin film, thickness, thermoelectric properties, size effect, oscillation period.

Introduction

$Bi_{1-x}Sb_x$ solid solutuions are well known as effective thermoelectric (TE) materials for refrigerating devices operating at temperatures below ~200 K [1, 2]. The growing interest in $Bi_{1-x}Sb_x$ solutions is due not only to the possibility of their practical use in TE power engineering but also to their unique properties associated with the characteristics of their energy spectrum and the possibility of its qualitative rearrangement with changing composition, accompanied by a number of phase transitions [3-7]. Bi exhibits semimetallic properties: the electron L_s – band and T – band of "heavy" holes overlap. As Sb is added to Bi, the distance between the electron L_s – band and L_a – band of "light" holes decreases and at $x = 0.023 \div 0.04$ (different authors report different values of x), the energy gap between them becomes zero, i.e. a gapless state occurs. With further increase in x, the gap between the L_s and $L\alpha$ bands increases again, simultaneously the

overlap of T and Ls bands decreases, and at $x = 0.06 \div 0.07$, a semimetal – indirect semiconductor phase transition takes place. Then at $x = 0.08 \div 0.09$, the tops of T and Ls valence bands coincide, and in the range $x \cong 0.09 \div 0.15$ the indirect semiconductor becomes a direct-gap one. In [8-12], it was shown that the concentration-dependent anomalies of the transport properties correspond to the critical compositions associated with electronic phase transitions and the percolation-type transition from dilute to concentrated solid solutions. According to [13,14], electronic phase transitions of such types take place in the $Bi_{1-x}Sb_x$ films.

Recently, interest in the properties of the $Bi_{1-x}Sb_x$ solid solutions has sharply increased after it was found that they exhibit the properties of topological insulators – the newest materials of quantum physics, in which the strong spin-orbit interaction leads to the appearance of topological metallic surface states with a linear Dirac E(k) dispersion [15-17]. The $Bi_{1-x}Sb_x$ solid solution with $x = 0.1$ was the first experimentally discovered 3D-topological insulator [16]. In recent years, after it was established that the best TE materials (including $Bi_{1-x}Sb_x$) belong to the topological insulators class, the possibility of using the unique properties of the topological surface layer to develop fundamentally new ways to increase in TE figure of merit ZT has been discussed.

The development of nanotechnologies and the possibility of enhancing ZT in low-dimensional structures [18] have stimulated studies of $Bi_{1-x}Sb_x$ thin-film structures. Besides, using thin films, in which the relative contribution of the metal layer to the conductivity is larger as compared to bulks, is beneficial for studying the properties of the topological layer. However, when studying thin films, it should be taken into account that in the thin-film state the manifestations of classical size effect (CSE) and quantum size effect (QSE) are possible, which can significantly change the properties of films in comparison with bulk crystals [19]. The CSE is caused by diffuse scattering of charge carriers at the film boundaries and manifests itself when the film thickness d is comparable to the mean free path l of charge carriers. The QSE results from the quantization of the charge carrier energy spectrum and is observed when the value of d becomes comparable to the Fermi wavelength, where h is Planck's constant, m^* is the effective mass, and EF is the Fermi energy. One of the manifestations of the QSE is an oscillatory behavior of the d-dependences of the transport properties. Due to the extremely low m^* value and anomalously high mobility of electrons in Bi and $Bi_{1-x}Sb_x$, these materials are very convenient for studying QSE. It is in thin Bi films that the d-dependent oscillations of the galvanomagnetic properties were observed for the first time [20] and explained theoretically [21].

After that a very large number of works dealing with size effects in Bi films have appeared (see, e.g. [19,22- 51]. Based on the results of studies of the d-dependences of transport properties, some authors [23,27,31,38,39,43,44,49,50] determined l and the surface scattering coefficient p (the fraction of charge carriers which are specularly reflected from the surface) for Bi films using the Fuchs- Sondheimer theory (FST) [52,53] or other methods. It was found that at room temperature in monocrystalline Bi films l lies in the range of 600-1000 nm, whereas in polycrystalline films $l = 100$ -250 nm, and $p = 0$ - 0.8. The discrepancy in l and p values obtained

by different authors was apparently connected with the fact that these parameters depend both on the film structure, which in turn is determined by the sample preparation technology, and on the method of l and p determination.

After the size-dependent oscillations of the kinetic coefficients had observed in Bi films in [20], the existence of such oscillations was confirmed in a large number of works [19,22-51] in which the oscillating dependences of electrical resistance ρ, the Hall coefficient RH, Seebeck coefficient S and magnetoresistance $\Delta\rho/\rho$ on d were also interpreted as a manifestation of the QSE. The oscillation periods Δd determined experimentally for Bi thin films by different authors were in the range of 25-45 nm. Some authors [54 – 60] even considered quantum corrections to conductivity, which are the result of quantum interference.

The next step was studying the transport properties of thin films of $Bi1-xSbx$ solid solutions [61 – 74] in order to identify CSEs and QSEs. It turned out that, like in Bi films, the d-dependences of the kinetic properties in $Bi1-xSbx$ exhibit CSE. The authors of [65] estimated l for epitaxial $Bi_{1-x}Sb_x$ films with x in the range of 0 - 0.142 from the d-dependences of electron mobility at 4.2 K using the FST theory. According to [65], l varies within the range of 1000 - 6000 nm. The authors of [71, 72] calculated l for polycrystalline $Bi_{1-x}Sb_x$ films from the room temperature $\sigma(d)$ and $S(d)$ dependences under the assumption of total diffuse scattering of carriers ($p = 0$) at $x = 0.07$ [71] and x = 0.12 [72], before and after annealing, and obtained $l = 60$ and 180 nm, $l = 150$ and 230 nm respectively.

The first studies [61 – 63] of the d-dependences of σ, S, and ρ of $Bi_{1-x}Sb_x$ films confirmed the presence of QSE in $Bi_{1-x}Sb_x$ thin films. The authors of [61,62] investigated the $\sigma(d)$ and $S(d)$ dependences at 90 K for polycrystalline $Bi_{1-x}Sb_x$ films ($d \leq 300$ nm) with $x = 0.018$ and 0.035 and found that as compared with Bi films Δd increases up to $\Delta d = 70$ and 90 nm, respectively. In [63], it was also shown that introduction of a small amount of Sb ($x \sim 0.04$) into Bi films with $d = 420$ - 570 nm prepared by thermal evaporation of Sb in vacuum and subsequent diffusion annealing, resulted in an increase in Δd from $\Delta d \sim 26$ nm for pure Bi to $\Delta d \sim 65$ nm for $Bi1-xSbx$ at 4.2 K. Further more detailed systematic studies of the d-dependences ($d = 400$ - 200 nm) of the σ, R_H and $\Delta\rho/\rho$ at 4.2 K, carried out by the authors of [64-68], showed that as x increases to 0.059, Δd increases to ~110 nm, however, further increase in x to 0.142 leads to a decrease in Δd down to ~50 nm, which was attributed by the authors of [64-68] to a change in the parameters of the band spectrum of $Bi_{1-x}Sb_x$ under changing composition.

It can be seen that in various studies of the size effects in $Bi_{1-x}Sb_x$ films, films with different compositions, different thicknesses, prepared using different technologies were used and measurements were carried out at different temperatures. Meanwhile, the properties of $Bi_{1-x}Sb_x$ crystals and, to even greater extent, of films are very sensitive to various types of external influences, and therefore the various physical parameters of thin films should be compared for the same temperatures, the same intervals of the studied d's, and the same technologies of the film

preparation. In addition, in the available literature, either CSEs or QSEs were usually investigated, although both types of size effects can manifest themselves simultaneously.

In [73, 74] we reported the observation of oscillations with $\Delta d = 80 \pm 5$ nm [73] and with $\Delta d = 105 \pm 5$ nm [74] in the room-temperature d-dependences of σ, R_H, $\Delta \rho / \rho$ and S for $Bi_{1-x}Sb_x$ polycrystalline thin films ($d = 5 - 400$ nm) prepared by the thermal evaporation in vacuum of the crystals with $x = 0.045$ and $x = 0.09$ and the subsequent deposition on (111) mica substrates at $T_S = 380 \div 5$ K. The earlier determined at room temperature Δd for Bi films prepared under similar conditions was ~ 30 nm [46]. Simultaneously in [73,74] we investigated CSE and estimated l using the FST theory as 800 ± 40 nm ($x = 0.045$) and as 900 ± 50 nm ($x = 0.09$). The value of p practically did not depend on composition and was equal to 0.8. The composition $x = 0.045$ corresponds to the semimetallic state and lies between the critical compositions corresponding to the transition to the gapless state ($x \sim 0.03$) and the transition from the semimetal to an indirect-gap semiconductor ($x \sim 0.06$). The composition $x = 0.09$ corresponds to the direct-gap semiconductor region.

Thus, the compositions of $Bi_{1-x}Sb_x$ films studied in [73, 74] and films of pure Bi [46] were prepared and investigated using the same preparation and measurement techniques, and all those compositions lay outside the phase transition regions, whose presence could distort the manifestation of size effects. It was of interest to study under identical conditions thin films obtained from semimetallic $Bi_{1-x}Sb_x$ crystals with compositions between the critical compositions corresponding to the percolation transition ($x \sim 0.01$) and the transition to the gapless state ($x \sim 0.03$). The composition $x = 0.02$ belongs to such compositions.

The purpose of this work is to prepare semimetallic films of various d with composition $x = 0.02$ using the technique similar to described in [46, 73, 74] and by measuring the d-dependences of TE characteristics to identify the manifestations of the classical and quantum size effects, estimate the values of l, p and Δd and compare them with those obtained in [46, 73, 74]

Results and discussions

The objects of this study are thin films of $Bi_{0.98}Sb_{0.02}$ solid solution with thicknesses $d = 5 - 250$ nm obtained by thermal evaporation in vacuum of $Bi_{0.98}Sb_{0.02}$ polycrystal and subsequent deposition on mica substrates at 380 K. The methods of preparing films, measuring their thickness, characterising the micro- and crystal structure, and measuring the TE properties are similar to those described in [46,73,74].

In Fig. 1,a,b,c,d, the dependences of σ, S, R_H and TE power factor $P = S^2 \sigma$ on d at 300 K are shown. A nonzero conductivity was observed starting from the critical thickness $d_c = 9$ nm, which corresponds to the transition from an island film to a channeled structure. According to earlier electron microscopic studies [46], the $Bi_{1-x}Sb_x$ films grow on mica substrates in an island-like

fashion in the epitaxial orientation (001) $Bi_{1-x}Sb_x$ ‖ (001) mica. $Bi1-xSbx$ films on mica represent mosaic single crystals with high-angle twin-type boundaries.

It is seen that all thickness dependences exhibit a distinctly non-monotonic behavior. With increasing film thickness, σ, S and R_H show a tendency to increase. However, along with the general trend to increase with increasing d, the kinetic coefficients exhibit an oscillatory behavior, too. For all d-dependences one can isolate a monotonic component and oscillatory one. We attribute the presence of the monotonic component to the CSE and the oscillatory component to QSE.

According to the FST of the CSE [52,53], the dependence of electrical conductivity on d, provided that $d \ll l$, is described by the following equation:

$$\frac{\sigma_d}{\sigma_\infty} = \frac{3}{4} \cdot \frac{1+p}{1-p} \cdot \frac{d}{l} \cdot \ln \frac{l}{d} ,$$

(1)

where l is the mean free path in the bulk material, p is the surface scattering coefficient; Δd is the electrical conductivity of a film with thickness d; and σ_∞ is the conductivity of a bulk crystal. The value of p lies between 0 (for entirely diffuse scattering) and 1 (for entirely specular reflection). In the latter case, the CSE will not be observed. The FST assumes that CSE occur when scattering is predominantly diffuse, i.e., at sufficiently low p values. It should be noted that the FST adopts a number of simplifiying assumptions: it considers a metal with a spherical Fermi surface and isotropic l independent of d; p is assumed to be constant, i.e. the same for both surfaces, independent of d, the angle of incidence on the surface, and electron trajectories. Assuming the value of electrical conductivity for $Bi_{0.98}Sb_{0.02}$ films with a thickness of d = 200-300 nm (σ ≈ 4000 (Ohm cm)$^{-1}$) as σ_∞ and varying the values of p and l, theoretical σ(d) dependences were calculated. Comparing the experimental and theoretical Δ(d) dependences calculated within the framework of the FST, we established that the best match of the results of theoretical calculations and experimental data was observed for $p = 0.5 \pm 0.05$ and $l = 800 \pm 40$ nm. In Fig. 1,a, the theoretical dependence Δ(d) calculated using equation (1) is shown as the dotted line.

In Fig. 1,b, the $S(d)$ dependence is presented. S has the negative sign, like in bulk Bi and $Bi_{0.98}Sb_{0.02}$. With increasing d, a tendency to an increase in the magnitude of the S values is observed. In Fig. 1,c, the $R_H(d)$ dependence is given. It can be seen that, in contrast to the sign of S in films and bulk crystal, the sign of R_H in films turns out to be positive. With increasing d, R_H exhibits a tendency to increase in magnitude. The oscillations are even more pronounced than in the σ(d) and $S(d)$ dependences.

The periods of oscillations observed in the dependences of σ, S, R_H on d are practically the same for all kinetic coefficients, amounting to $\Delta d = 45 \pm 5$ nm.

Using the data for σ and S, the TE power factor was calculated as $P = S^2\sigma$. The behavior of the $P(d)$ dependences is similar to that of the σ(d) and $S(d)$ curves (Fig. 1,d). The values of TE

power factor for "thick" films ($d \sim 200$-400 nm) were practically equal to those for bulk Bi$_{0.98}$Sb$_{0.02}$ crystals, from which the films were obtained.
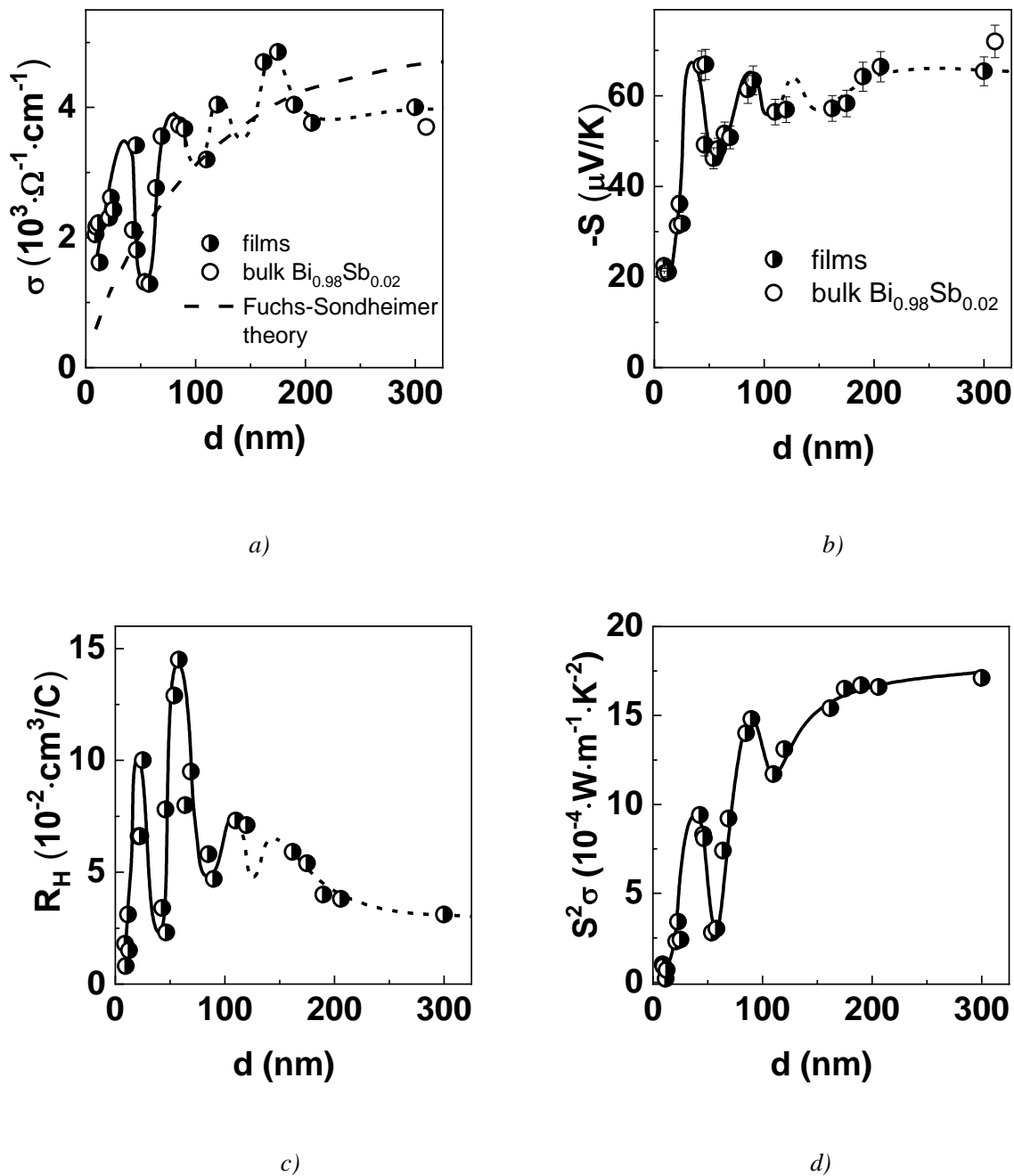

a)

b)

c)

d)

Fig. 1. Room-temperature dependences of the
electrical conductivity σ (a), the Seebeck coefficient S(b),
the Hall coefficient R$_H$(c), and the thermoelectric power
factor P = S^2 σ (d) on Bi$_{0.98}$Sb$_{0.02}$ thin
films thickness d for Bi$_{0.98}$Sb$_{0.02}$ thin films
prepared by thermal evaporation in vacuum on mica substrates.

In Fig. 1,a the theoretical dependence σ (*d*) calculated using the Fuchs - Sondheimer theory (FST) is shown as a dotted line.

It is natural to assume that the oscillating behavior observed in the *d*-dependences of σ, R_H, and *S* is the result of size quantization in the Bi$_{0.98}$Sb$_{0.02}$ thin films. For observing QSEs in polycrystalline films, the formation of texture is required, though the film does not need to be monocrystalline. Due to the axial symmetry of the Bi band structure relative to the trigonal axis, oscillations of the electrical conductivity appear, if the trigonal axes are normal to the film surface in all crystallites.

A thin film of a semimetal is a quantum well, within which the movement of charge carriers is limited in one direction. Such a system is a convenient model object, since its properties are close to the model of a potential well with infinitely high walls. This model is simpler as compared to the finite width and height barrier model. The possibility of the observation of the oscillations in a film grown on an amorphous substrate is explained by the presence of texture in Bi$_{0.98}$Sb$_{0.02}$ thin films in the direction of electron confinement [19].

Restricting the motion of electrons leads to the quantization of the transverse component of quasimomentum and, accordingly, the energy spectrum. For a barrier of an infinite height, using the effective mass approximation, the energy levels can be presented as:

$$E_n = \frac{\hbar^2}{2m_z^*}\frac{\pi^2}{d^2}n^2 + \frac{\hbar^2 k_x^2}{2m_x^*} + \frac{\hbar^2 k_y^2}{2m_y^*} \tag{2}$$

where m_x^*, m_y^* are the components of the effective mass for motion parallel to the film surface and m_z^* is the effective mass for motion perpendicular to the film surface, *n* is the discrete quantum number. At fixed *n* values, the energy changes continuously as a function of κ_x and κ_y, corresponding to each subband *n*, and the energy spectrum consists of overlapping subbands. The Bi$_{0.98}$Sb$_{0.02}$ solid solution is a semimetal with degenerate charge carriers; therefore, the quantization condition for this material can be expressed in terms of the Fermi wavelength and the Fermi energy E_F:

Using this approximation, one can estimate the oscillation period Δ*d*:

$$\Delta d = \frac{h}{\sqrt{8m_z^* \varepsilon_F}} \tag{3}$$

Knowing the effective mass of electrons and the Fermi energy for the *Bi1-xSbx* solid solution with *x* = 0.02 from the literature data [4] for bulk crystals (*m* *x* = 0.02 = 0.8 *m* *$_{Bi}$, *m* *$_{Bi}$ = 0.012 ± 0.002 *m$_o$* E_F = 22.7 meV) and using equation (3), we calculated the theoretical period of quantum oscillations as Δ*d* = 52 nm. It can be seen that the theoretical value is in good agreement

with the experimentally determined Δd. It should be noted that although σ, R_H and S were measured independently, in all d–dependent studies, distinct oscillations with approximately the same periods were observed for all measured chatracteristics. Comparing the value of Δd obtained in this work with the one we obtained earlier for $Bi_{1-x}Sb_x$ films prepared by a similar procedure but with different concentration x [46,73,74], we found that with increasing x, Δd increases, amounting to 30, 45, 80, and 105 nm for films with x equal to 0, 0.02, 0.045, and 0.1, respectively.

As follows from the data obtained, R_H for all $Bi_{0.98}Sb_{0.02}$films has a positive sign, while S is negative. This difference can be explained by the strong anisotropy of Bi single crystals, which also occurs, but to a lesser extent, when Sb is introduced into Bi. According to [75], in Bi single crystals R_H has a positive sign only in the direction of a trigonal axis, while in the perpendicular directions the R_H sign changes to negative. In contrast to R_H, the Seebeck coefficient remains negative in any crystallographic direction [75]. That is why in all Bi films grown along the trigonal axis [001] a positive sign of R_H and a negative sign of S were observed [46]. However, let us note that we observed a change in the sign of R_H with increasing d in films with a high Sb content [73, 74] and explained this by the fact that for such samples the perpendicular orientation of the trigonal axis [001] relative to the substrate becomes less perfect. This explanation is confirmed by the results obtained in [29], where in polycrystalline Bi films the R_H sign, as well as the S sign, was negative, since there was no anisotropy in those films and the contribution of the bisector and bipolar components responsible for the negative sign of R_H was predominant. The fact that the positive sign of R_H in $Bi_{0.98}Sb_{0.02}$films was observed for all d's indicates that upon the introduction of a small amount of Sb (2 at.%), the degree of texture of the film remains rather high.

It follows from the experimental data obtained in this work that the thickness oscillations of the transport properties of $Bi_{0.98}Sb_{0.02}$ are distinctly manifested even at room temperature, although it is expected that thermal smearing of energy levels increases with increasing temperature and can become comparable to the spacing between the quantized levels. In a number of works on Bi and $Bi_{1-x}Sb_x$ films, measurements were carried out at 4.2 K, however, the oscillations did not manifest themselves more clearly. In our works on IV-VI and V$_2$VI$_3$ films (see, for example, [76,77]) we reported that the amplitude of the quantum oscillations in the room temperature thickness dependences is quite large. That is why, perhaps, the weak temperature dependence of the oscillation amplitude is not determined by the specificity of $Bi_{0.98}Sb_{0.02}$ thin films but is common for films of different types and requires theoretical interpretation.

Conclusions

1. In the room-temperature dependences of the electrical conductivity σ, the Hall coefficient R_H, and the Seebeck coefficient S of $Bi_{0.98}Sb_{0.02}$thin films on d (d = 5 - 250 nm), monotonic and oscillating components can be distinguished, which indicates the manifestation of classical and quantum size effects.

2. The monotonic component of is well described within the framework of the Fuchs - Sondheimer theory with the mean free path of electrons $l \approx 800 \pm 40$ nm and the surface scattering coefficient $p \approx 0.5 \pm 0.05$.

3. The experimentally measured period of quantum oscillations ($\Delta d = 45 \pm 5$ nm) is in good agreement with that calculated theoretically within the framework of the model of an infinitly deep potential well. Comparing the value of Δd obtained in this work with those obtained earlier for *Bi1-xSbx* films prepared by a similar procedure but with different values of *x*, we found that with increasing *x*, Δd increases, amounting to 30, 45, 80, and 105 nm for films with *x* equal to 0, 0.02, 0.045, and 0.1, respectively.

4. In contrast to the previously investigated films with $x = 0.045$ and $x = 0.09$, in which the $R_H$sign depended on the film thickness, in $Bi_{0.98}Sb_{0.02}$films, the R_H sign remained positive for all *d*'s, like in pure *Bi*. At the same time, the sign of *S* was negative. The observed effect is associated with the fact that the sign of R_H is different in different directions and with the increasing degree of texture disorientation under increasing *x*.

5. The room-temperature *d*-dependence of the TE power factor *P* also exhibits an oscillatory behavior. The values of power factor for "thick" films ($d\sim$200-400 nm) were practically similar to those for bulk $Bi_{0.98}Sb_{0.02}$ crystals, which were used as a charge for thin film preparation.

References

1. Rowe D.M. (Ed.) (1995). *CRC Handbook of Thermoelectrics*. London, New York, Washington: CRC Press, Boca Raton.

2. Anatychyk L.I. (1979). *Termoelementy i termoelektricheskiie ustroistva. Spravochnik. [Thermoelements and thermoelectric devices. Reference book].* Kyiv: Naukova dumka [in Russian].

3. Brandt N.B., Chudinov S.M, Karavaev V.G. (1976). Study of a gapless state induced by a magnetic field in bismuth-antimony alloys. *Zh. Eksper. Teor. Fiz.* 70(6), 2296.

4. Brandt N.B.,. Chudinov S.M (1970). Oscillatory effects in semimetallic $Bi_{1-x}Sb_x$ alloys under pressure. *Zh. Eksper. Teor. Fiz.*, 59(5), 1494-1507.

5. Oelgart G., Schneider G., Kraak W. (1976). The semiconductor-semimetal transition in $Bi_{1-x}Sb_x$ alloys. *Phys.Stat.Sol*, 74(b), 1976, 75-78.

6. Brandt N.B., Semenov M.V., Falkovsky L.A. (1977). Experiment and theory on the magnetic susceptibility of Bi-Sb alloys. *J. Low Temp. Phys.*, 27(1,2), 75-90.

7. Lenoir B., Cassart M., Michenaud J.-P. (1996). Transport properties of Bi-rich Bi-Sb alloys. *J. Phys. Chem. Solids*, 57(1), 89-99.

8. Rogacheva E.I., Drozdova A.A., Nashchekina O.N., Dresselhaus M.S., Dresselhaus G. (2009). Transition into a gapless state and concentration anomalies in the properties of Bi$_{1-x}$Sb$_x$ solid solutions. *Appl. Phys. Lett*., 94 (20), 202111.

9. Rogacheva E.I., Drozdova A.A., Nashchekina O.N. (2010). Percolation effects in semimetallic Bi-Sb solid solutions. *Phys.Stat. sol*, 207(A), 344–347.

10. Rogacheva E.I., Doroshenko A.N., Drozdova A.A., Nashchekina O.N., Men'shov Yu.V. (2020). Galvanomagnetic properties of polycrystalline Bi$_{1-x}$Sb$_x$ solid solutions in the concentration range x = 0-0.25. *Functional Materials*, 27(3), 488-496.

11. Rogacheva E.I. and Drozdova A.A. (2006). Thermoelectric properties of polycrystalline Bismuth-Antimony Solid Solutions. *J. Thermoelectricity*, 2, 22-28.

12. Doroshenko A.N., Rogacheva E.I., Drozdova A.A., Martynova K.V., Men'shov Yu.V.(2016). Thermoelectric properties of the polycrystalline Bi1-xSbx solid solutions in the concentration interval   x = 0 – 0.25. *J. Thermoelectricity*, 4, 23-36.

13. Rogacheva E.I., Nashchekina O.N., Orlova D.S., Doroshenko A.N., Dresselhaus M.S. (2017). Influence of composition on the thermoelectric properties of Bi1−xSbx thin films. *J. Electronic Mater.* 46(7), 3821-3825.

14. Rogacheva E.I., Doroshenko A.N., Sipatov A.Yu. (2020). Electronic phase transitions in thin Bi1-XSbX films. *J. Thermoelectricity*, 2, 12-24.

15. Fu L., Kane C.L., Mele E.J. (2007). *Phys. Rev. Lett*., 98, 106803.

16. Hsieh D., Qian D., Wray L., Xia Y.,. Hor Y.S, Cava R.J.,. Hasan M.Z. (2008). *Nature*, 452, 970.

17. Hasan M.Z. Kane C.L. (2010). *Rev. Mod. Phys*., 82, 3045.

18. Dresselhaus M.S. , Yu-Ming Lin, Koga T. , Cronin S.B. , Rabin O., Black M.R. , Dresselhaus G. (2001). In *Semiconductors and Semimetals, Recent Trends in Thermoelectric Materials Research* III, USA, San Diego, CA, Academic Press, 2001, 1–121.

19. Komnik Yu.F. (1979). *Fizika metalicheskikh plionok [Physics of metal films]*. Moscow: Atomizdat [In Russian].

20. Ogrin Y.F., Lutsky V.N., Yelinson M.I. (1966). Observation of quantum size effects in thin bismuth films. *Sov. Phys. JETP Lett*., 3, 71-73.

21. Sandomirskii V.B. (1967). *Quantum size effect in semimetal films*. Soviet Phys. JETP, 25(1), 101-106.

22. Duggal P., Rup R., Tripathi P. (1966). Quantum size effect in thin bismuth films. *Appl. Phys. Let*., 9(8), 293-295.

23. Komnik Yu.F., Buchsztab E.I. (1968). Observation of the quantum and classical size effects in polycrystalline thin bismuth films. *Soviet Physics JETP*, 54, 34-37.

24. Traon JJ.Y.le, Combet H.A. (1969). Electrical conductivity and Hall effect in thin layers of

bismuth between 4,2K and 300K. *J. Phys.*, 30, 419-426.

25. Thornburg D.D., Wayman C.M. (1969). Quantum and classical size effects in the thermoelectric power of thin bismuth films. *Philos. Magaz.*, 20(167), 1153-1161.

26. Lal A., Duggal V.P. (1970). Thermoelectric power of thin single crystal bismuth films. *Philos. Magaz.*, 22(175), 189-191.

27. Hoffman R.A., Frankl D.R. (1971). Electrical transport properties of thin bismuth films. *Phys. Rev. B.*, 3(6), 1825-1833.

28. Komnik Yu.F., Andrievskii V.V., Buhshtab E.I. (1970). Features of the magnetoresistance of thin bismuth films. *Physics of the Solid State*, 12(11), 3266 – 3269.

29. Petrosyan V.I., Molin V.N., Dagman E.I., Tavger B.A., Skripkina P.A., Aleksandrov L.N. (1971). Features of quantum size effects in thin non-textured polycrystalline bismuth films obtained by the electric flash method. *Fizika Metallov i Metallovedenie*, 32, 725 – 730 [in Russian].

30. Garcia N., Kao Y.H., Strongin M. (1972). Galvanomagnetic studies of bismuth films in the quantum-size-effect region. *Phys. Rev. B.*, 5(6), 2029-2039.

31. Subotowicz M., Jalochowski M., Mikolajczak B, Mikolajczak P. (1973). Measurements of the physical properties of thin Bi films from 180 to 40000 AA. *Phys. Stat. Sol. A.*, 17(1), 79-87.

32. Abrasimov V.M., Yegorov B.N., Krykin M.A. (1973).Size effect of kinetic coefficients in polycrystalline bismuth films. *Sov. Phys. JETP*, 37(1), 113-116.

33. Inoue M., Yagi H., Tamaki Y. (1973). Anomalies in the Hall coefficient of bismuth films. Japan. *J. Appl. Phys.*, 12, 310.

34. Mikolajczak P., Piasek W., Subotowicz M. (1974). Thermoelectric power in bismuth thin films. *Phys. Stat. Sol. A.*, 25(2), 619-628.

35. Borzyak P.G., Vatamanyuk V.I., Kulyupin Yu.A. (1974). Peculiarties of the thickness dependences of the bismuth films structure and resistivity. *Phys. Stat. Sol. A.*, 22, 3-6.

36. Baba S., Sugawara H., Kinbara A. (1976). Electrical resistivity of thin bismuth films. *Thin Solid Films*, 31, 329-335.

37. Bondar E. A., Vatamanyuk V.I., Chumak A.A. (1976). Thickness dependence of the current carrier concentration in bismuth films. *Thin Solid Films*, 34, 387-389.

38. Komnik Yu.F., Andrievsky V.V. (1977). Kinetic properties of electrons in bismuth thin films. *Thin Solid Films*, 42, 1-6.

39. Kochowski S., Opilski A. (1978). Concentration and mobility of charge carriers in thin polycrystalline films of bismuth. *Thin Solid Films*, 48, 345-351.

40. Saleh M., Buxo J., Dorville G., Sarrabayrouse G. (1979). Electrical and elastoresistance properties of evaporated thin films of bismuth. *Revue de Physique Applique*, 14, 405-413.

41. Asahi H., Kinbara A. (1980). Size effect in electrical properties of thin epitaxial bismuth films. *Thin Solid Films*, 66, 131-137.

42. Boxus J., Uher C., Heremans J., Issi J -P. (1981). Size dependence of the transport properties of trigonal bismuth. *Phys. Rev. B.*, 23, 449–452.

43. Akhtar S.M., Khawaja E.E. (1985). A study of the resistivity and the. thermoelectric power of thin films of Sb and Bi. *Phys. Stat. Sol. A.*, 87, 335-340.

44. Damodara Das V., Soundararajan N. (1987). Size and temperature effects on the Seebeck coefficient of thin bismuth films. *Phys. Rev. B.*, 35(12), 5990-5996.

45. Chu H.T., Zhang W. (1992). Quantum size effect and electric conductivity in thin films of pure bismuth. *J. Phys. Chem. Solids*, 53, 1059.

46. Rogacheva E.I., Grigorov S.N., Nashchekina O.N., Lyubchenko S.G., Dresselhaus M.S. (2003). Quantum-size effects in n-type bismuth thin films. *Appl. Phys. Let.*, 82(15), 2628-2630.

47. Rogacheva E.I., Lyubchenko S.G., Nashchekina O.N., Meriuts A.V., Dresselhaus M.S. (2009). Quantum size effects and transport phenomena in thin Bi layers. *Microelectronics Journal*, 40, 728-730.

48. Rogacheva E.I., Lyubchenko S.G., Drozdova A.A. (2009). Effect of magnetic field on galvanomagnetic properties of mica/Bi/EuS heterostructures. *Microelectronics Journal*, 40, 821–823.

49. Mustafaev Z., Fraiman B.S., Chudnovskiy A.F. (1971). Thermal conductivity of thin layers of bismuth. *Semiconductors*, 5(1), 242-246 [in Russian].

50. Okun I.Z., Fraiman B.S., Chudnovskiy A.F. (1972). Magnetoresistance of thin bismuth layers. *Semiconductors*, 6(4), 715-717 [in Russian].

51. Burchakova V.I., Gitsu D.V., Kozlovskiy M.I. (1972). Features of thermoelectric power of bismuth thin films. *Physics of the Solid State*, 14(3), 1972, 907-909 [in Russian].

52. Fuchs K. (1938).The conductivity of thin metallic films according to the electron theory of metals *Proc. Cambridge Philos. Soc.*, 34, 100-108.

53. Sondheimer E.H. (1952). The mean free path of electrons in metals. *Adv. Phys.*, 1(1), 1-42.

54. Savchenko A.K., Lutskiy V.N., Rilik A.S. (1981). About the influence of quantum corrections on the resistance of thin bismuth films. *Sov. Phys. JETP Lett.*, 34(6), 367-371.

55. Buhshtab E.I., Komnik Yu.F., Butenko A.V. Andrievskiy V.V. (1982). Features of the magnetoresistance of thin bismuth films in the region of manifestation of quantum corrections. *Sov. J. Low Temp. Phys.*, 8(4), 440-445.

56. Komnik Yu.F., Buhshtab E.I., Butenko A.V. Andrievskiy V.V. (1982). Localization effects in bismuth films in a weak magnetic field. Sov. *J. Low Temp. Phys.*, 8(12), 1289-1292.

57. Komnik Yu.F., Bukhshtab E.I., Butenko A.V., Andrievsky V.V. (1982). Separation of the electron localization and interaction in bismuth film resistance. *Solid State Communs.*, 44(6), 865-867.

58. Fumio Komori, Shun-inhi Kobayashi, Wataru Sasaki (1983). The anti-localization effect in

Bi thin films. *J. Phys. Soc. Japan*, 52(2), 368-371.

59. Woerlee P.H., Verkade G.C., Jansen G.M. (1983). An experimental investigation on weak localisation, spin-orbit and interaction effects in thin bismuth films. *J. Phys. C: Solid State Phys.*, 16, 3011-3024.

60. McLachlan D.S. (1983). Weak-localization, spin-orbit, and electron-electron interaction effects in two- and three-dimensional bismuth films. *Phys. Rev. B*., 28(12), 6821-6832.

61. Favennec M.M.E., Le Contellec M., Le Traon J.Y. (1972). Study of quantum size effects by elastroresistance, thermoelectric power and conductivity measurements in Bi and Bi_xSb_{1-x}. *Thin Solid Films*, 13(1), 73-79.

62. Favennec M.P., Le Contellec M. (1973). Quantum size effects in the thermoelectric power of Bi and Bi_xSb_{1-x} thin films. *Solid State Communs*., 13(2), 141-146.

63. Komnik Yu. F., Bukhshtab E. I., Nikitin Yu. V. (1975). Quantum size effect in bismuth films with antimony adding. *Sov. J. Low Temp. Phys*., 1, 243–246.

64. Bukhshtab E. I., Komnik Yu. F., Nikitin Yu. V. (1978). Electrical properties of thin bismuth-antimony films. I. Changes in the properties with varying composition. *Sov. J. Low Temp. Phys*., 4(8), 474 – 479.

65. Komnik Yu. F., Nikitin Yu. V., Bukhshtab E. I. (1978). Electrical properties of thin bismuth-antimony films. II. Changes in the properties with varying thickness. *Sov. J. Low Temp. Phys*., 4(9), 538 – 544.

66. Komnik Yu. F., Nikitin Yu. V., Bukhshtab E. I. (1878). Electrical properties of thin bismuth-antimony films. III. Quantum size effect. *Sov. J. Low Temp. Phys*., 4(10), 591 – 595.

67. Nikitin Yu. V., Bukhshtab E. I., Komnik Yu. F. Electrical properties of thin bismuth-antimony films. IV. Temperature dependence, Sov. J. Low Temp. Phys., 4(11), 1978. 679 – 684.

68. Komnik Yu. F., Bukhshtab E. I., Nikitin Yu. V. (1978). Specific features of the galvanomagnetic properties of thin films of $Bi_{1-X}Sb_X$ in the semimetal and semiconductor regions. *Thin Solid Films*., 52, 361 – 364.

69. Damodara Das V., Meena N. (1981). Electrical properties of Bi80Sb20 alloy thin films, vacuum-deposited at different substrate temperatures. *J. Mater. Science*, 16(12), 3489–3495.

70. Tang M.Y., Dresselhaus M.S., A band structure phase diagram calculation of 2D BiSb films, Materials research society symposium proceedings, 886, 2006, 129134.

71. Mallik R.C., Damodara Das V. (2005). Study of structural-, and thickness-dependent thermoelectric and electrical properties of $Bi_{93}Sb_7$ alloy thin films. *J. Appl. Phys*. 98, 0237101-0237108.

72. Mallik R.C., Damodara Das V. (2005). Size- and temperature-dependent thermoelectric and electrical properties of $Bi_{88}Sb_{12}$ alloy thin films. *Vacuum*, 77(3), 275-285.

73. Rogacheva E.I., Orlova D.S., Dresselhaus M.S., Tang S. (2011). Size effects in Bi-Sb solid solutions thin films. *MRS Online Proceedings Library*, 1314, 1-6.

74. Rogacheva E.I., Orlova D.S., Nashchekina O.N., Dresselhaus M.S., Tang S. (2012). Thickness dependence oscillations of transport properties in thin films of atopological insulator Bi₉₁Sb₉. *Appl. Phys. Lett*., 101, 023108(1-4).

75. Michenaud J-P., Issi J-P. (1972). Electron and hole transport in bismuth. *J. Phys. C:Solid State Phys*., 5, 3061-3072.

76. Rogacheva E.I., Nashchekina O.N., Tavrina T.V., Us M.A., Dresselhaus M.S., Cronin S.B., Rabin O. (2003). Quantum size effects in IV-VI quantum wells. *Physica E*, 17, 313-315.

77. Rogacheva E.I., Budnik A.V., Sipatov A.Yu., Nashchekina O.N., Dresselhaus M.S.(2015). Thickness dependent quantum oscillations of transport properties in topological insulator Bi₂Te₃ thin films. *Appl. Phys. Lett*. 106, 053103.

Рогачова О.І., *док. фіз.-мат. наук, професор*

Новак К.В., Орлова Д.С.,

Нащекіна О.М., *канд. фіз.-мат. наук, доцент*

Сіпатов О.Ю., *докт. фіз.-мат. наук, професор*

Лісачук Г.В. *докт. техн. наук, професор*

Національний технічний університет
«Харківський політехнічний інститут»,
вул. Кирпичова 2., Харків 61002, Україна

РОЗМІРНІ ЕФЕКТИ ТА ТЕРМОЕЛЕКТРИЧНІ ВЛАСТИВОСТІ ТОНКИХ ПЛІВОК $BI_{0.98}SB_{0.02}$

При кімнатній температурі отримано залежності термоелектричних властивостей (коефіцієнта Зеєбека S, електропровідності σ, коефіцієнта Холла R_H і термоелектричної потужності $P = S^2 \cdot \sigma$) від товщини (d = 5 - 250 нм) тонких плівок твердих розчинів $Bi_{98}Sb_2$, вирощених на підкладках зі слюди методом термічного випаровування у вакуумі із одного джерела. Показано, що монотонна складова залежності σ(d) добре описується в рамках теорії Фукса-Зондгеймера для класичного розмірного ефекту. Виявлена осцилююча складова d-залежностей σ, S, R_H та $S^2 \cdot \sigma$ пов'язується з проявом квантового розмірного ефекту, і визначений експериментально період квантових осциляцій Δd = 45 ± 5 нм добре узгоджується зі значенням Δd, теоретично розрахованим в рамках моделі нескінченно глибокої потенційної ями. Бібл. 77, рис. 1.

Ключові слова: Bi$_{0.98}$Sb$_{0.02}$ твердий разчин, тонка плівка, товщина, термоелектричні властивості,, розмірний ефект, період осциляцій.

Рогачева Е.И., *докт. физ.-мат. наук, профессор*

Новак К.В., Орлова Д.С.

Нащекина О.М., *канд. физ.-мат. наук, доцент*

Сипатов А.Ю., *докт. физ.-мат. наук, профессор*

Лисачук Г.В., *докт. техн. наук, профессор*

Национальный Технический Университет
«Харьковский Политехнический Институт»,
ул. Кирпичева, 2, Харьков, 61002, Украина

РАЗМЕРНЫЕ ЭФФЕКТЫ И ТЕРМОЭЛЕКТРИЧЕСКИЕ СВОЙСТВА ТОНКИХ ПЛЕНОК Bi$_{0.98}$Sb$_{0.02}$

При комнатной температуре получены зависимости термоэлектрических свойств (коэффициента Зеебека S, электропроводности σ, коэффициента Холла R$_H$ и термоэлектрической мощности P=S^{2}σ) от толщины (d = 5 - 250 nm) тонких пленок твердых растворов Bi$_{98}$Sb$_2$, выращенных на подложках из слюды методом термического испарения в вакууме из одного источника. Показано, что монотонная составляющая зависимости σ(d) хорошо описывается в рамках теории Фукса-Зондгеймера для классического размерного эффекта. Обнаружена осциллирующая составляющая d-зависимостей σ, S, R$_H$ и S^{2}σ связывается с проявлением квантового размерного эффекта, и определенный экспериментально период квантовых осцилляций Δd = 45 ± 5 нм хорошо согласуется со значением Δd, теоретически рассчитанным в рамках модели бесконечно глубокой потенциальной ямы. Библ. 77, рис. 1.

Ключевые слова: Bi$_{0.98}$Sb$_{0.02}$, твердый раствор, тонкая пленка, толщина, термоэлектрические свойства, размерный эффект, период осцилляций.

References

1. Rowe D.M. (Ed.) (1995). *CRC Handbook of Thermoelectrics*. London, New York, Washington: CRC Press, Boca Raton.

2. Anatychyk L.I. (1979). *Termoelementy i termoelektricheskiie ustroistva. Spravochnik. [Thermoelements and thermoelectric devices. Reference book].* Kyiv: Naukova dumka [in Russian].

3. Brandt N.B., Chudinov S.M, Karavaev V.G. (1976). Study of a gapless state induced by a magnetic field in bismuth-antimony alloys. *Zh. Eksper. Teor. Fiz.* 70(6), 2296.

4. Brandt N.B.,. Chudinov S.M (1970). Oscillatory effects in semimetallic Bi$_{1-x}$Sb$_x$ alloys under pressure. *Zh. Eksper. Teor. Fiz.*, 59(5), 1494-1507.

5. Oelgart G., Schneider G., Kraak W. (1976). The semiconductor-semimetal transition in Bi$_{1-x}$Sb$_x$ alloys. *Phys.Stat.Sol*, 74(b), 1976, 75-78.

6. Brandt N.B., Semenov M.V., Falkovsky L.A. (1977). Experiment and theory on the magnetic susceptibility of Bi-Sb alloys. *J. Low Temp. Phys.*, 27(1,2), 75-90.

7. Lenoir B., Cassart M., Michenaud J.-P. (1996). Transport properties of Bi-rich Bi-Sb alloys. *J. Phys. Chem. Solids*, 57(1), 89-99.

8. Rogacheva E.I., Drozdova A.A., Nashchekina O.N., Dresselhaus M.S., Dresselhaus G. (2009). Transition into a gapless state and concentration anomalies in the properties of Bi$_{1-x}$Sb$_x$ solid solutions. *Appl. Phys. Lett.*, 94 (20), 202111.

9. Rogacheva E.I., Drozdova A.A., Nashchekina O.N. (2010). Percolation effects in semimetallic Bi-Sb solid solutions. *Phys.Stat. sol*, 207(A), 344–347.

10. Rogacheva E.I., Doroshenko A.N., Drozdova A.A., Nashchekina O.N., Men'shov Yu.V. (2020). Galvanomagnetic properties of polycrystalline Bi$_{1-x}$Sb$_x$ solid solutions in the concentration range x = 0-0.25. *Functional Materials*, 27(3), 488-496.

11. Rogacheva E.I. and Drozdova A.A. (2006). Thermoelectric properties of polycrystalline Bismuth-Antimony Solid Solutions. *J. Thermoelectricity*, 2, 22-28.

12. Doroshenko A.N., Rogacheva E.I., Drozdova A.A., Martynova K.V., Men'shov Yu.V.(2016). Thermoelectric properties of the polycrystalline Bi1-xSbx solid solutions in the concentration interval x = 0 – 0.25. *J. Thermoelectricity*, 4, 23-36.

13. Rogacheva E.I., Nashchekina O.N., Orlova D.S., Doroshenko A.N., Dresselhaus M.S. (2017). Influence of composition on the thermoelectric properties of Bi1−xSbx thin films. *J. Electronic Mater.* 46(7), 3821-3825.

14. Rogacheva E.I., Doroshenko A.N., Sipatov A.Yu. (2020). Electronic phase transitions in thin Bi1-XSbX films. *J. Thermoelectricity*, 2, 12-24.

15. Fu L., Kane C.L., Mele E.J. (2007). *Phys. Rev. Lett.*, 98, 106803.

16. Hsieh D., Qian D., Wray L., Xia Y.,. Hor Y.S, Cava R.J.,. Hasan M.Z. (2008). *Nature*, 452, 970.

17. Hasan M.Z. Kane C.L. (2010). *Rev. Mod. Phys.*, 82, 3045.

18. Dresselhaus M.S. , Yu-Ming Lin, Koga T. , Cronin S.B. , Rabin O., Black M.R. , Dresselhaus G. (2001). In *Semiconductors and Semimetals, Recent Trends in Thermoelectric Materials Research* III, USA, San Diego, CA, Academic Press, 2001, 1–121.

19. Komnik Yu.F. (1979). *Fizika metalicheskikh plionok [Physics of metal films].* Moscow: Atomizdat [In Russian].

20. Ogrin Y.F., Lutsky V.N., Yelinson M.I. (1966). Observation of quantum size effects in thin

bismuth films. *Sov. Phys. JETP Lett.*, 3, 71-73.

21. Sandomirskii V.B. (1967). *Quantum size effect in semimetal films*. Soviet Phys. JETP, 25(1), 101-106.

22. Duggal P., Rup R., Tripathi P. (1966). Quantum size effect in thin bismuth films. *Appl. Phys. Let.*, 9(8), 293-295.

23. Komnik Yu.F., Buchsztab E.I. (1968). Observation of the quantum and classical size effects in polycrystalline thin bismuth films. *Soviet Physics JETP*, 54, 34-37.

24. Traon JJ.Y.le, Combet H.A. (1969). Electrical conductivity and Hall effect in thin layers of bismuth between 4,2K and 300K. *J. Phys.*, 30, 419-426.

25. Thornburg D.D., Wayman C.M. (1969). Quantum and classical size effects in the thermoelectric power of thin bismuth films. *Philos. Magaz.*, 20(167), 1153-1161.

26. Lal A., Duggal V.P. (1970). Thermoelectric power of thin single crystal bismuth films. *Philos. Magaz.*, 22(175), 189-191.

27. Hoffman R.A., Frankl D.R. (1971). Electrical transport properties of thin bismuth films. *Phys. Rev. B.*, 3(6), 1825-1833.

28. Komnik Yu.F., Andrievskii V.V., Buhshtab E.I. (1970). Features of the magnetoresistance of thin bismuth films. *Physics of the Solid State*, 12(11), 3266 – 3269.

29. Petrosyan V.I., Molin V.N., Dagman E.I., Tavger B.A., Skripkina P.A., Aleksandrov L.N. (1971). Features of quantum size effects in thin non-textured polycrystalline bismuth films obtained by the electric flash method. *Fizika Metallov i Metallovedenie*, 32, 725 – 730 [in Russian].

30. Garcia N., Kao Y.H., Strongin M. (1972). Galvanomagnetic studies of bismuth films in the quantum-size-effect region. *Phys. Rev. B.*, 5(6), 2029-2039.

31. Subotowicz M., Jalochowski M., Mikolajczak B, Mikolajczak P. (1973). Measurements of the physical properties of thin Bi films from 180 to 40000 AA. *Phys. Stat. Sol. A.*, 17(1), 79-87.

32. Abrasimov V.M., Yegorov B.N., Krykin M.A. (1973).Size effect of kinetic coefficients in polycrystalline bismuth films. *Sov. Phys. JETP*, 37(1), 113-116.

33. Inoue M., Yagi H., Tamaki Y. (1973). Anomalies in the Hall coefficient of bismuth films. Japan. *J. Appl. Phys.*, 12, 310.

34. Mikolajczak P., Piasek W., Subotowicz M. (1974). Thermoelectric power in bismuth thin films. *Phys. Stat. Sol. A.*, 25(2), 619-628.

35. Borzyak P.G., Vatamanyuk V.I., Kulyupin Yu.A. (1974). Peculiarties of the thickness dependences of the bismuth films structure and resistivity. *Phys. Stat. Sol. A.*, 22, 3-6.

36. Baba S., Sugawara H., Kinbara A. (1976). Electrical resistivity of thin bismuth films. *Thin Solid Films*, 31, 329-335.

37. Bondar E. A., Vatamanyuk V.I., Chumak A.A. (1976). Thickness dependence of the current carrier concentration in bismuth films. *Thin Solid Films*, 34, 387-389.

38. Komnik Yu.F., Andrievsky V.V. (1977). Kinetic properties of electrons in bismuth thin films. *Thin Solid Films*, 42, 1-6.

39. Kochowski S., Opilski A. (1978). Concentration and mobility of charge carriers in thin polycrystalline films of bismuth. *Thin Solid Films*, 48, 345-351.

40. Saleh M., Buxo J., Dorville G., Sarrabayrouse G. (1979). Electrical and elastoresistance properties of evaporated thin films of bismuth. *Revue de Physique Applique*, 14, 405-413.

41. Asahi H., Kinbara A. (1980). Size effect in electrical properties of thin epitaxial bismuth films. *Thin Solid Films*, 66, 131-137.

42. Boxus J., Uher C., Heremans J., Issi J -P. (1981). Size dependence of the transport properties of trigonal bismuth. *Phys. Rev. B.*, 23, 449–452.

43. Akhtar S.M., Khawaja E.E. (1985). A study of the resistivity and the. thermoelectric power of thin films of Sb and Bi. *Phys. Stat. Sol. A.*, 87, 335-340.

44. Damodara Das V., Soundararajan N. (1987). Size and temperature effects on the Seebeck coefficient of thin bismuth films. *Phys. Rev. B.*, 35(12), 5990-5996.

45. Chu H.T., Zhang W. (1992). Quantum size effect and electric conductivity in thin films of pure bismuth. *J. Phys. Chem. Solids*, 53, 1059.

46. Rogacheva E.I., Grigorov S.N., Nashchekina O.N., Lyubchenko S.G., Dresselhaus M.S. (2003). Quantum-size effects in n-type bismuth thin films. *Appl. Phys. Let.*, 82(15), 2628-2630.

47. Rogacheva E.I., Lyubchenko S.G., Nashchekina O.N., Meriuts A.V., Dresselhaus M.S. (2009). Quantum size effects and transport phenomena in thin Bi layers. *Microelectronics Journal*, 40, 728-730.

48. Rogacheva E.I., Lyubchenko S.G., Drozdova A.A. (2009). Effect of magnetic field on galvanomagnetic properties of mica/Bi/EuS heterostructures. *Microelectronics Journal*, 40, 821–823.

49. Mustafaev Z., Fraiman B.S., Chudnovskiy A.F. (1971). Thermal conductivity of thin layers of bismuth. *Semiconductors*, 5(1), 242-246 [in Russian].

50. Okun I.Z., Fraiman B.S., Chudnovskiy A.F. (1972). Magnetoresistance of thin bismuth layers. *Semiconductors*, 6(4), 715-717 [in Russian].

51. Burchakova V.I., Gitsu D.V., Kozlovskiy M.I. (1972). Features of thermoelectric power of bismuth thin films. *Physics of the Solid State*, 14(3), 1972, 907-909 [in Russian].

52. Fuchs K. (1938).The conductivity of thin metallic films according to the electron theory of metals *Proc. Cambridge Philos. Soc.*, 34, 100-108.

53. Sondheimer E.H. (1952). The mean free path of electrons in metals. *Adv. Phys.*, 1(1), 1-42.

54. Savchenko A.K., Lutskiy V.N., Rilik A.S. (1981). About the influence of quantum corrections on the resistance of thin bismuth films. *Sov. Phys. JETP Lett.*, 34(6), 367-371.

55. Buhshtab E.I., Komnik Yu.F., Butenko A.V. Andrievskiy V.V. (1982). Features of the magnetoresistance of thin bismuth films in the region of manifestation of quantum corrections.

Sov. J. Low Temp. Phys., 8(4), 440-445.

56. Komnik Yu.F., Buhshtab E.I., Butenko A.V. Andrievskiy V.V. (1982). Localization effects in bismuth films in a weak magnetic field. Sov. *J. Low Temp. Phys.*, 8(12), 1289-1292.

57. Komnik Yu.F., Bukhshtab E.I., Butenko A.V., Andrievsky V.V. (1982). Separation of the electron localization and interaction in bismuth film resistance.*Solid State Communs.*, 44(6), 865-867.

58. Fumio Komori, Shun-inhi Kobayashi, Wataru Sasaki (1983). The anti-localization effect in Bi thin films. *J. Phys. Soc. Japan*, 52(2), 368-371.

59. Woerlee P.H., Verkade G.C., Jansen G.M. (1983). An experimental investigation on weak localisation, spin-orbit and interaction effects in thin bismuth films. *J. Phys. C: Solid State Phys.*, 16, 3011-3024.

60. McLachlan D.S. (1983). Weak-localization, spin-orbit, and electron-electron interaction effects in two- and three-dimensional bismuth films. *Phys. Rev. B*., 28(12), 6821-6832.

61. Favennec M.M.E., Le Contellec M., Le Traon J.Y. (1972). Study of quantum size effects by elastroresistance, thermoelectric power and conductivity measurements in Bi and Bi$_x$Sb$_{1-x}$. *Thin Solid Films*, 13(1), 73-79.

62. Favennec M.P., Le Contellec M. (1973). Quantum size effects in the thermoelectric power of Bi and Bi$_x$Sb$_{1-x}$ thin films. *Solid State Communs.*, 13(2), 141-146.

63. Komnik Yu. F., Bukhshtab E. I., Nikitin Yu. V. (1975). Quantum size effect in bismuth films with antimony adding. *Sov. J. Low Temp. Phys.*, 1, 243–246.

64. Bukhshtab E. I., Komnik Yu. F., Nikitin Yu. V. (1978). Electrical properties of thin bismuth-antimony films. I. Changes in the properties with varying composition. *Sov. J. Low Temp. Phys.*, 4(8), 474 – 479.

65. Komnik Yu. F., Nikitin Yu. V., Bukhshtab E. I. (1978). Electrical properties of thin bismuth-antimony films. II. Changes in the properties with varying thickness. *Sov. J. Low Temp. Phys.*, 4(9), 538 – 544.

66. Komnik Yu. F., Nikitin Yu. V., Bukhshtab E. I. (1878). Electrical properties of thin bismuth-antimony films. III. Quantum size effect. *Sov. J. Low Temp. Phys.*, 4(10), 591 – 595.

67. Nikitin Yu. V., Bukhshtab E. I., Komnik Yu. F. Electrical properties of thin bismuth-antimony films. IV. Temperature dependence, Sov. J. Low Temp. Phys., 4(11), 1978. 679 – 684.

68. Komnik Yu. F., Bukhshtab E. I., Nikitin Yu. V. (1978). Specific features of the galvanomagnetic properties of thin films of Bi$_{1-X}$Sb$_X$ in the semimetal and semiconductor regions. *Thin Solid Films*., 52, 361 – 364.

69. Damodara Das V., Meena N. (1981). Electrical properties of Bi80Sb20 alloy thin films, vacuum-deposited at different substrate temperatures. *J. Mater. Science*, 16(12), 3489–3495.

70. Tang M.Y., Dresselhaus M.S., A band structure phase diagram calculation of 2D BiSb films, Materials research society symposium proceedings, 886, 2006, 129134.

71. Mallik R.C., Damodara Das V. (2005). Study of structural-, and thickness-dependent thermoelectric and electrical properties of Bi$_{93}$Sb$_7$ alloy thin films. *J. Appl. Phys.* 98, 0237101-0237108.

72. Mallik R.C., Damodara Das V. (2005). Size- and temperature-dependent thermoelectric and electrical properties of Bi$_{88}$Sb$_{12}$ alloy thin films. *Vacuum*, 77(3), 275-285.

73. Rogacheva E.I., Orlova D.S., Dresselhaus M.S., Tang S. (2011). Size effects in Bi-Sb solid solutions thin films. *MRS Online Proceedings Library*, 1314, 1-6.

74. Rogacheva E.I., Orlova D.S., Nashchekina O.N., Dresselhaus M.S., Tang S. (2012). Thickness dependence oscillations of transport properties in thin films of atopological insulator Bi$_{91}$Sb$_9$. *Appl. Phys. Lett.*, 101, 023108(1-4).

75. Michenaud J-P., Issi J-P. (1972). Electron and hole transport in bismuth. *J. Phys. C:Solid State Phys.*, 5, 3061-3072.

76. Rogacheva E.I., Nashchekina O.N., Tavrina T.V., Us M.A., Dresselhaus M.S., Cronin S.B., Rabin O. (2003). Quantum size effects in IV-VI quantum wells. *Physica E*, 17, 313-315.

77. Rogacheva E.I., Budnik A.V., Sipatov A.Yu., Nashchekina O.N., Dresselhaus M.S.(2015). Thickness dependent quantum oscillations of transport properties in topological insulator Bi$_2$Te$_3$ thin films. *Appl. Phys. Lett.* 106, 053103.

Rybchakov D.E.

Institute of Thermoelectricity of the NAS and MES of Ukraine,
1 Nauky str., Chernivtsi, 58029, Ukraine,
e-mail: anatych@gmail.com

Rybchakov D.E.

COMPUTER SIMULATION OF THE EXTRUSION PROCESS OF *Bi-Te* BASED THERMOELECTRIC MATERIAL OF RECTANGULAR SHAPE

During hot extrusion, the thermoelectric material heated to a temperature below its melting point passes through the mold (die) under the action of pressure. In the present paper, this process has been simulated with the use of Comsol Multiphysics application package of object-oriented simulation. In this model, the extruded material is presented as a liquid with a very high viscosity, which depends on the velocity and temperature. As a result of simulation, the distributions of temperature and material flow velocity in the die were obtained as well as stress distribution in the die due to external pressure and thermal loads during the tape extrusion process. These studies make it possible to optimize the installation for the production of extruded thermoelectric material. Bibl. 4, Fig. 6, Tabl. 2.

Key words: thermoelectric material, hot extrusion, computer simulation, die.

Introduction

There are various methods for obtaining thermoelectric materials, which are solid solutions based on bismuth telluride. These solutions have a number of specific features that make it difficult to obtain high- quality materials. Among the existing methods for obtaining thermoelectric materials, the most common is the method of zone melting, mainly vertical [1].

Another method for obtaining thermoelectric materials is the hot extrusion process when the thermoelectric material heated to a temperature below its melting point passes through the mold (die) under the action of pressure [2]. This method has the following advantages:

– High degree of homogeneity of the obtained samples.
– The ability to obtain samples of the required shape, which reduces the loss of material during further cutting.
– Higher mechanical strength of the samples compared to those obtained by zone melting.

However, the hot extrusion method also has disadvantages, the main of which is that texture in extruded materials is worse than in materials obtained by zone melting, but the figure of merit of extruded material is achieved not only by texture, but also by phonon scattering at grain boundaries [3].

Summarizing the advantages and disadvantages of the hot extrusion method, we can conclude that the materials obtained in this way have a high consumer potential. Thus, the main task in the study of the hot extrusion is to improve starting samples. This is achieved by optimizing the geometry of the die and experimenting with the input conditions of the process such as temperature, pressure and more. However, such experiments involve large financial and labor costs, which, as a result, may not be justified at all. To reduce these costs and formulate the theoretical part of this technology, computer simulation is a very relevant method. This method allows revealing critical shortcomings of the influence of conditions on the obtained samples. Of course, it is not able to reproduce real conditions of the hot extrusion with 100% reliability, but even the existing imperfect reliability can reduce costs several times.

The purpose of this work is to create a computer model of the process of hot extrusion of thermoelectric material based on bismuth telluride, in order to study the temperature distribution and the velocity of formation of extruded material in the form of tapes, which can be the basis for optimizing the hot extrusion work equipment.

Physical, mathematical and computer models

To accomplish this task, Comsol Multiphysics application package of object-oriented simulation was used [4]. In this model, the thermoelectric material is considered as a liquid with a high viscosity which depends on velocity and temperature. Computer model makes it possible to study the distribution of mechanical stresses in the die due to external pressure and loads.
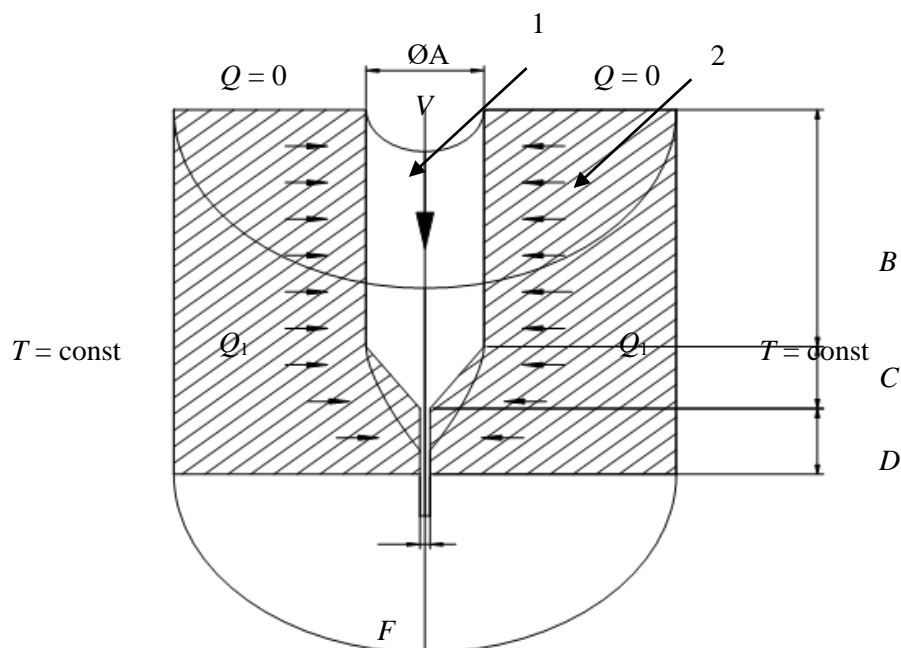
Fig. 1. Physical model of the extrusion process of tape thermoelectric material.

The used physical model of the tape material extrusion process is shown in Fig. 1. The model considers the case of extrusion of a cylindrical billet of material 1 through a matrix 2, at the output of which a tape of thermoelectric material is formed. The geometrical dimensions: A and B are the diameter and length of the input cell of the die in which the thermoelectric material billet is located; C is the length of the beveled part of the die; D and F are the thickness and length of the die outlet, the width of which is A. The case is considered when the ratio of the length to the thickness of the outlet is in the range 2 - 10.

During simulation, one also has to take into account a large number of parameters of the operating environment, some of which are shown in Table 1.

Model environment conditions

1.	Ambient temperature	25˚C
2.	Die temperature (T = const)	450˚C
3.	Coefficient of heat exchange between the material and the die	11000 W/(m^2*K)
4.	The speed of the piston that presses material (V)	0.03 mm/s

The properties of thermoelectric material and the material of which the die is made are given in Table 2.

Material properties

1.	Thermoelectric material	Thermal conductivity, W/(m*K)	4
		Density, kg/m^3	7600
		Heat capacity, J/(kg/K)	150
2.	Steel (die)	Thermal conductivity, W/(m*K)	24.3
		Density, kg/m^3	7850
		Heat capacity, J/(kg/K)	500

Fig. 2 shows a grid of the investigated model in Comsol Multiphysics.
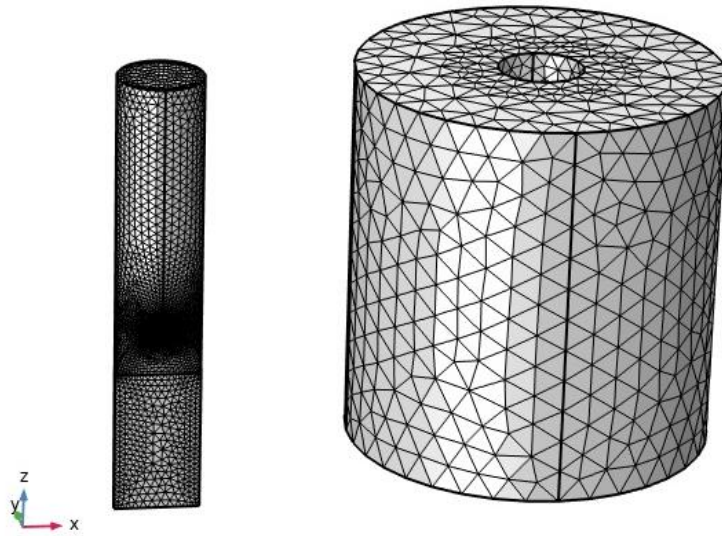
Fig. 2. The grid is built for the die configurations shown in Fig.1.

Computer simulation results

As a result of computer simulation, the following indicators were obtained:

Velocity field of thermoelectric material inside the die is shown in Figs.3 and. 4.
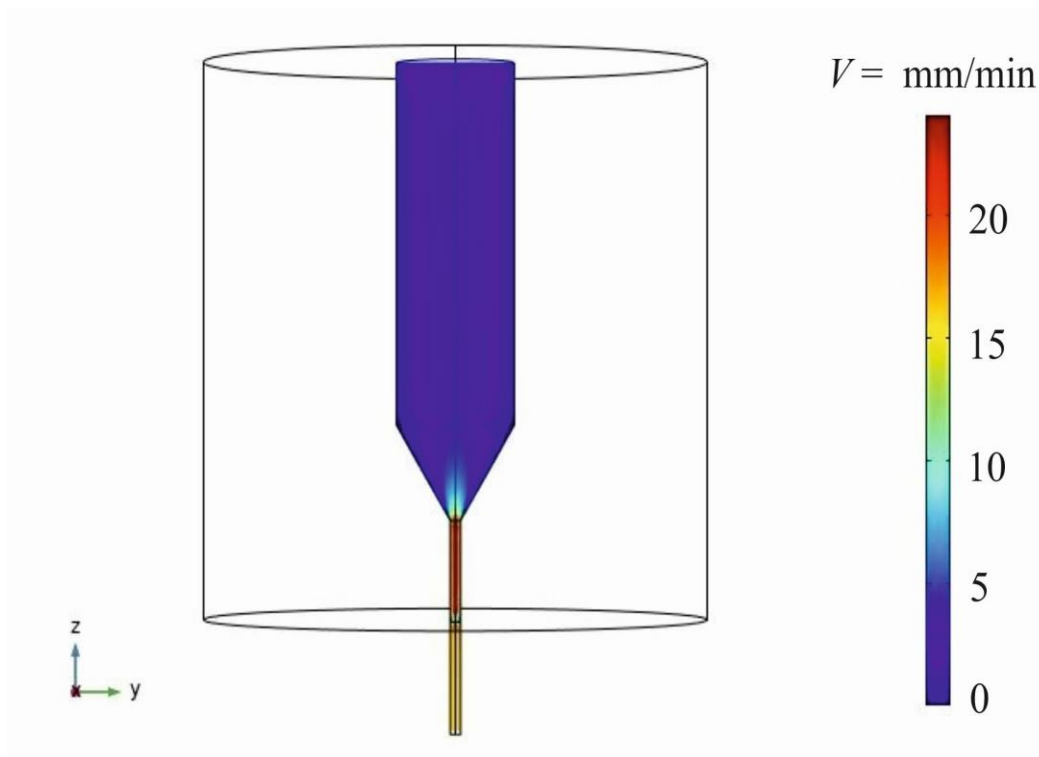
Fig. 3. Velocity field of thermoelectric material
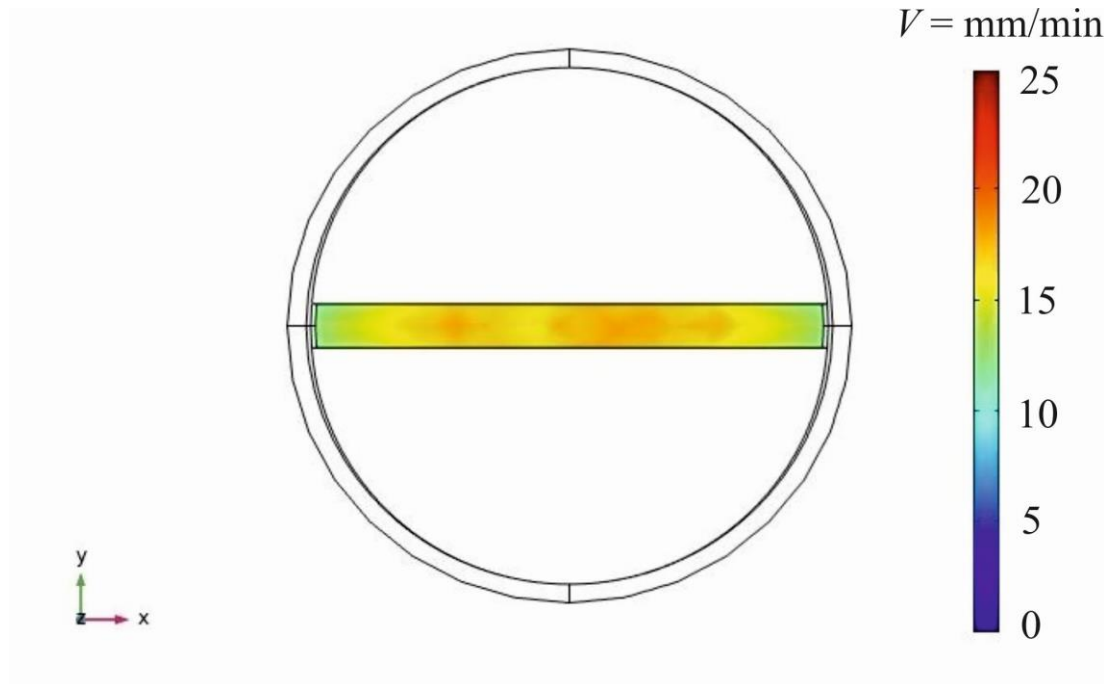
Fig. 4.Velocity field of thermoelectric material at the output

Temperature distributions in thermoelectric material and die are shown in Figs. 5 and 6.
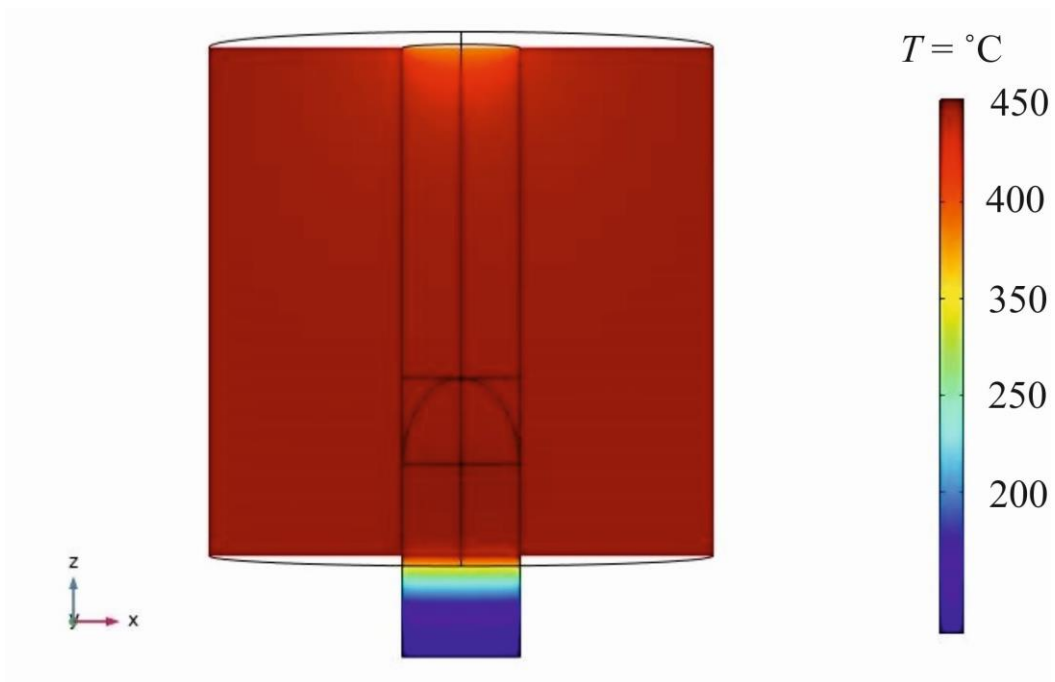
Fig. 5. Temperature distributions
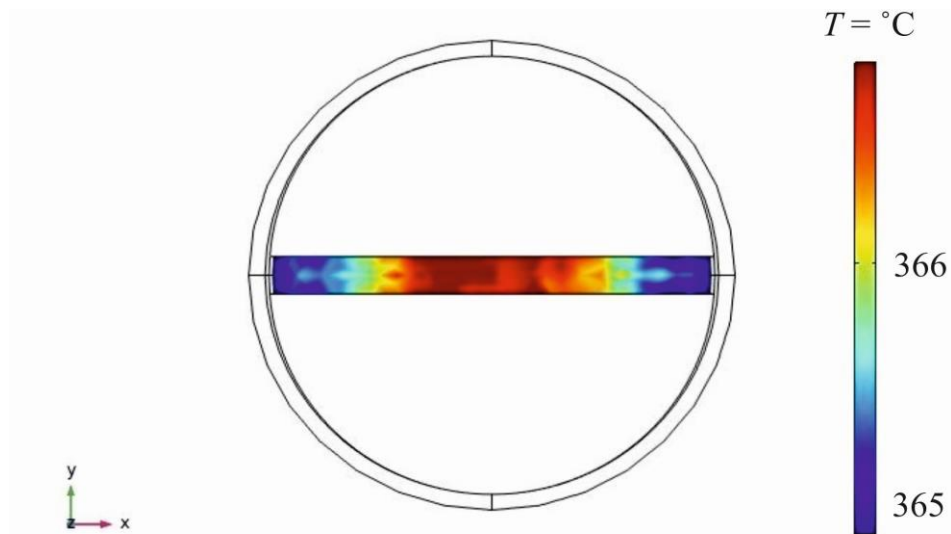
Fig. 6. Temperature distributions at the output

The developed computer model can serve as a basis for optimizing the installation for extrusion of thermoelectric material based on bismuth telluride in order to increase its efficiency, as well as to improve starting product.

Conclusions

1. A computer model of the process of hot tape extrusion of a thermoelectric material based on bismuth telluride has been created, which can be used to study the distributions of temperature and velocity of material movement in a die of a given shape, as well as the distribution of stresses in the die due to external pressure and thermal loads.
2. The behavior of thermoelectric material passing through the die for the case of tape extrusion of thermoelectric material based on bismuth telluride has been studied.
3. The distributions of temperature and velocity fields have been obtained depending on the configuration of the die for the case of one-stage tape extrusion of a thermoelectric material based on bismuth telluride.

References

1. Goltsman B.M**.,** Kudinov V.A., Smirnov I.A. (1972). *Termoelektricheskiie materialy na osnove tellurida vismuta (Bi$_2$Te$_3$) [Thermoelectric materials based on bismuth telluride (Bi$_2$Te$_3$)].* Moscow: Nauka [in Russian].
2. Sabo E.P. (2006). Tekhnologiia khalkogenidnykh termoelementov. Fizicheskiie osnovy. [Technology of chalcogenide thermoelements. Physical fundamentals]. *J.Thermoelectricity*, 1, 45-66.

3. Gorskyi P.V. (2020). On the fundamental difference between thermoelectric composites and doped thermoelectric materials and the consequences it implies. *J.Thermoelectricity*, 1, 27-37.

4. Fluid-structure interaction in aluminum extrusion. Structural Mechanics Module Model Library. *COMSOLAB*, 2008, 301-316.

Рибчаков Д.Е.

Інститут термоелектрики НАН і МОН України,
вул. Науки, 1, Чернівці, 58029, Україна,
e-mail: anatych@gmail.com

КОМП'ЮТЕРНЕ МОДЕЛЮВАННЯ ПРОЦЕСУ ЕКСТРУЗІЇ ТЕРМОЕЛЕКТРИЧНОГО МАТЕРІАЛУ НА ОСНОВІ *Bi-Te* ПРЯМОКУТНОЇ ФОРМИ

Процес гарячої екструзії являє собою проходження розігрітого до температури нижче температури плавлення термоелектричного матеріалу через прес-форму (філь'єру) під дією тиску. В даній роботі проведено моделювання цього процесу з використанням пакету прикладних програм об'єктно-орієнтованого моделювання Comsol Multiphysics. В даній моделі екструдованих матеріал представляється як рідина з дуже високою в'язкість, яка залежить від швидкості та температури. В результаті моделювання було отримано розподіли температури й швидкості течії матеріалу в матриці, а також розподіл напруг у матриці за рахунок зовнішнього тиску і теплових навантажень в процесі стрічкової екструзії. Дані дослідження дають змогу оптимізувати установку для одержання екструдованого термоелектричного матеріалу. Бібл. 4. рис. 6, табл. 2.

Ключові слова: термоелектричний матеріал, гаряча екструзія, комп'ютерне моделювання, філь'єра.

Рыбчаков Д.Е.

Институт термоэлектричества НАН и МОН Украины,
ул. Науки, 1, Черновцы, 58029, Украина,
e–mail: anatych@gmail.com

КОМПЬЮТЕРНОЕ МОДЕЛИРОВАНИЕ ПРОЦЕССА ЭКСТРУЗИИ ТЕРМОЭЛЕКТРИЧЕСКИХ МАТЕРИАЛОВ ПРЯМОУГОЛЬНОЙ ФОРМЫ НА ОСНОВЕ *Bi-Te*

Процесс горячей экструзии представляет собой прохождение разогретого до температуры ниже температуры плавления термоэлектрического материала через пресс-форму (фильеру) под действием давления. В данной работе проведено моделирование этого процесса с использованием пакета прикладных программ объектно-ориентированного моделирования Comsol Multiphysics. В данной модели экструдированный материал представляется как жидкость с очень высокой вязкостью, которая зависит от скорости и температуры. В результате моделирования было получено распределения температуры и скорости течения материала в матрице, а также распределение напряжений в матрице за счет внешнего давления и тепловых нагрузок в процессе ленточной экструзии. Данные исследования позволяют оптимизировать установку для получения экструдированного термоэлектрического материала. Библ. 4, рис. 6, табл. 2.

Ключевые слова: термоэлектрический материал, горячая экструзия, компьютерное моделирование, фильеры.

References

1. Goltsman B.M. Semiconductor thermoelectric materials based on bismuth telluride (Bi_2Te_3) / B.M. Goltsman, V.A. Kudinov, I.A Smirnov. - Moscow: Science. - 1972. - 320 p. (In Russian)

2. Sabo E.P. Tekhnology of chalcogenide thermoelements. Physical fundamentals / E.P. Sabo // J. Thermoelectricity. – 2006. – No. 1. – P. 45 - 66.

3. Gorskiy P.V About the principles of the development of thermoelectric composites in lightweight thermoelectric materials and inheritance from it / P.V. Gorskiy. // J. Thermoelectricity. – 2020. – No. 1. – P. 27-37.

4. Fluid-Structure Interaction in Aluminum Extrusion // Structural Mechanics Module Model Library. - COMSOL AB. - 2008. - p. 301-316.

V.G. Kolobrodov, *doc. techn. sciences, professor*
V.I. Mykytenko, *doc. techn. sciences, assistant professor*
G.S. Tymchyk, *doc. techn. sciences, professor*
Sokol B.V.

National Technical University of Ukraine
"Igor Sikorsky Kyiv Polytechnic Institute"
37 Peremohy Ave., Kyiv, 03056, Ukraine
e-mail: deanpb@kpi.ua

TEMPERATURE RESOLUTION OF COMPUTER-INTEGRATED POLARIZATION THERMAL IMAGER

The work is devoted to the development of a method for determining the energy (temperature) resolution of a polarization thermal imager, which contains a linear polarizer and a phase plate. For this purpose it is proposed to use the noise equivalent temperature difference (NETD). A physico-mathematical model of an optoelectronic system of the polarization thermal imager has been developed, which allows one to calculate its signal transmission function. Based on this function, a method for calculating NETD has been developed. The formula describing functional dependence of a polarization thermal imager temperature resolution on the angular orientation of the polarizer relative to the optical axis of the phase plate at a given degree of polarization is obtained. A study of the impact of a test object radiation degree of polarization on the polarization thermal imager temperature resolution was performed. Bibl. 8, Fig. 7, Tabl. 1.

Key words: polarization thermal imager, energy resolution, noise equivalent temperature difference, degree of polarization

Introduction

Polarization is one of the four parameters of the electromagnetic field of radiation, and the other three are intensity, wavelength and coherence [1,2]. Polarimetry measures the vector nature of the radiation and provides important information about the surface orientation of the object, its shape and surface quality. The polarization properties of radiation from objects of observation differ from the background radiation and are not correlated with their intensity and spectrum. As a rule, the radiation from the object is partially polarized, and from the background - natural [3, 4]. Thus, polarimetric images are very useful for magnifying the signal from an object and suppressing background noise.

The main characteristics of polarized radiation are intensity, degree of polarization, ellipticity and polarization angle [5,6]. To measure these characteristics in the infrared (IR) region of the spectrum, polarization thermal imagers (PT) are used [7, 8]. The main characteristics of any thermal imager used to study thermoelectric phenomena and devices are energy (temperature), spatial and temporal resolution, which depend on the transmittance of its optical system, the sensitivity of the

radiation detector and the characteristics of the electronic video signal processing system [9 – 11]. There are a significant number of standards, monographs and articles devoted to modeling, calculation and measurement of the thermal resolution of thermal imagers, by which we mean the minimum radiation contrast between the object and the background that a thermal imager can detect [12 – 14]. At the same time, there is practically no scientific and technical information on methods for calculating the temperature resolution of a PT.

Formulation of the problem

The purpose of this paper is to develop and study a method for determining the temperature (energy) resolution of a polarization thermal imager.

Model of a polarization thermal imager

A polarization thermal imager can be viewed as a linear system that converts the brightness of the observation plane from the IR region of the spectrum to the brightness of the image of the object and background on the display screen in the visible region of the spectrum. The process of such a transformation can be investigated using the generalized scheme of the system "object of observation - atmosphere – thermal imager - observer" [12, 13].

Radiation (intrinsic or reflected) from the object of observation and the background passes through the atmosphere and enters the optical system of the thermal imager, which forms an image of the object and the background in the plane of the matrix radiation detector (MRD). The radiation detector converts the radiation stream, which forms an image, into an electrical video signal, which, after amplification, goes to analog and digital processing devices. After the necessary transformations, the video signal goes to the display, on the screen of which a visible analogue of the object and the background is formed, is perceived by the observer.

Consider the opto-electronic system of PT, which consists of an optical system and MRD (Fig. 1). The optical system, in turn, consists of an IR polarizer, a quarter-wave retarder, and an IR thermal imager lens arranged in series on the optical axis.

One of important characteristics of thermal imager is signal transfer function (*SiTF*) $u_s(L_t)$ – the dependence of the electrical signal at the output of the electronic unit of the thermal imager on the brightness of the object of observation. To obtain functional dependence $u_s(L_t)$, we will consider Fig. 1. Let the observation object have a spectral brightness uniform over the area $L_t(\lambda)$, and its angular dimensions $\zeta_{tx} \times \zeta_{ty}$ significantly exceed the instantaneous field of view of the thermal imager, which is located at a distance R from the observation object. We assume that the surface of the object and the background radiates according to Lambert's law.

Then the spectral brightness of the object surface is determined by the formula as

$$L_t(\lambda) = \frac{1}{\pi}\varepsilon_t(\lambda)M_\lambda(\lambda, T_t),$$

(1)

where $\varepsilon_t(\lambda)$ is the spectral coefficient of radiation of the object surface; $M_\lambda(\lambda, T_t)$ is Planck's function. If the normal to the surface of the object is placed at an angle φ to the optical axis of observation, then the input pupil of the lens receives a spectral flux of radiation

$$\Phi_\lambda(\lambda) = \tau_A(\lambda, R) L_{\lambda_t}(\lambda) \Omega_o A_t \cos \varphi, \tag{2}$$

where $\tau_A(\lambda)$ is spectral transmittance of the atmosphere; A_t is the area of the object within the instantaneous field of view of the thermal imager; $\Omega_0 = A_p/R^2$ is body angle within which the radiation from the object reaches the entrance pupil of the lens area A_p.
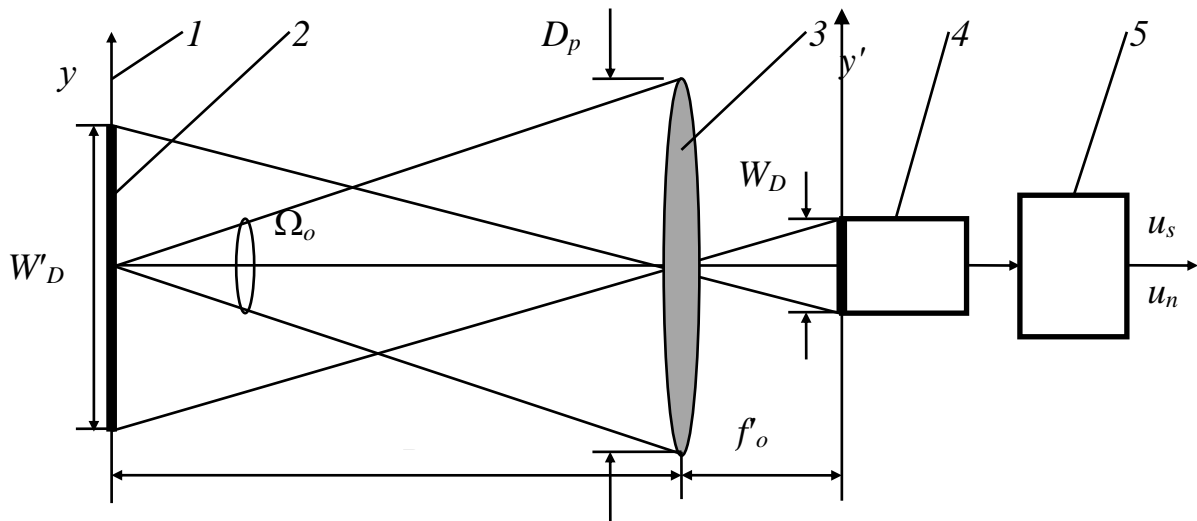
Fig. 1. To calculation of transmission function of thermal imager signal:
1 – the plane of the radiation object; 2 – instantaneous linear field of view;
3 – optical system; 4 – MRD; 5 – video amplifier

The signal at the output of MRD with spectral sensitivity $R_D(\lambda)$ will be equal to

$$u_s = \int_\lambda^{\lambda_2} \Phi_\lambda(\lambda) \tau_o(\lambda) R_D(\lambda) d\lambda = A_t \frac{A_p}{R^2} \cos \varphi \int_\lambda^{\lambda_2} \tau_A(\lambda) L_{\lambda t}(\lambda) \tau_o(\lambda) R_D(\lambda) d\lambda. \tag{3}$$

When measuring the SiTF function, it is assumed that the test object is located at a short distance from the thermal imager, i.e. $\tau_A(\lambda) \approx 1$, and the spectral transmittance of the optical system within the operating spectral range has an average value τ_0. Then the function *SiTF* (3) of the thermal imager taking into account the gain of the electronic unit C_{EI} and the relationships $A_p = \pi D_p^2/4$ i $A_t/R^2 = A_D/f_o'^2$, following from Fig.1, will be given by

$$u_s(L_t) = \frac{\pi}{4} C_{EI} A_D \left(\frac{D_p}{f_o}\right)^2 \tau_o \cos\varphi \int_{\lambda_1}^{\lambda_2} L_t(\lambda) R_D(\lambda) d\lambda. \tag{4}$$

The function $u_s(L_t)$, has a complex form, which depends, first of all, on the working spectral range and spectral sensitivity of MRD, which makes it difficult to measure the true brightness of the object. Formula (4) does not take into account the spectral composition of the electrical signal, which is determined by the readout system. In addition, the magnitude of the signal u_s is influenced by the gain C_{EI} and noise of the system.

As can be seen from formulae (1) – (4), the value of thermal imager signal $u_s(x',y')$, at the output of MRD is a function of absolute temperature T_t of the object surface and its spectral radiation coefficient $E_t(\lambda,T)$. Moreover, video signal $u_s(x',y')$ depends on spectral transmittance of the atmosphere $\tau_A(\lambda,R)$, the characteristics of optimal system D_p, f_o', τ_o and MRD $R_D(\lambda)$, $\lambda_1, \dots \lambda_2$, A_D, as well as on the modulation transfer functions of separate elements of optoelectronic system of the thermal imager.

Determination of temperature resolution of PT

As the temperature resolution of PT, we will use classical parameter which is called *NETD* (Noise Equivalent Temperature Difference). The *NETD* parameter is understood as the temperature difference between the standard test object and the background, emitting as the absolutely black body, whereby the ratio of the peak signal value at the output of the standard reference filter of the thermal imager which considers the test object, to the noise is equal to unity [15,16]. The test must have angular dimensions that are several times the angular size of the sensitive area of the MRD pixel $\alpha_D \times \beta_D$, in order to eliminate the effect of spatial resolution on the measurement results.

To obtain formulae for the calculation of $NETD$, consider the signal transmission function of the thermal imager (4). Additionally, we make a number of assumptions:

1. The test object is located at a short distance from the thermal imager. Then we can assume that the radiation is little absorbed during passage through the atmosphere, i.e. in the operating spectral range $\tau_A(\lambda) \approx 1$.
2. The electronic system of the thermal imager has an effective noise bandwidth Δf.
3. A large test object is placed on a uniform background and has a temperature contrast ΔT. The test object and background emit as a blackbody.

Since the object is always in the background, a red (informative) signal appears when there is a temperature contrast between the object and the background, that is

$$u_s = u_{st} - u_{sb}, \tag{5}$$

where u_{st} and u_{sb} are signals formed by the object and background, respectively.

If the object and background radiate according to Lambert's law, then formula (5), taking into

account (4), provided that the gain $C_{El} = 1$, can be represented as

$$
u_s = \frac{1}{\pi} A_t \frac{A_p}{R^2} \tau_o \int_{\lambda_1}^{\lambda_2} R_D(\lambda)[M_\lambda(\lambda, T_b + \Delta T) - M_\lambda(\lambda, T_b)]d\lambda =
$$

$$
= \frac{1}{\pi} A_t \frac{A_p}{R^2} \tau_o \cdot \Delta T \int_{\lambda_1}^{\lambda_2} R_D(\lambda) \frac{\partial M_\lambda(\lambda, T_b)}{\partial T} d\lambda, \tag{6}
$$

where τ_o is the average transmittance of the optical system.

The spectral sensitivity of MRD can be expressed in terms of the specific detective ability $D^*(\lambda)$ according to formula [13]

$$
R_D(\lambda) = D^*(\lambda) \frac{u_n}{\sqrt{A_D \Delta f}}, \tag{7}
$$

where A_D and u_n are area and noise signal of MRD pixel, respectively.

Substituting (7) into (6), we find the signal-noise ratio at the output of the reference filter

$$
SNR = \frac{u_s}{u_n} = \frac{1}{\pi} A_t \tau_o \frac{A_o}{R^2} \frac{\Delta T}{\sqrt{A_D \Delta f}} \int_{\lambda_1}^{\lambda_2} D * (\lambda) \frac{\partial M_\lambda(\lambda, T_b)}{\partial T} d\lambda. \tag{8}
$$

We find the formula for calculating *NETD* from (8), assuming that $SNR = 1$. Then

$$
NETD = \Delta T = \frac{\pi R^2 \sqrt{A_D \Delta f}}{A_t \tau_o A_p \int_{\lambda_1}^{\lambda_2} D*(\lambda) \frac{\partial M_\lambda(\lambda, T_b)}{\partial T} d\lambda}. \tag{9}
$$

The resulting formula is most general for calculating *NETD*. We present Eq.(9) in another form, using Fig. 1. It is obvious that $A_p = \pi D_p^2/4$ i $A_t/R^2 = A_D/f_o'^2$. Then

$$
NETD = \frac{4k_o^2}{\tau_o \int_{\lambda_1}^{\lambda_2} D*(\lambda) \frac{\partial M_\lambda(\lambda, T_b)}{\partial T} d\lambda} \sqrt{\frac{\Delta f}{A_D}}, \tag{10}
$$

where $k_o = f_o'/D_p$ is lens aperture number.

Using relation (10), we define the following ways to reduce the *NETD* parameter:

1. Use fast lenses with a small aperture number $k_o = f_o'/D_p$ and high transmittance τ_o. This is the most efficient way, because $NETD \sim k_o^2$.

2. Use MRD with a high specific detective ability $D^*(\lambda)$.

3. Reduction of effective noise band Δf of reference filter. However, to obtain a high spatial resolution, this band should be increased [15]. Therefore, Δf is chosen from a compromise between spatial and temperature resolutions.

The obtained formula (10) for energy resolution is valid for the case when the thermal imager converts the brightness of the object of observation from the IR region of the spectrum into its image on the display screen in the visible region of the spectrum. In other words, in a classical thermal imager there is a transformation of radiation intensity. A polarization thermal imager records the polarization characteristics of the object and background by changing the angular orientation of the polarizer and phase plate in the optical system. The transmittance τ_0 of the optical system of PT with such a change in the angular orientation will be different, which according to formula (10) will lead to different values of the energy resolution of the thermal imager.

The paper [16] investigates the method of calculating the energy transmittance of the optical system of polarization thermal imager for partially polarized radiation depending on the angular orientation of the polarizer and the phase plate. In the PT, the characteristics of the polarization image are determined using the Stokes parameters, which are measured for angles α between the transmission plane of the polarizer and the optical axis of a quarter-wave retarder equal to 0°, 90°, 45°, and 135°.

The results of these studies testify that the normalized transmittance of the optical system of PT $\tau_{os,n} = \tau_{os} / \tau_p \tau_{hp} \tau_o$, where τ_p, τ_{hp} and τ_o are transmittances caused by the Fresnel losses on the input and output surfaces of optical elements and the absorption in the optical medium of the polarizer and the phase plate, respectively; τ_o are transmittances of IR lens:

1. For natural radiation, the transmittance does not depend on the angular orientation of the phase plate and is equal to 0.5.

2. For partially polarized radiation, the transmittance depends on the angle α. For angles α equal to 0º, 90º, 45º and 135º, the normalized transmittance τ_{-} (os, n) for the degree of polarization 0.5 is equal to 0.75, 0.25, 0.5 and 0.5, respectively. This feature of the optical system of PT will be taken into account when calculating the temperature resolution of the thermal imager.

Method of calculating the temperature resolution of PT

An important step in determining is the selection of a test object that should be used in the calculations and measurements of the temperature resolution of the PT. In this case, one should take into account:

1. Polarization characteristics of the object of observation: intensity, degree of polarization and polarization angle.
2. Energy parameters of the object of observation (test object) and background, which are determined by temperature, radiation and reflection coefficients of the object and the background.
3. Orientation of the test object surface and background relative to the optical surface of the

thermal imager.

Taking these features into account requires a detailed study that goes beyond this article. The research will be based on NATO standard 4347 for ground forces "Determination of nominal characteristics of static range for infrared surveillance systems" [17].

Therefore, in this paper, in the formula of energy resolution of classical thermal imagers (10) we will additionally take into account the following:

1. Test object and background parameters:

   1.1. The surfaces of the object and background have a uniform distribution of temperature T_t and T_b, radiation coefficients ε_t and ε_b and reflection coefficients R_t and R_b. The background temperature $T_b = 288$ K.

   1.2. The degree of polarization of radiation from the test object is P_t, and from the background $P_b = 0$.

2. The transmittance of the optical system $\tau_{os}(\alpha) = \tau_{os,n}(\alpha)(\tau_p\tau_{hp}\tau_o)$ depends on the angular orientation α of the polarizer relative to the optical axis of the phase plate.

3. Radiation detector – microbolometric matrix (MBM), which has temperature sensitivity $NETD_D$, format $p_D \times q_D$, pixel size $V_D \times W_D$, frame frequency f_f.

The specific detective ability D^*_{th} of the thermal radiation detector, such as MBM, does not depend on the radiation wavelength, and, therefore, in formula (10) it can be factored outside the integral. To determine $NETD$ as MBM parameter in formula (10), it is assumed that [18]:

   – aperture number of the optical system $k_0 = 1$;

   – effective noise band $\Delta f = 1/(2t_i)$, where t_i is matrix integration time, which may be equal to the pixel time constant t_D.

In the case of such assumptions, the MBM parameter $NETD_D$ is calculated by the formula

$$NETD_D = \frac{4}{\sqrt{2A_D t_i} \cdot D^*_{th} \int_{\lambda_1}^{\lambda_2} \frac{\partial M_\lambda(\lambda, T_{th})}{\partial T} d\lambda}, \tag{11}$$

where T_{th} is the temperature of the test object whereby the parameter $NETD_D$ is determined.

From formula (11) we find the specific detective ability D^*_{th} and substitute it to (10)

$$NETD = NETD_D \frac{k_o^2}{\tau_{os}(\alpha)\varepsilon_t} k_D(T_{th}, T_b), \tag{12}$$

where $k_D(T_{th}, T_b)$ is a coefficient which takes into account the difference of the differential luminosity of the surface of the test object at temperature T_{th} whereby the specific detective ability of MBM was measured, from the real background temperature T_b when testing PT,

$$k_D(T_{th}, T_b) = \frac{\int_{\lambda_1}^{\lambda_2} \frac{\partial M_\lambda(\lambda, T_{th})}{\partial T} d\lambda}{\int_{\lambda_1}^{\lambda_2} \frac{\partial M_\lambda(\lambda, T_b)}{\partial T} d\lambda}. \tag{13}$$

Formula (12) is valid, provided that radiation coefficients of the test object ε_t and background ε_b have close values, i.e. $\varepsilon_t \approx \varepsilon_b$. The effect of degree of polarization P of partially polarized light from the test object is taken into account in the transmittance $\tau_{os}(\alpha)$ of the optical system of PT. In [16], it was established that the transmittance $\tau_{os}(\alpha)$ is determined by the function:

$$\tau_{os}(\alpha) = \tau_p \tau_{hp} \tau_o \left[\frac{1}{2}(1 - P) + P\cos^2\alpha \right]. \tag{14}$$

Thus, the resulting formula (12) allows calculating the energy resolution of the polarization thermal imager.

Example of calculating the temperature resolution of PT

Consider an example of calculating the temperature resolution of PT under the following conditions:

1. Test object parameters:

- Background temperature $T_b = 288$ K.
- Temperature contrast $\Delta T = 2$ K .
- Radiation coefficient of test object surface $\varepsilon_t = 1$.
- Angular position of the normal to the surface relative to observation axis $\varphi = 85\,°$
- Degree of polarization $P = 0.5$.
- Polarization angle $\Psi = 0\,°$.

2. Integral transmittance of the atmosphere in the spectral range $\lambda_1 \ldots \lambda_2 = 8$ μm $\tau_A = 1$.

3. Optical system parameters:

- Input pupil diameter and infrared lens focal length – $D_p = 50$ mm and $f_0 = 50$ mm.

Input pupil diameter and IR lens focal length

- Integral transmittances of individual elements of optical system:
  - polarizer $\tau_p = 0.9$;
  - phase plate $\tau_{hp} = 0.9$;
  - IR lens $\tau_0 = 0.85$.

4. Parameters of radiation detector – microbolometric matrix GWIR 0304X2A, which has parameters:

- * Working spectral range $\lambda_1 \ldots \lambda_2 = 8 \ldots 14$ μm.
- Temperature sensitivity $NETD_D = 0.05$ K
- Matrix format $p_D \times q_D = 640 \times 512$ pixel.
- Pixel size $V_D \times W_D = 17 \times 17$ μm.
- Frame frequency $f_f = 50$ Hz.

To calculate the temperature separation of PT, we use formula (12), in which, according to the condition of the example, we know:

1. Noise equivalent temperature difference of MBM $NETD_D = 0.05$ K.

- Radiation coefficient of test object surface $\varepsilon_t = 1$.
2. Aperture number of the optical system $k_0 = D_p / f_0 = 1$.

Coefficient of MBM $k_D(T_{th}, T_b)$ for the temperatures $T_{th} = 300$ K and $T_b = 288$ K will be calculated by the formula (13) [13]:

$$k_D(T_{th}, T_b) = \frac{\int_8^{14} \frac{\partial M_\lambda(\lambda, 300)}{\partial T} d\lambda}{\int_8^{14} \frac{\partial M_\lambda(\lambda, 288)}{\partial T} d\lambda} = \frac{232 \frac{\text{мкВт}}{\text{см}^2 K}}{263 \frac{\text{мкВт}}{\text{см}^2 K}} = 0{,}88 \ \mu W$$

Determination of the transmittance of the optical system of PT depending on the angular orientation α of the polarizer relative to the optical axis of the phase plate is investigated in detail in [16]. For partially polarized radiation, the transmittance depends on the angle α. For angles α equal to 0º, 90º, 45º and 135º, the normalized transmittance $\tau_{os,n}$ for the degree of polarization $P = 0.5$ is equal to 0.75, 0.25, 0.5 and 0.5, respectively. This feature of the optical system of PT will be taken into account when calculating the temperature resolution of the thermal imager.

Let us substitute the above parameters of PT into formula (12) and calculate the temperature resolution for different values of angle α:

$$NETD(\alpha = 0°) = 0{,}05 \cdot \frac{1}{0{,}9 \cdot 0{,}9 \cdot 0{,}85 \cdot 0{,}75 \cdot 1} 0{,}88 = 0{,}085 \ K;$$

$$NETD(\alpha = 90°) = 0{,}26 \ K; \ NETD(\alpha = 45°) = 0{,}13 \ K; \ NETD(\alpha = 135°) = 0{,}13 \ K$$

Let us establish the dependence of the temperature resolution of PT on the degree of polarization P of partially polarized radiation, which affects the transmittance $\tau_{os}(P)$ of the optical system of the thermal imager. In [16], it was found that for angles α = 45◦ and 135◦ the normalized transmittance does not depend on the degree of polarization and is equal to $\tau_{os}(P) = 0.5$. For the angles α = 0◦ and 90◦ we have, respectively:

$$\tau_{os}(P, \alpha = 0°) = \frac{1}{2} \tau_p \tau_{hp} \tau_o (1 + P); \tag{15}$$

$$\tau_{os}(P, \alpha = 90°) = \frac{1}{2} \tau_p \tau_{hp} \tau_o (1 - P). \tag{16}$$

After substituting (15) and (16) into equation (12), we obtain the dependence of the temperature resolution of the PT on the degree of polarization of the radiation of the test object. The graph of this dependence for the previously selected parameters of the thermal imager is shown in Fig. 1.

$$NETD(P, \alpha = 0°) = NETD_D \frac{2k_o^2}{\tau_p \tau_{ph} \tau_o (1+P)\varepsilon_t} k_D(T_{th}, T_b); \qquad (17)$$

$$NETD(P, \alpha = 90°) = NETD_D \frac{2k_o^2}{\tau_p \tau_{ph} \tau_o (1-P)\varepsilon_t} k_D(T_{th}, T_b). \qquad (18)$$

It was also important to establish the dependence of the temperature resolution of the PT for an arbitrary angle α of orientation of the phase plate relative to the transmission plane of the polarizer. In [16], the dependence of the transmittance of the optical system on the angle α and degree of polarization *P* was obtained:

$$\tau_{os}(\alpha, P) = \tau_p \tau_{hp} \tau_o [0,5(1-P) + P \cos^2 \alpha]. \qquad (19)$$

On substituting (19) into Eq. (12) we obtain a dependence of the temperature resolution of the PT on the angular orientation α of the polarizer with respect to the optical axis of the phase plate with a given degree of polarization *P*.

$$NETD(\alpha, P) = NETD_D \frac{1}{0,9 \cdot 0,9 \cdot 0,85 \cdot [0,5(1-P) + P \cos^2 \alpha]} 0,88. \qquad (20)$$

The plots of this dependence for the previously selected parameters of the thermal imager are given in Fig. 2 and 3.
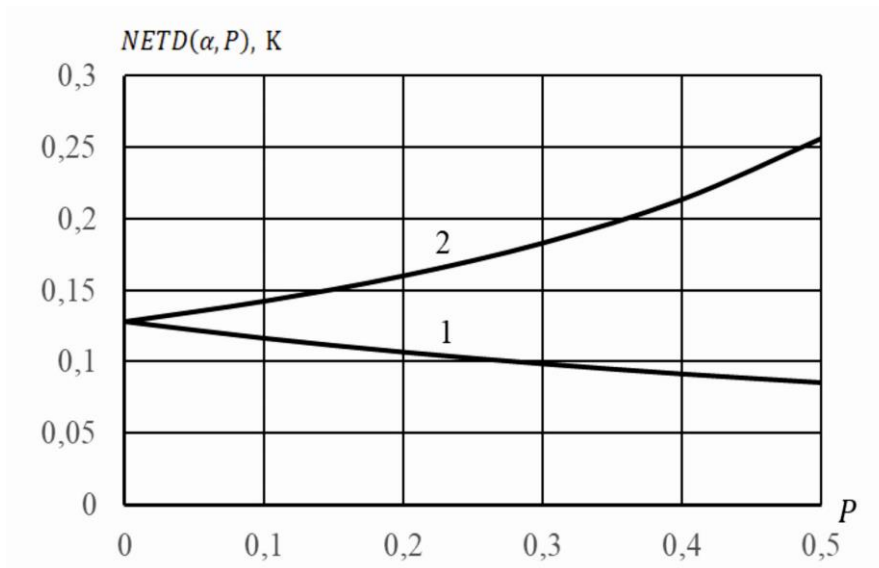
Fig. 2. Dependence of the temperature resolution of the polarization thermal imager on the degree of polarization P of test object radiation for the angular orientation α of the polarizer relative to the optical axis of the phase plate which is equal to: 1 – 0°; 2 – 90°
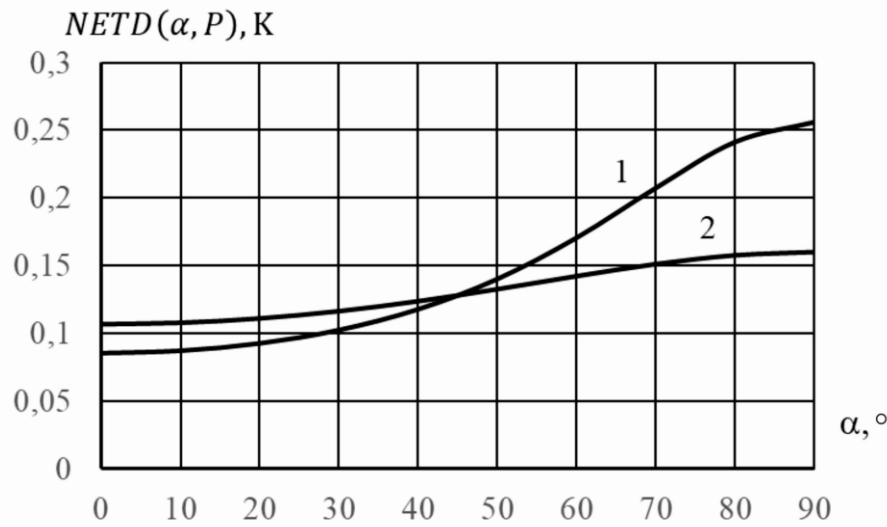
Fig. 3. Dependence of temperature resolution of the polarization
thermal imager on the angular orientation α of the polarizer relative
to optical axis of the phase plate for the degree
of polarization: 1 – P = 0.5; 2 – P = 0.2.

Analysis of the obtained theoretical simulation results allows for the following conclusions:

1. As the degree of polarization P increases, the temperature resolution of the PT for the radiation component that is polarized in the observation plane ($α = 0°$) decreases, and for the perpendicular component ($α = 90°$) it increases.

2. For nonpolarized radiation ($P = 0$), the transmittance of the optical system does not depend on the angle α, so the temperature resolution remains unchanged at arbitrary orientation of the polarizer relative to the axis of the phase plate.

3. For fully polarized radiation ($P = 1$), the temperature resolution depends on the angle α and varies according to the law $NETD$ ($α$, $P = 1$) $\sim cos^{-2}α$. If $α = 0°$, then the PT has the lowest temperature resolution.

4. If the optical axis of the phase plate forms an angle $α = 45°$ with the plane of the polarizer, then the temperature resolution of the PT does not depend on the degree of polarization P and is equal to 0.13 K.

Conclusions

The proposed physics-mathematical model of the optoelectronic system of a polarization thermal imager, which consists of a polarizer, a quarter-wave retarder and a lens arranged in series on the optical axis, allowed developing a method for determining the temperature (energy) resolution of the thermal imager. The study of this method made it possible to:

1. Obtain an equation for the thermal imager signal transmission function which was used to determine the temperature resolution of the thermal imager.

2. As a temperature resolution of polarization thermal imager it is proposed to use a classical parameter – the noise equivalent temperature difference *NETD* and NATO standard 4347 [17-19].

3. Obtain an equation for calculating the *NETD* parameter, which takes into account the dependence of the transmittance of the optical system on the angular orientation of the polarizer and the phase plate. A study of this equation showed that

3.1. The polarization thermal imager records the polarization characteristics of the test object and the background by changing the angular orientation of the polarizer and the phase plate in the optical system. The transmittance τ_0 of the optical system of PT with such a change in angular orientation will be different, which leads to different values of the temperature resolution of the thermal imager [19].

3.2. The temperature resolution depends on the degree of polarization of the studied radiation. For unpolarized radiation the temperature resolution remains unchanged at an arbitrary orientation of the polarizer relative to the axis of the phase plate.

3.3. The lowest temperature resolution will be in the case when the optical axis of the phase plate forms and angle $\alpha = 0°$ with the plane of the polarizer.

The obtained results must be taken into account when developing an electronic system for processing video signals from a matrix radiation detector. In further research, it is also important to develop a model of a test object with specified polarization characteristics of IR radiation such as the degree, ellipticity and azimuth of polarization.

References

1. Goldstein D.H. (2011). *Polarized light*. 3d ed. London - New York: CRC Press.
2. Born M.,Wolf E. (2002). *Principles of optics*, 7th ed. Cambridge University.
3. Yanga Bin, Wub Taixia, Chenc Wei, Lic Yanfei, Knjazihhind Juri, Asundie Anand, Yan Lei (2017). Polarization remote sensing physical mechanism, key methods
1. and application. *The International Archives of the Photogrammetry, Remote Sensing and Spatial Information Sciences.* Vol. XLII-2/W7, Wuhan, China.
4. Zhang Y., Shi Z.G., Qiu T.W. (2017). Infrared small target detection method based on decomposition of polarization information. *J.of Electronic Imaging*, T 33004, №1.
5. *Fizicheskii entsyklopedicheskii slovar' [Physical encyclopedic dictionary]* (1984). A.M.Prokhorov (Ed.). Moscow: Soviet Encyclopedia [in Russian].
6. Vollmer M., Karstadt S., Mollman K.-P., Pinno F. (2001). Identification and suppression of thermal imaging. *InfraMation Proceedings*. University of Applied Sciences, Brandenburg (Germany). ITC 104 A.
7. Zhao Yongqiang, Yi Chen, Kong Seong G., Pan Quan, Cheng Yongmei (2016). *Multi-band polarization imaging and applications*. National Defense Industry Press, Beijing and Springer-Verlag Berlin Heidelberg.
8. Gurton K.P., Yuffa A.J., Videen G.W. (2014). Enhanced facial recognition for thermal imagery

using polarimetric imaging. *Optical Society of America*, 39(13), 3857–3859.

9. Sivukhin D.V. (2004). *Obshchii kurs fiziki [General physics course]*. 4th ed. Moscow: MFTI [in Russian].

10. Anatychuk L.I., Vikhor L.M., Kotsur M.P., Kobylianskyi R.R., Kadenyuk T.Ya. (2016). Optimal control of time dependence of cooling temperature in thermoelectric devices. *J.Thermoelectricity*, 5, 5-11.

11. Kolobrodov V.H., Mykytenko V.I., Tymchyk H.S. (2020) Poliaryzatsiina model teplokontrastnykh obiektiv sposterezhennia [Polarization model of heat-contrast objects of observation]. *J.Thermoelectricity*, 1, 36-52.

12. Vollmer Michael, Mollman Klaus-Peter (2018). *Infrared thermal imaging. fundamentals, research and applications. 2nd ed.* Weinheim: Wiley – VCH.

13. Kolobrodov V.G., Lykholit M.I. (2007). *Proektuvannia teploviziinykh i televiziinykh system sposterezhennia [Design of thermal imaging and television surveillance systems]*. Kyiv: KPI [in Ukrainian].

14. Chrzanowski K. (2010). *Testing thermal imagers. Practical guidebook*. Military University of Technology, 00-908 Warsaw, Poland.

15. Lloyd G. (1978). *Thermal imaging systems*. Moscow: Mir [Russian transl].

16. Kolobrodov V.G. (2020). Determination of transmittance of optical system of polarizing thermal imager. *Visnyk NTUU KPI Seriia – Radiotekhnika Radioaparatobuduvannia*, 78, 78–85.

17. NATO Military Agency for standardization (1995). *Definition of nominal static range performance for thermal imaging systems.*

18. Khrebtov I.A., Maliarov V.G. (1997). Neokhlazhdaiemyie teplovyie metrichnye priiomniki IK izlucheniia [Uncooled thermal array IR detectors]. *Soviet Journal of Optical Technology*, 6, 3–17 [in Russian].

19. Tymchik G.S., Kolobrodov V. H., Kolobrodov M. S., Vasyura Anatoliy S., Komada Paweł, Azeshova Zhanar. (2018). The output signal of a digital optoelectronic processor. *Proc. SPIE 10808, Photonics Applications in Astronomy, Communications, Industry, and High-Energy Physics Experiments* 2018, 108080W (1 October 2018).

Колобродов В.Г., *докт. техн. наук, професор*
Микитенко В.І., *докт. техн. наук, доцент*
Тимчик Г.С. *докт. техн. наук, професор*
Сокол Б.В.

Національний технічний університет України
«Київський політехнічний інститут імені Ігоря Сікорського»
проспект Перемоги, 37, Київ, 03056, Україна
e-mail: deanpb@kpi.ua

ТЕМПЕРАТУРНЕ РОЗДІЛЕННЯ КОМП'ЮТЕРНО-ІНТЕГРОВАНОГО ПОЛЯРИЗАЦІЙНОГО ТЕПЛОВІЗОРА

Робота присвячена розробці методу визначення енергетичного (температурного) розділення поляризаційного тепловізора. Запропоновано використовувати для цього величину еквівалентної шуму різниці температур NETD (Noise Equivalent Temperature Difference). Розроблено фізико-математичну модель оптико-електронної системи поляризаційного тепловізора, яка дозволяє обраховувати її функцію передачі сигналу. На основі цієї функції розроблено методику обчислення NETD. Отримано формулу, що описує функціональну залежність температурного розділення поляризаційного тепловізора від кутової орієнтації поляризатора відносно оптичної осі фазової пластини при заданому ступені поляризації. Виконано дослідження впливу ступеня поляризації випромінювання тест-об'єкта на температурне розділення поляризаційного тепловізора, який містить лінійний поляризатор і фазову пластину. Бібл. 8, рис. 7, табл. 1.

Ключові слова: *поляризаційний тепловізор, енергетичне розділення, еквівалентна шуму різниця температур, ступень поляризації*

Колобродов В.Г., *докт. техн. наук, профессор*
Мыкытенко В.И., *докт. техн. наук, доцент*
Тымчык Г.С., *докт. техн. наук, профессор*
Сокол Б.В.

Национальный технический университет Украины
"Киевский политехнический
институт имени Игоря Сикорского», проспект Победы,
37, Киев, 03056, Украина, *e-mail: deanpb@kpi.ua*

ТЕМПЕРАТУРНОЕ РАЗДЕЛЕНИЕ КОМПЬЮТЕРНО-ИНТЕГРИРОВАННЫХ ПОЛЯРИЗАЦИОННЫХ ТЕПЛОВИЗОРОВ

В статье предложена поляризационная модель тепловизора с целью его применения при исследовании термоэлектрических явлений и устройств, позволяет повысить эффективность работы таких устройств. Для исследования и проектирования таких тепловизоров рассмотрена физико-математическая модель поляризации излучения от объектов наблюдения, которая учитывает поляризационные свойства собственного теплового излучения и отраженного внешнего излучения. Разработанная модель была применена для определения поляризационных свойств излучения плоской железной пластины. Анализ полученных результатов свидетельствует о том, что для теплового излучения при углах наблюдения $\psi < 40°$, составляющие коэффициента излучения почти одинаковы $\varepsilon_{//} \approx \varepsilon_{\perp} \approx 0.16$, но $\varepsilon_{//} < \varepsilon_{\perp}$. С увеличением угла наблюдения $\psi > 40°$ перпендикулярная поляризационная компонента $\varepsilon_{\perp}$ монотонно уменьшается до нуля, а параллельная компонента $\varepsilon_{//}$ увеличивается и достигает максимального значения при угле $\psi = 84°$, а затем уменьшается до нуля. Степень поляризации излучения возрастает с увеличением угла ψ и при угле $\psi = 84°$ равна 0.96. Полученные результаты исследований целесообразно использовать при разработке модели термоэлектриков, которая может использоваться при проектировании поляризационного тепловизора. Библ. 8, рис. 7, табл. 1.

Ключевые слова: Поляризационный тепловизор, температурное разделение, частично поляризованное излучение, степень поляризации.

References

1. Goldstein D.H. (2011). *Polarized light*. 3d ed. London - New York: CRC Press.

2. Born M.,Wolf E. (2002). *Principles of optics*, 7th ed. Cambridge University.

3. Yanga Bin, Wub Taixia, Chenc Wei, Lic Yanfei, Knjazihhind Juri, Asundie Anand, Yan Lei (2017). Polarization remote sensing physical mechanism, key methods and application. *The International Archives of the Photogrammetry, Remote Sensing and Spatial Information Sciences.* Vol. XLII-2/W7, Wuhan, China.

4. Zhang Y., Shi Z.G., Qiu T.W. (2017). Infrared small target detection method based on decomposition of polarization information. *J.of Electronic Imaging*, T 33004, №1.

5. *Fizicheskii entsyklopedicheskii slovar' [Physical encyclopedic dictionary]* (1984). A.M.Prokhorov (Ed.). Moscow: Soviet Encyclopedia [in Russian].

6. Vollmer M., Karstadt S., Mollman K.-P., Pinno F. (2001). Identification and suppression of thermal imaging. *InfraMation Proceedings*. University of Applied Sciences, Brandenburg (Germany). ITC 104 A.

7. Zhao Yongqiang, Yi Chen, Kong Seong G., Pan Quan, Cheng Yongmei (2016). *Multi-band polarization imaging and applications*. National Defense Industry Press, Beijing and Springer-Verlag Berlin Heidelberg.

8. Gurton K.P., Yuffa A.J., Videen G.W. (2014). Enhanced facial recognition for thermal imagery using polarimetric imaging. *Optical Society of America*, 39(13), 3857–3859.

9. Sivukhin D.V. (2004). *Obshchii kurs fiziki [General physics course]*. 4th ed. Moscow: MFTI [in Russian].

10.   Anatychuk L.I., Vikhor L.M., Kotsur M.P., Kobylianskyi R.R., Kadenyuk T.Ya. (2016). Optimal control of time dependence of cooling temperature in thermoelectric devices. *J.Thermoelectricity*, 5, 5-11.

11.   Kolobrodov V.H., Mykytenko V.I., Tymchyk H.S. (2020) Poliaryzatsiina model teplokontrastnykh obiektiv sposterezhennia [Polarization model of heat-contrast objects of observation]. *J.Thermoelectricity*, 1, 36-52.

12.   Vollmer Michael, Mollman Klaus-Peter (2018). *Infrared thermal imaging. fundamentals, research and applications. 2nd ed.* Weinheim: Wiley – VCH.

13. Kolobrodov V.G., Lykholit M.I. (2007). *Proektuvannia teploviziinykh i televiziinykh system sposterezhennia [Design of thermal imaging and television surveillance systems].* Kyiv: KPI [in Ukrainian].

14.   Chrzanowski K. (2010). *Testing thermal imagers. Practical guidebook.* Military University of Technology, 00-908 Warsaw, Poland.

15.   Lloyd G. (1978). *Thermal imaging systems*. Moscow: Mir [Russian transl].

16.   Kolobrodov V.G. (2020). Determination of transmittance of optical system of polarizing thermal imager. *Visnyk NTUU KPI Seriia – Radiotekhnika Radioaparatobuduvannia*, 78, 78–85.

17.   NATO Military Agency for standardization (1995). *Definition of nominal static range performance for thermal imaging systems.*

18.   Khrebtov I.A., Maliarov V.G. (1997). Neokhlazhdaiemyie teplovyie metrichnye priiomniki IK izlucheniia [Uncooled thermal array IR detectors]. *Soviet Journal of Optical Technology*, 6, 3–17 [in Russian].

19.   Tymchik G.S., Kolobrodov V. H., Kolobrodov M. S., Vasyura Anatoliy S., Komada Paweł, Azeshova Zhanar. (2018). The output signal of a digital optoelectronic processor. *Proc. SPIE 10808, Photonics Applications in Astronomy, Communications, Industry, and High-Energy Physics Experiments* 2018, 108080W (1 October 2018).

Submitted 28.08.2020

Anatychuk L.I., *acad. of the NAS of Ukraine* [1,2]

[1]Institute of Thermoelectricity of the NAS and MES of Ukraine,

1 Nauky str., Chernivtsi, 58029, Ukraine,

[2]Yu.Fedkovych Chernivtsi National University,

2, Kotsiubynskyi str., Chernivtsi, 58000, Ukraine

e-mail: anatych@gmail.com

Anatychuk L.I.

EFFICIENCY CRITERION OF THERMOELECTRIC ENERGY CONVERTERS USING WASTE HEAT

The paper analyzes the efficiency criterion of thermoelectric energy converters using waste heat (thermoelectric recuperators). Conclusions are drawn in which cases it is economically feasible to use such recuperators. Bibl. 7, Fig. 2.

Kay words: thermoelectric generator, waste heat recovery.

Introduction

General characterization of the problem.

The use of thermoelectricity for the utilization of waste heat in order to obtain electrical energy has been and remains the subject of interest of specialists dealing with thermoelectricity for the last almost three decades. Among them, waste heat from internal combustion engines, smelting furnaces, cement kilns, chemical and oil refining industries and much more, where a significant part of the waste heat is simply released into the environment. Waste heat in everyday life also takes a significant place [1, 2].

Due to the growing trend of combating CO_2 emissions, many countries have begun to assess the potential of their thermal waste [3, 4]. Paper [5] analyzes the available statistics and concludes that in developed countries, industry accounts for 50% to 80% of energy consumed by the country as a whole. At the same time, on average, 20% of the consumed energy is lost with thermal waste, and in some countries, such as Ireland, Turkey, Spain, Cyprus, this value reaches 50 - 70%.

Therefore, it is *currently important* to create thermoelectric generators (TEG), which will be used as waste heat recuperators and return part of the heat loss in the form of electricity.

The classical theory of thermoelectric generators determines the efficiency of the main criterion of their quality. The difference in the use of a heat generator as a recuperator is that the waste heat is free, and therefore the efficiency of the generator does not play a decisive role. The question of what criterion should be used to evaluate thermoelectric energy converters that will use thermal waste becomes *relevant*. Thus, there is a fundamentally new situation to describe the quality of the

thermoelectric recuperator.

The purpose of this work is to determine the efficiency criterion for a thermoelectric recuperator that uses waste heat.

Quality criterion for TEG as a waste heat recuperator

In conditions when the efficiency is not a governing factor for assessing the quality of a thermoelectric recuperator, the first place should be given to the economic feasibility of using a TEG as a recuperator.

Proceeding from the fact that the result of the TEG operation is additional electrical energy, it will be expedient to use it if the cost of the electrical energy produced by it is economically rational for its use in each specific case, and in the presence of an electrical network should be lower than the cost of industrial electrical energy. It is clear that this cost in the recuperation mode does not include the price of heat energy, which is determined by the cost of energy carriers, such as hydrocarbons, nuclear fuel and others, since waste heat is free.

Therefore, the cost of electric energy m_0 produced by a thermoelectric recuperator will be determined as follows:

$$m_0 = \frac{S_0}{N},$$

(1)

where S_0 is the unit cost of the thermoelectric recuperator, N is the service life.

Therefore, in the case of using TEG as a heat waste recuperator in the first place are the requirements for its minimum unit cost S_0 and maximum service life N.

The unit cost of the recuperator includes the cost of the generator S_1, the cost of its installation and maintenance S_2, the cost of heat removal from the generator S_3 and the cost of voltage stabilization S_4 (Fig.1). Depending on the operating conditions, there may be other costs

Unit cost of the generator			
The cost of TEG	Installation and maintenance cost	The cost of heat removal from the generator	The cost of the generator voltage stabilization
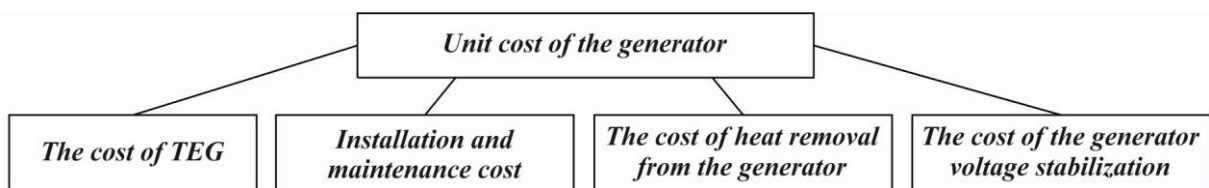
Fig. 1. Components of the unit cost of the generator.

The combination of these costs forms the unit cost of the recuperator S_0 ($/W), which is the ratio of all costs to its electrical power W:

$$S_0 = \frac{s_1 + s_2 + s_3 + s_4}{W}.$$

(2)

Estimates show that at present this value is about \$ 25/W [6]. According to (1), this value should be minimized.

On the other hand, the longer the generator's operating life N (hours), the lower the cost of the electrical energy m_0 produced by it.

The service life of the thermoelectric recuperator mainly depends on the service life of the thermoelectric modules used in the TEG. The best examples of thermoelectric generator modules, specially designed for thermoelectric recuperators, have a service life of about 100.000 hours [6].

Hence, it is possible to estimate the minimum cost of electrical energy of the thermoelectric recuperator. It will be about $ 0.25 per kWh, provided the optimal temperature on the TEG modules is ensured.

In the presence of industrial electrical networks, the economic feasibility of using a TEG as a recuperator is achieved when the cost of the electricity it produces is lower than the cost of industrial electrical energy, that is, on condition that

$$\frac{m}{m_0} > 1, \tag{3}$$

where m is the cost of industrial electrical energy, m_0 is the cost of electrical energy produced by thermoelectric recuperator.

Substituting (3) into (1), we obtain the efficiency criterion of thermoelectric recuperator A that should be more than unity:

$$A = \frac{mN}{S_0} > 1. \tag{4}$$

This criterion will characterize the feasibility of using thermoelectric generator as a waste heat recuperator and determine its payback period.
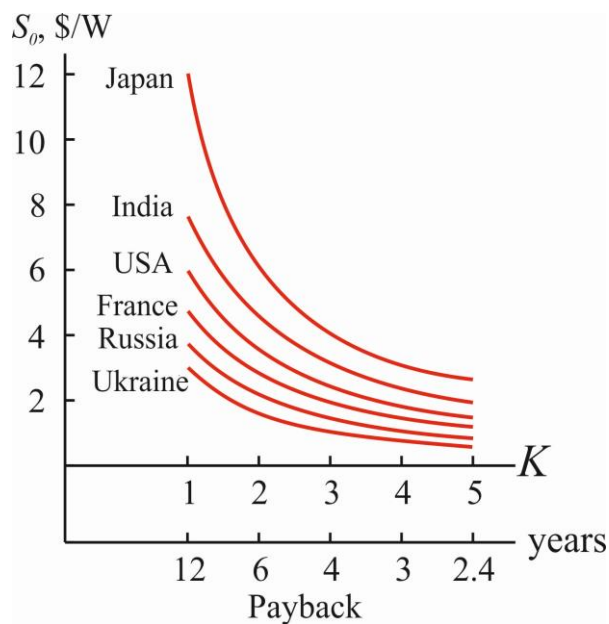
Fig. 2. Reasonable unit cost of TEG depending on the payback period.

The payback period of thermoelectric recuperator N_0 will be

$$N_0 = \frac{N}{A}.$$ (5)

The rest of the time $(N - N_0)$ the recuperator will be profitable. The net profit P from the use of a thermoelectric recuperator will be determined as

$$P = mW(N - N_0).$$ (6)

For example, Fig. 2 shows the calculations of the reasonable unit cost of a thermoelectric recuperator depending on the payback time for different countries. The unit cost of the generator was determined based on the price of electricity in a particular country [7].

As can be seen from Fig. 2, at present, in order to achieve the economic feasibility of using thermoelectric recuperators, it is necessary to work towards a significant reduction in its unit cost. It is more appropriate to use thermoelectric generators in countries where electricity is the most expensive.

Conclusions

1. A universal criterion A for the efficiency of thermoelectric recuperators using waste heat has been obtained. It determines the economic feasibility of using the recuperator, the payback period and the profit obtained through its use.
2. It has been established that the economically feasible use of a thermoelectric generator is when the criterion *A > 1*.
3. It is shown that in order to reduce the payback period of the thermoelectric recuperator, and, accordingly, increase the net profit, it is necessary to increase the criterion A, that is, to work towards reducing the unit cost of the recuperator and increasing its service life.
4. It is more economically efficient to use thermoelectric recuperators in countries where electricity is more expensive.

References

1. Neild Jr. A.B. (1963). *Portable thermoelectric generators*. Society of Automotive Engineers, New York, SAE-645A.
2. Zhang X., Chau K.T., Chan C.C. (2017). Overview of thermoelectric generation for hybrid vehicles. *Journal of Asian Electric Vehicles*, 6(2), 1119-1124.
3. Heghmanns A., Wilbrecht S., Beitelschmidt M., Geradts K. (2016). Parameter optimization and operating strategy of a TEG system for railway vehicles. *Journal of Electronic Materials*. DOI: 10.1007/s11664-015-4145-2
4. Bosch Henry (2016). From modules to a generator: An integrated heat exchanger concept for car applications of a thermoelectric generator (2016). *Journal of Electronic Materials*, 45(3). DOI: 10.1007/s11664-015-4129-2.

5. Kuz R. (2017). Dreams and realities of the use of thermoelectric generators in automobile transport. *XVII International Forum on Thermoelectricity* (Belfast, May 15-18, 2017).

6. Anatychuk L.I., Kuz R.V. (2011). Computer designing and test results of automotive thermoelectric generator. *Thermoelectrics goes automotive*. Berlin: Expert Verlag, P. 191 - 208.

7. http://worlwideenergy.com

Анатичук Л.І., *акад. НАН України*[1,2]

[1]Інститут термоелектрики НАН і МОН України,
вул. Науки, 1, Чернівці, 58029, Україна;
e-mail: anatych@gmail.com;
[2]Чернівецький національний університет
ім. Юрія Федьковича, вул. Коцюбинського 2,
Чернівці, 58000, Україна

КРИТЕРІЙ ЕФЕКТИВНОСТІ ТЕРМОЕЛЕКТРИЧНИХ ПЕРЕТВОРЮВАЧІВ ЕНЕРГІЇ, ЩО ВИКОРИСТОВУЮТЬ ТЕПЛОВІ ВІДХОДИ

У роботі проведено аналіз критерію ефективності термоелектричних перетворювачів енергії, що використовують відходи тепла (термоелектричних рекуператорів). Зроблено висновки, в яких випадках є економічно доцільним використання таких рекуператорів. Бібл. 7, рис. 2.

Ключові слова: термоелектричний генератор, утилізація відходів тепла.

Анатычук Л.И., *акад. НАН Украины*[1,2]

[1]Институт термоэлектричества НАН и МОН Украины,
ул. Науки, 1, Черновцы, 58029, Украина,
e–mail: anatych@gmail.com;
[2]Черновицкий национальный университет
им. Юрия Федьковича, ул. Коцюбинского, 2,
Черновцы, 58012, Украина

КРИТЕРИЙ ЭФФЕКТИВНОСТИ ТЕРМОЭЛЕКТРИЧЕСКИХ ПРЕОБРАЗОВАТЕЛЕЙ ЭНЕРГИИ, ИСПОЛЬЗУЮЩИХ ТЕПЛОВЫЕ ОТХОДЫ

В работе проведен анализ критерия эффективности термоэлектрических преобразователей энергии, использующих отходы тепла (термоэлектрических рекуператоров). Сделаны выводы, в каких случаях экономически целесообразно использование таких рекуператоров. Библ. 7, рис.2.

Ключевые слова: *термоэлектрический генератор, утилизация отходов тепла.*

References

1. Neild Jr. A.B. (1963). *Portable thermoelectric generators*. Society of Automotive Engineers, New York, SAE-645A.

2. Zhang X., Chau K.T., Chan C.C. (2017). Overview of thermoelectric generation for hybrid vehicles. *Journal of Asian Electric Vehicles*, 6(2), 1119-1124.

3. Heghmanns A., Wilbrecht S., Beitelschmidt M., Geradts K. (2016). Parameter optimization and operating strategy of a TEG system for railway vehicles. *Journal of Electronic Materials*. DOI: 10.1007/s11664-015-4145-2

4. Bosch Henry (2016). From modules to a generator: An integrated heat exchanger concept for car applications of a thermoelectric generator (2016). *Journal of Electronic Materials*, 45(3). DOI: 10.1007/s11664-015-4129-2.

5. Kuz R. (2017). Dreams and realities of the use of thermoelectric generators in automobile transport. *XVII International Forum on Thermoelectricity* (Belfast, May 15-18, 2017).

6. Anatychuk L.I., Kuz R.V. (2011). Computer designing and test results of automotive thermoelectric generator. *Thermoelectrics goes automotive*. Berlin: Expert Verlag, P. 191 - 208.

7. http://worlwideenergy.com

Filin S. O., *doc. tech. Sciences*

Zakrzewski Bogusław, *doc. tech. Sciences*

Filin S.O.

West-Pomeranian Technological University,
Szczecin, 17, al.Piastow, Szczecin,
70-310, Poland, *e-mail: sergiy.filin@zut.edu.pl*

Zakrzewski B.

EXPERIMENTAL STUDIES OF THE INFLUENCE OF THE FAN AND MODULE OPERATING MODE ON THE CHARACTERISTICS OF THERMOELECTRIC BEVERAGE COOLER

Using a beverage cooler as an example, the dependence of the temperature T_c of the chamber (container) of the cooler on the supply voltage U_f of the fan on the hot side of the unit was experimentally determined for various values of the supply voltage U_m. of the module. The correct choice of the supply voltage U_f of this fan allows not only to reduce the power consumption of the entire product, but also to reduce the temperature of the cooler chamber by 1-6 ° C, which automatically leads to an increase in its speed. When the supply voltage of the thermoelectric module U_m changes in the range from 0.3-0.4 to 0.75-0.8 of the nominal value, a minimum of the $T_c (U_f)$ function is observed. Bibl. 14, Fig. 4, Tabl. 2.

Key words: thermoelectric beverage cooler, cooling depth, fan, supply voltage, experimental studies.

Introduction

A number of previous author's publications [1-5] were devoted to the design of thermoelectric beverage coolers in original containers, i.e. in metal cans and plastic bottles. As part of the research, the market of modern household and car thermoelectric beverage coolers was analyzed in terms of their cooling rate. It has been shown that the speed of these devices does not satisfy the needs of consumers. The use of "wet" contact is proposed to increase the speed of coolers, and the efficiency of this solution is shown both by calculation and experimentally. This work is a continuation of previous research. The next phase is devoted to the analysis of the influence of various factors on the main technical characteristics of the mentioned coolers.

As can be seen from Table 1, the choice of the most important technical characteristics of a thermoelectric device depends on its purpose and mode of operation (permanent or occasional work). For refrigerators and minibars, such characteristics are the average power consumption P, the daily or

annual energy consumption E and the temperature difference ΔT created. For beverage coolers, these are the cooling rate V, also called the speed, and the cooling depth ΔT.

<div align="right">*Table 1*</div>

Qualitative analysis of the degree of influence of the selected design and operational factors on the most important technical characteristics of household thermoelectric devices

Group of products Factor	Mini bar coolers	Beverage coolers	Ice makers	Air conditioners
Operation (operating mode)	Permanent	Occasional	Occasional	Long-term, seasonal
The most important characteristics	P or E, ΔT	V, ΔT, \$	G, \$	E or P, ΔT, \$
Efficiency of thermoelectric material and modules	++	++	++	++
General layout, form	+	+	++	+
Heat transfer conditions on radiators (heat exchangers)	++	++	+	++
The effectiveness of thermal insulation of the chamber (containers, ice molds)	++	+	0	0
Efficiency of AC/DC power supply	+	+	+	+
Temperature control method	++	+	0	+
Cost-effectiveness of auxiliary equipment (chamber lighting, automation, fans, etc.)	+	+	0	++

where: E – energy consumption, [kWh/day]; P – power consumption, [W]; ΔT – created temperature difference (for refrigerator), cooling depth (for beverage cooler), [°C]; operating temperature range (for air-conditioner); V – cooling rate, [°C/h]; G – productivity, [kg/h]; $\$$ – price [$\$$].

++ – strong influence, + – moderate influence, 0 – there is no or negligible influence.

Table 1 shows the factors that influence the characteristics of the selected types of devices. The experience of creating and operating household thermoelectric products shows that improving their characteristics is not limited only to increasing the efficiency of thermoelectric materials. The total influence of other factors is comparable, and in some cases exceeds the influence of the effectiveness of materials. Among these other factors, the conditions of heat exchange on the radiators on both sides of the thermoelectric module or modules should be highlighted. Temperatures of overcooling the cold radiator and overheating the hot radiator have a direct effect on the cooling capacity and energy efficiency of a thermoelectric module [6,7]. Therefore, the conditions of heat transfer on the radiators are highlighted as a factor of strong influence.

Brief analysis of literature, purpose and object of research

The efficiency of heat exchange on both sides of the thermoelectric module depends on the fan performance, which, in turn, depends on its supply voltage. Therefore, the main variable parameter was the fan supply voltage. It should be remembered that in household appliances powered from a 220-230 *V* AC mains through a rectifier, it is easy to implement an independent power supply for the module and the fan. The study of the influence of the supply voltage of the fan placed in the refrigerator or display cabinet on the average temperature in the chamber was carried out quite a long time ago and is described in [8-10]. At the same time, the study of the influence of the fan operating mode on the hot side of the module on the temperature characteristics of a thermoelectric product is of even greater interest. In addition to [10], where such studies were carried out in a very limited scope, such experimental work has not yet been carried out. Recent works devoted to experimental studies of thermoelectric coolers [11-14] also do not address these issues. The aim of the study was to fill this gap.

A thermoelectric beverage cooler with "wet contact" of the TSSN-0.5 type, presented in Fig. 1 and described in detail in [1-5], was chosen as the object of research. The cooler is designed for cooling drinks in metal cans with a volume of 0.33 and 0.5 liters and in plastic bottles of the same volume. The cooler contains one thermoelectric module of the MT2-1.6-127 type, whose cold side is in contact with the bottom of a thermally insulated cylindrical container made of aluminum. The hot side of the module is connected to a radiator, which is blown by an Everflow type R128025DM fan with a nominal supply voltage of 12V DC. An independent power supply for the module and the fan is provided in the investigated object. The aluminum radiator located under the fan plays the role of a stand and a distancer and practically does not participate in heat exchange.

a)   *b)*
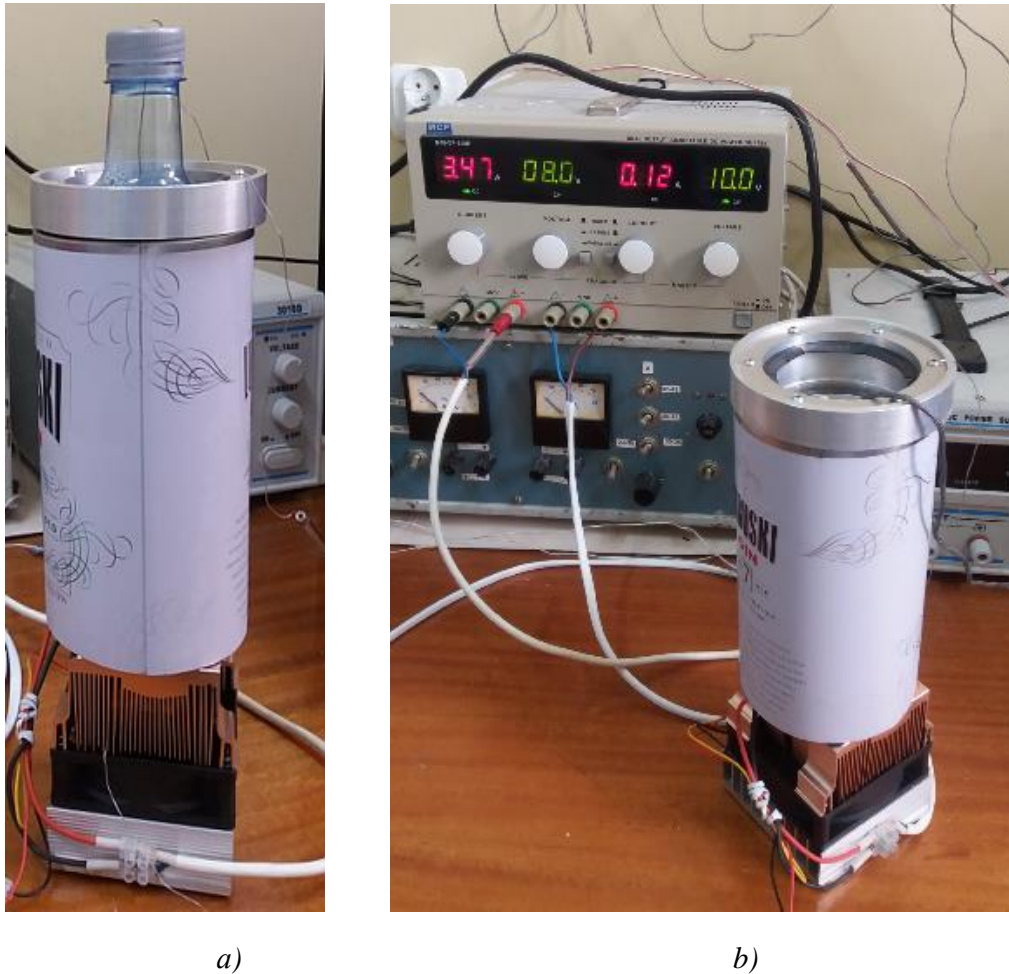
Fig.1. Prototype of a household thermoelectric beverage cooler TSSN-0.5 [3]:
a – general view, b – testing moment.

Research method, brief description of the experimental bench and test procedure

To achieve this goal, the way of doing experimental research was chosen. The tests were carried out in the laboratory of thermoelectric cooling of the Department of Air Conditioning and Refrigerated Transport of the West Pomeranian University of Technology in Szczecin in the period 2020-2021.

A simplified diagram of the experimental bench and the installation diagram of temperature sensors are shown in Fig. 2. To measure temperatures, resistance temperature sensors TSM-100 were used, which are part of the IT-10 measuring complex. The measurement results were recorded with a frequency of 10 seconds using the Channel 2.0 software. The module and the fan were powered from an external two-channel power supply of the M10-DP-305E type with independent control of the output electrical parameters. After the chamber temperature stabilized at the next value of the fan supply voltage, the power supply switched to the next voltage value at a constant value of the supply voltage of the thermoelectric module. Typical dynamics of the chamber temperature change during the tests is shown in Fig. 3.

The tests were carried out at a laboratory room temperature of 22 + 1 ºC, maintained with a split-type household air conditioner. The tests were carried out for two operating modes of the cooler: with

an empty chamber (container) and with a drink in a 0.33 liter can (Fig. 1 b).
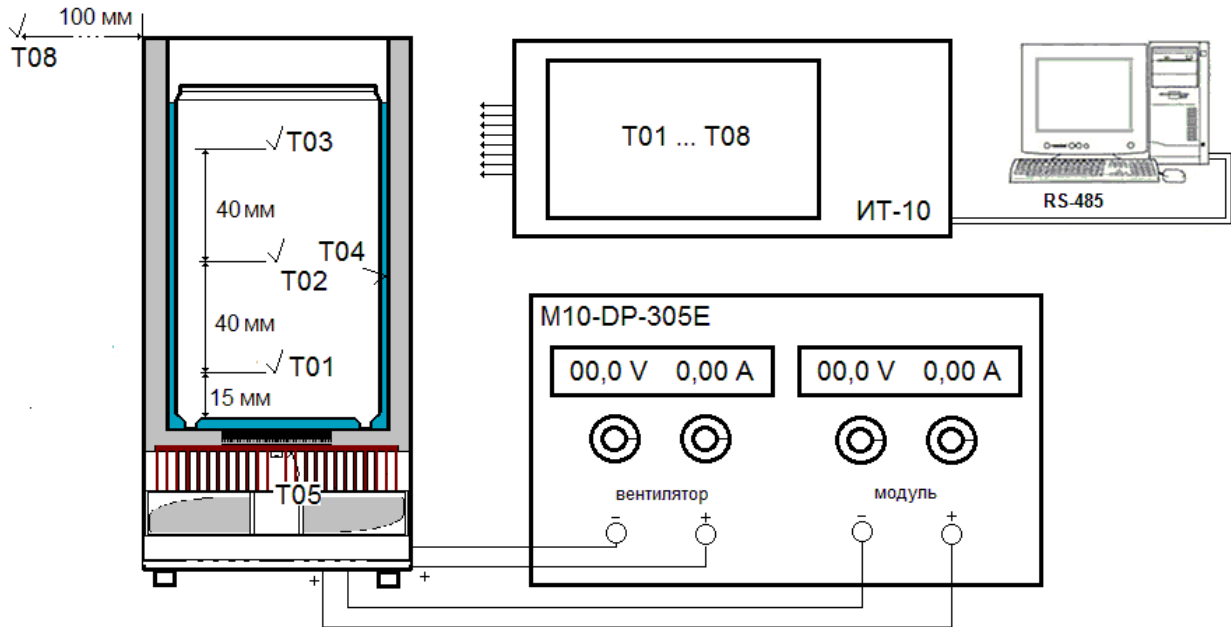
Fig.2. Block diagram of the experimental bench with indication of the thermocouple installation locations.
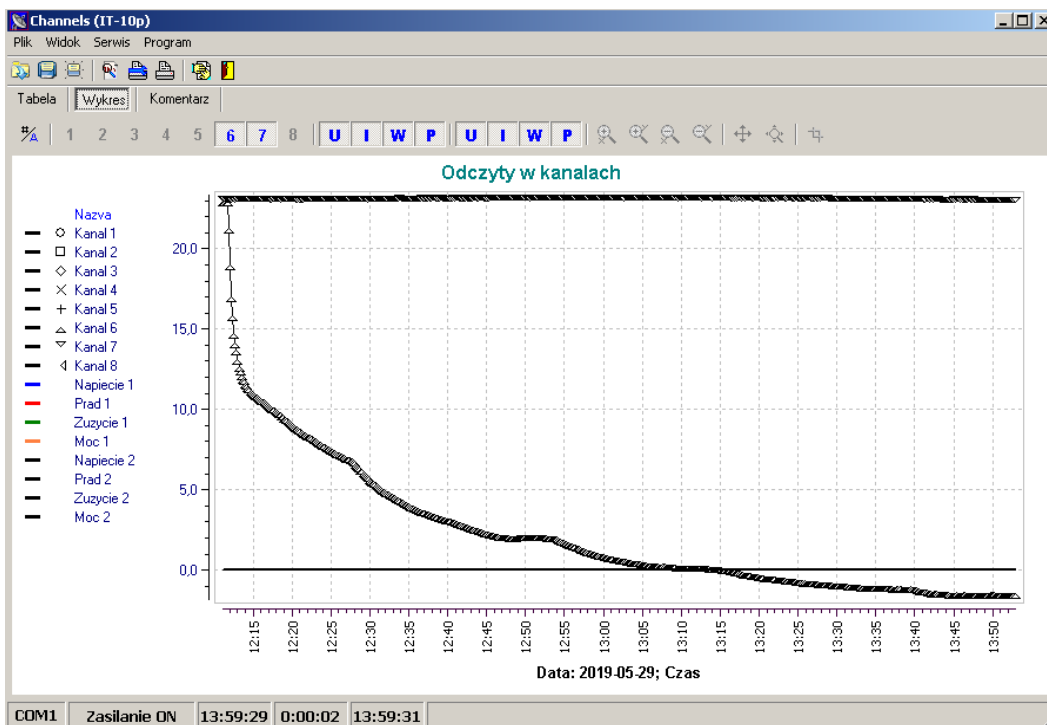
Fig.3. The dynamics of change in the temperature of the chamber T_c during tests at $U_m = 10$V.

Test results and their analysis

The test results of a cooler with a metal can in synthetic form are presented in Table 2. The fan supply voltage was regulated in the range from 6 to 14 V, which follows from many years of experience in operating this type of axial fans. They remain operational when the supply voltage changes in the range from 5 to 15 volts. In the experiment, we limited ourselves to the range of 6-14 volts for the following reasons. At a voltage below 6V, problems arise with the start of the fan, although with a gradual decrease in voltage from 6 to 5V, it continues to work at low speeds. Voltage over 14V is associated with increased power consumption and increased noise.

Table 2

Results of testing the thermoelectric cooler at variable values of
supply voltage of module U_m and fan U_w

Temperatures °C →	T_c			T_h			ΔT		
Voltages $U_m \rightarrow$ $\downarrow U_f$	6V	8V	10V	6V	8V	10V	6V	8V	10V
6V	5.1	5.9	6.7	34.3	39.3	50.2	29.2	33.4	43.5
8V	4.3	4.3	2.0	32.2	35.9	45.2	27.9	31.6	43.2
10V	4.1	4.3	0.1	31.0	34.7	42.3	26.9	30.4	42.2
12V	4.4	4.3	-1.0	30.3	32.7	40.4	25.9	28.4	41.4
14V	4.6	5.4	-1.3	29.6	31.9	39.4	25.0	26.5	40.4

The range of voltage variations of the module was narrowed to the limits from 6 to 10V, which followed from previous experiments [3]. Changes in the temperature of the hot radiator T_h fully corresponded to our expectations: for each constant value of the module supply U_m (6, 8, and 10 V), with an increase in the fan supply voltage U_f, the temperature of the hot radiator T_h decreased, and this decrease was more significant at higher values of U_m. The situation looked completely different on the cold side, where the temperature of the wall of the container (chamber), in which the can with the drink was located, was measured. Here, the minimum values of the container temperature T_c were observed at the supply voltage $U_f = 10$V at the module supply voltages of 6V and 8V, and at $U_m = 8$V the minimum was blurred. At $U_m = 10$V, a monotonic decrease in the temperature T_c with an increase in U_f was observed (Fig. 4).
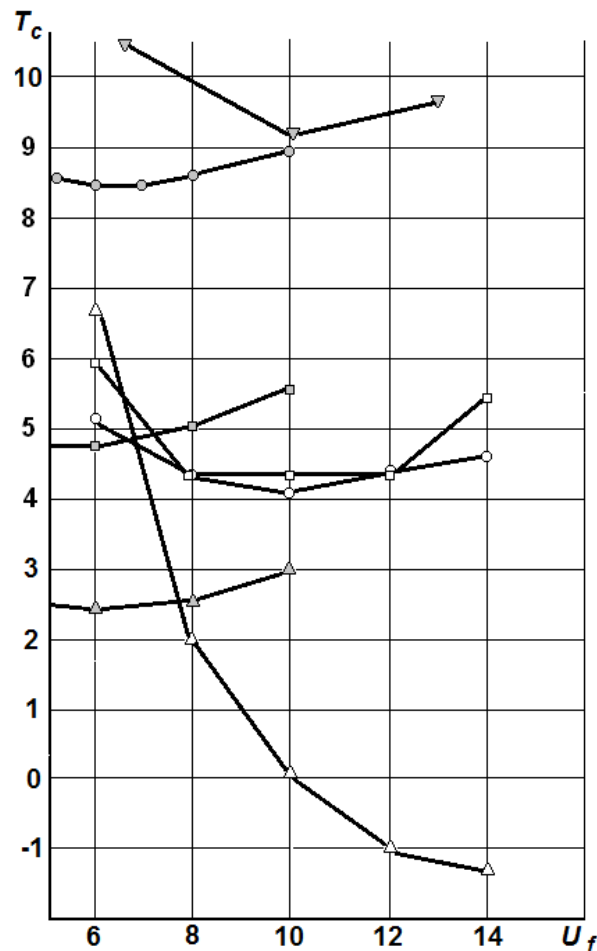
Fig.4. Dependence of the container (chamber) temperature T_c on the supply voltage of fan U_f Installed on the hot side of the module at different values of its supply voltage, namely: ○ - $U_m = 6$V; □ - $U_m = 8$V; △ - $U_m = 10$V; the rest of the graphs and symbols relate to the comparison of results with the data of other studies, and are explained in the text.

Fig.4 also shows a comparison of the results obtained with the results of known, earlier works. The symbol $\triangledown$ denotes the dependence of the temperature in the chamber of a 103^{-1} thermoelectric refrigeration display case on the supply voltage of the fans on the hot side of the unit [10], and the symbols $\bigcirc$ $\square$ $\triangle$ show the dependence of the temperature in the chamber of the thermoelectric beverage cooler with a volume of 13.5 l on the supply voltage of the fan in the chamber, i.e. on the cold side of the unit [8]. The first of the above dependences ($\triangledown$) has minimum near $U_f = 10$V. This value coincides with the results obtained in the present work. Does this mean a universal recommendation for choosing U_f?

With regard to the fact that $U_{f(opt)}$ is influenced not only by the module supply voltage, but also by the design of the hot heat exchanger, fan type, temperature control method and a number of other factors, it is too early to make a final conclusion about the optimal value of $U_{f(opt)}$. At the same time, we can confidently draw a qualitative conclusion: there is an optimal fan supply voltage on the hot side from the point of view of temperature reduction in the chamber T_c, and it is less than the nominal fan supply voltage. Another, not so obvious, but important conclusion: the larger the heat exchange surface the hot radiator has, the lower the optimal fan supply voltage will be. In stationary thermoelectric refrigerators and other devices in which weight reduction is not a priority task, the use of a radiator with a larger surface leads to an increase in the cost of the refrigerator within 5-6 %. In this case, a corresponding decrease in the fan supply voltage means a 2% to 4% reduction in power consumption. The result of the feasibility study depends on the frequency (intensity) of using the refrigerator. If a stationary refrigerator or beverage cooler is used 24 hours a day for more than 3 months a year for a minimum of 5 years, operating cost savings are prioritized over investment cost savings.

A similar dependence of T_c on U_f, but this time on the cold side of the unit, also demonstrates a minimum for various values of U_m ($\bigcirc$ $-U_m = 6$V; $\square$ $-U_m = 8$V; $\triangle$ $-U_m = 10$V), which corresponds to the minimum value of the fan supply voltage, i.e. 6V. The physical meaning of this behavior of the function $T_c (U_f)$ is as follows. In going from natural to forced convection, which is observed at $U_f = 5$-6 V, there is an abrupt decrease in the average temperature in the refrigerator chamber. However, a further increase in the fan supply voltage, which corresponds to an increase in the air circulation rate in the chamber, leads to the fact that the total thermal resistance to heat transfer on the chamber walls (taking into account the leakage of the door insulation) decreases faster than the resistance on the cold heat sink. As a result, an increase in the heat flux through the chamber insulation prevails in the balance of heat fluxes.

Conclusions

The studies carried out have once again shown the importance of coordinating the operating modes of the module (modules) and fans used in the units of various thermoelectric products. Using a beverage cooler as an example, the dependence of the temperature T_c of the chamber (container) of the cooler on the supply voltage U_f of the fan on the hot side of the unit was experimentally determined

for various values of the supply voltage of the module U_m. The correct choice of the supply voltage U_f of this fan allows not only to reduce the power consumption of the entire product, but also to reduce the temperature of the cooler chamber by 1-6 ° C, which automatically leads to an increase in its speed. When the supply voltage of the thermoelectric module U_m changes in the range from 0.3-0.4 to 0.75-0.8 of the nominal value, a minimum of the T_c (U_f) function is observed.

References

1. Filin S.O. (2018). The influence of thermal contact between cooling surface and object on quick-speed thermoelectric coolers for beverages. *J.Thermoelectricity*,1, 66-77.

2. Filin S.O. (2018). Poprawa dynamicznych charakterystyk małych termoelektrycznych schładzaczy i podgrzewaczy napojów. *Ciepłownictwo, ogrzewnictwo, wentylacja*, 12, 525-529. DOI: 10.15199/9.2018.12.9

3. Filin S.O., Zakrzewski B. (2021). Experimental studies of the performance of thermoelectric coolers of drinks with wet contact. *JEPTER*, 94 (1).

4. Filin S.O. (2020). Calculation of the cooling speed of the thermoelectric beverage cooler with "wet" contact. *J. Thermoelectricity*, 2 .

5. Filin S., Anatychuk L. Termoelektryczne schładzacze napojów. Zgłoszenie patentowe nr 426737 z dnia 22.08.2018.

6. Anatychuk L.I. (1979). *Termoelementy i termoelektricheskiie ustroistva: Spravochnik [Thermoelements and thermoelectric devices: Handbook]*. Kyiv: Naukova dumka [in Russian].

7. Naer V.A., Garachuk V.K. (1982). *Teoreticheskiie osnovy termoelektricheskogo okhlazhdeniia [Theoretical foundations of thermoelectric cooling]*. Odessa: OPI [in Russian].

8. Filin S., Owsicki A. (2005). Badania wpływu parametrów pracy wentylatora w komorze na cechy eksploatacyjne chłodziarki termoelektrycznej. *Chłodnictwo*, XL, 4, 8-12,30.

9. Filin S.O, Owsicki A. (2006). Experimental research of thermoelectric glass door refrigerators. *J.Thermoelectricity*, 2, 68-73.

10. Zakrzewski B., Filin S., Owsicki A. (2006). Design and experimental research of glass door refrigeration of 100 l volume with thermoelectric cooling unit. *Proceedings of 4-th Congress CEFood* (Bulgaria, Sofia, May 22-24, 2006).

11. Fairuz Remeli M., Ezzah Bakaruddin N., Shawal S., Husin H., Fauzi Othman M., Singh B. (2020). Experimental study of a mini cooler by using Peltier thermoelectric cell. *IOP Conference Series: Materials Science and Engineering* 788(1), 012076, DOI: 10.1088/1757-899X/788/1/012076.

12. Reid E., Barkes J., Morrison C., Ung A., Patel R., Rebarker C., Panchal P., Vasa S. (2018). Design and testing of a thermoelectrically-cooled portable vaccine cooler. *Journal of Young Investigators*, 35(2), 50–55, DOI: 10.22186/jyi.35.2.50-55.

13. Mirmanto Mirmanto, Syahrul Syahrul, Yusi Wirdan. (2018). Experimental performances of a thermoelectric cooler box with thermoelectric position variations. *Engineering Science and Technology an International Journal*, 22(1), DOI: 10.1016/j.jestch.2018.09.006.

14. Yasser Abdulrazak Alghanima, Osama Mesalhy, Ahmed Farouk Abdel Gawad. (2021). Effect of position and design parameters of a fan-cooled cold-side heat-sink of a thermoelectric cooling-module on the performance of a hybrid refrigerator. *Proceedings of ICFD14: Fourteenth International Conference of Fluid Dynamics* (Egypt, Cairo, April 2-3, 2021).

Філін С.О. *докт. техн. наук*

Закшевський Богуслав, *докт. техн. наук*

Західнопоморський технологічний університет у Щецині,
алея Піаст 17, Щецін, 70-310, Польща;
e-mail: *sergiy.filin@zut.edu.pl*

ЕКСПЕРИМЕНТАЛЬНІ ДОСЛІДЖЕННЯ ВПЛИВУ РЕЖИМУ РОБОТИ ВЕНТИЛЯТОРА І МОДУЛЯ НА ХАРАКТЕРИСТИКИ ТЕРМОЕЛЕКТРИЧНОГО ОХОЛОДЖУВАЧА НАПОЇВ

На прикладі охолоджувача напоїв експериментально визначена залежність температури T_c камери (ємності) охолоджувача від напруги живлення U_f вентилятора на гарячій стороні агрегату при різних значеннях напруги живлення модуля U_m. Правильний вибір напруги живлення U_f цього вентилятора дозволяє не лише знизити споживану потужність виробу в цілому, а й на 1-6°С знизити температуру камери охолоджувача, що автоматично призводить до підвищення його продуктивності. При зміні напруги живлення термоелектричного модуля U_m в діапазоні від 0,3-0,4 до 0,75-0,8 номінального значення спостерігається мінімум функції $T_c (U_f)$. Бібл. 14, рис. 4, табл. 2.

Ключові слова: термоелектричний охолоджувач напоїв, глибина охолодження, вентилятор, напруга живлення, експериментальні дослідження

Филин С.О. *докт. техн. наук*

Закшевский Богуслав, *докт. техн. наук*

Западнопоморський технологический
университет у Щецине
алея Пиастив 17, Щецин, 70-310, Польша;
e-mail: sergiy.filin@zut.edu.pl

ЕКСПЕРЫМЕНТАЛЬНЫЕ ИСЛЕДОВАНИЯ ВЛЕЯНИЯ РЕЖИМА РОБОТЫ ВЕНТИЛЯТОРА И МОДУЛЯ НА ХАРАКТЕРИСТИКИ ТЕРМОЭЛЕКТРИЧЕСКОГО ОХЛАДИТЕЛЯ НАПИТКОВ

На примере охладителя напитков экспериментально определена зависимость температуры T_c камеры (емкости) охладителя от напряжения питания U_f вентилятора на горячей стороне агрегату при различных значениях напряжения питания модуля U_m. Правильный вібор напряжения питания U_f этого вентилятора позволяет не только снизить потребляемую мощность всего изделия, но и на 1-6°C снизить температуру камеры охладителя, что автоматически приводит к повешению его производности. При изменении напряжения питания термоэлектрического модуля U_m в диапазоне від 0,3-0,4 до 0,75-0,8 номинального значения наблюдается минимум функции $T_c (U_f)$. Библ. 14, рис. 4, табл. 2.

Ключевые слова: термоэлектрический охладитель напитков, глубина охлаждения, вентилятор, напряжение питания, экспериментальные исследования.

References

1. Filin S.O. (2018). The influence of thermal contact between cooling surface and object on quick-speed thermoelectric coolers for beverages. *J.Thermoelectricity*,1, 66-77.

2. Filin S.O. (2018). Poprawa dynamicznych charakterystyk małych termoelektrycznych schładzaczy i podgrzewaczy napojów. *Ciepłownictwo, ogrzewnictwo, wentylacja*, 12, 525-529. DOI: 10.15199/9.2018.12.9

3. Filin S.O., Zakrzewski B. (2021). Experimental studies of the performance of thermoelectric coolers of drinks with wet contact. *JEPTER*, 94 (1).

4. Filin S.O. (2020). Calculation of the cooling speed of the thermoelectric beverage cooler with "wet" contact. *J. Thermoelectricity*, 2 .

5. Filin S., Anatychuk L. Termoelektryczne schładzacze napojów. Zgłoszenie patentowe nr 426737 z dnia 22.08.2018.

6. Anatychuk L.I. (1979). *Termoelementy i termoelektricheskiie ustroistva: Spravochnik [Thermoelements and thermoelectric devices: Handbook]*. Kyiv: Naukova dumka [in Russian].

7. Naer V.A., Garachuk V.K. (1982). *Teoreticheskiie osnovy termoelektricheskogo okhlazhdeniia [Theoretical foundations of thermoelectric cooling].* Odessa: OPI [in Russian].

8. Filin S., Owsicki A. (2005). Badania wpływu parametrów pracy wentylatora w komorze na cechy eksploatacyjne chłodziarki termoelektrycznej. *Chłodnictwo*, XL, 4, 8-12,30.

9. Filin S.O, Owsicki A. (2006). Experimental research of thermoelectric glass door refrigerators. *J.Thermoelectricity*, 2, 68-73.

10. Zakrzewski B., Filin S., Owsicki A. (2006). Design and experimental research of glass door refrigeration of 100 l volume with thermoelectric cooling unit. *Proceedings of 4-th Congress CEFood* (Bulgaria, Sofia, May 22-24, 2006).

11. Fairuz Remeli M., Ezzah Bakaruddin N., Shawal S., Husin H., Fauzi Othman M., Singh B. (2020). Experimental study of a mini cooler by using Peltier thermoelectric cell. *IOP Conference Series: Materials Science and Engineering* 788(1), 012076, DOI: 10.1088/1757-899X/788/1/012076.

12. Reid E., Barkes J., Morrison C., Ung A., Patel R., Rebarker C., Panchal P., Vasa S. (2018). Design and testing of a thermoelectrically-cooled portable vaccine cooler. *Journal of Young Investigators*, 35(2), 50–55, DOI: 10.22186/jyi.35.2.50-55.

13. Mirmanto Mirmanto, Syahrul Syahrul, Yusi Wirdan. (2018). Experimental performances of a thermoelectric cooler box with thermoelectric position variations. *Engineering Science and Technology an International Journal*, 22(1), DOI: 10.1016/j.jestch.2018.09.006.

14. Yasser Abdulrazak Alghanima, Osama Mesalhy, Ahmed Farouk Abdel Gawad. (2021). Effect of position and design parameters of a fan-cooled cold-side heat-sink of a thermoelectric cooling-module on the performance of a hybrid refrigerator. *Proceedings of ICFD14: Fourteenth International Conference of Fluid Dynamics* (Egypt, Cairo, April 2-3, 2021).

Submitted 17.09.2020

L.I. Anatychuk *acad. National Academy of Sciences of Ukraine*[1,2],

N.V. Pasechnikova *doc. med. sciences, Corresponding Member of the National Academy of medical sciences of Ukraine*[3]**,**

V.O. Naumenko *doc. med. sciences*[3],

O.S. Zadorozhnyi *doc. med. sciences*[3],

P.E. Nazaretian[3]**, Havryliuk M.V.** [1,2],

V.A. Tiumentsev[1]**, R.R. Kobylianskyi** *cand. phys.-math. sciences*[1,2]

[1]*Institute of Thermoelectricity of the NAS and MES of Ukraine, Chernivtsi, Ukraine*
e–mail: anatych@gmail.com
[2]*Yuriy Fedkovych Chernivtsi National University, Chernivtsi, Ukraine*
[3] *State Institution "The Filatov Institute of Eye Diseases and Tissue Therapy of the NAMS of Ukraine", Odesa, Ukraine*

THERMOELECTRIC DEVICE FOR NON-CONTACT COOLING OF THE HUMAN EYES

The paper presents the results of the development of a thermoelectric device for non-contact cooling of the human eyes. The device is designed for the treatment of acute and chronic eye diseases, reducing intraocular pressure, reducing pain and inflammation of the eye. The developed thermoelectric medical device makes it possible to cool the eye structures without contact, which will allow developing and implementing the technology of controlled local therapeutic hypothermia in ophthalmology. The design features of the device, the principle of its operation and technical characteristics are described. Bibl. 22, Fig. 2, Tabl. 1.
Key words: thermoelectric device, non-contact cooling, hypothermia of the human eye.

Introduction

Therapeutic hypothermia consists in artificially lowering the patient's body temperature by forcibly removing heat from the body (general hypothermia) or internal organs (local hypothermia) for therapeutic purposes.

Local therapeutic hypothermia is successfully employed in various fields of medicine. For example, cold cardioplegia is used to protect the heart tissue during cardiac surgery performed in the conditions of artificial circulation, which allows to uniformly reduce the temperature of the

myocardium to (+8÷10 °C) [1]. Craniocerebral hypothermia is used to prevent hypoxia of brain structures during neurosurgery, as well as in newborns born with severe asphyxia [2]. In reconstructive surgery on renal vessels or kidney transplantation, local hypothermia can protect its tissues from hypoxia and prevent the development of renal failure in the postoperative period [3].

In ophthalmology, local hypothermia of the eye structures can also be used to solve some therapeutic problems. Thus, J.M. Katsimpris suggests using local cooling of the eye to combat intraocular inflammation [4]. Local therapeutic hypothermia can be used to reduce intraocular pressure [5]. After local cooling in the eye there is an increase in blood supply to the vascular tract, increased pulse volume and blood flow velocity, which can be used for anti-ischemic purposes in ophthalmic diseases [6]. Local hypothermia during vitreoretinal eye surgery can lead to decreased fibrin production and reduced bleeding [7].

Artificial local contact hypothermia is a fairly simple way to achieve a decrease in intraocular temperature and, unlike general hypothermia, is free from the risk of severe complications from the internal organs, and therefore its use looks promising. There are different ways of local cooling of the eye. During intraocular surgery, local hypothermia of the eye can be created by lowering the temperature of irrigation solutions [8]. A decrease in the temperature of the intraocular media of the eye is possible, both when cooling directly the outer surface of the cornea, and when exposed to cold through closed eyelids. For contact cooling of the structures of the eye, one can use, for example, an ice pack applied to the eyelids [9]. The development of special thermoelectric devices for local contact cooling of the eye allows more efficient and controlled use of the beneficial effects of therapeutic hypothermia for the treatment of ophthalmic diseases [10, 11].

It is known that the heat transfer by the surface tissues of the human body, including the structures of the eye, to the environment is carried out mainly by radiation in the form of electromagnetic waves in the infrared spectrum (wavelength 3-50 μm with a peak of 9.6 μm), i.e. in the areas of long-wave infrared radiation [12]. Thus, at room temperature (+21 ÷ +23 °C) and relative humidity (within 40-60%) about 60% of heat is removed from the human body by radiation. About 20% of heat is removed by evaporation and 15 -20% - by convection. Conduction is situational and depends on the contact of the body with objects in the environment [13]. Thus, the above features of heat transfer of the human body create certain opportunities for cooling the surface structures of the body by non-contact means. Further research in this direction is required to develop the technology of artificial non-contact controlled local hypothermia of the eye and assess the feasibility of its use in the treatment and prevention of ophthalmic diseases.

Therefore, the *purpose of this work* is to develop a design and manufacture an experimental prototype of a thermoelectric device for non-contact cooling of the human eyes.

Design and technical characteristics of the device

At the Institute of Thermoelectricity of the NAS and MES of Ukraine within cooperation agreement with the State Institution "The Filatov Institute of Eye Diseases and Tissue Therapy of the NAMS of Ukraine", a thermoelectric device was developed for non-contact cooling of the human eyes (Fig.1). The technical characteristics of the device are given in Table 1.

The device is designed to treat acute and chronic eye diseases, reduce intraocular pressure, alleviate pain and inflammatory processes in the human eye. The developed thermoelectric medical device allows non-contact cooling of the structures of the eye, which will make it possible to develop and implement the technology of non-contact controlled local therapeutic hypothermia in ophthalmology [8, 14 - 20]. Such a device is original and has no analogues in the world.

Fig.1. Experimental prototype of thermoelectric device for non-contact cooling of the human eyes: 1 – thermoelectric cooling modules, 2 – electronic control and power supply unit

The device consists of two main functional units: a cooling device based on thermoelectric cooling modules 1 and an electronic control and power supply unit 2 (Fig. 1). The cooling device is made on the basis of the Peltier thermoelectric modules 1 [21, 22] and is designed to cool two metal surfaces located in close proximity to the surface of the human eyes. Due to the exchange of radiant energy between these surfaces, the surface of the human eye is cooled by several degrees Celsius. The degree of cooling of the eye surface depends on the temperature of the metal heat exchange surfaces and the duration of the procedure. The temperature of the eye surface during cooling is controlled by a non-contact thermometer. To increase the efficiency of radiation heat transfer, the metal cooling surfaces are blackened. Cooling of the hot sides of TE cooling modules is carried out by an external liquid circuit, which is connected to the water supply network. On the back panel of the cooling device there are liquid heat exchangers (made of highly thermally conductive material - copper) with fittings for connecting the water supply network. Water

consumption in the cooling circuit of the hot sides of TE cooling modules is small - enough 2-3 l/min at a water temperature of up to 20 ºC. In addition, the cooling device is placed on a tripod, which makes it possible to adjust its height and, accordingly, to select the individual placement of the cooling surfaces of the TE cooling modules in close proximity to the surfaces of the human eye.

<div align="right">

Table 1

</div>

Technical characteristics of the device

№	Technical characteristics of the device	Parameter values
1.	Range of setting and maintenance of working temperatures	(-25 ÷ +10) °C
2.	Temperature stabilization error, not more	1 ºC
3.	Temperature measurement error, not more	1 ºC
4.	Cooling the hot side of TE cooling module	liquid, from the water supply network
5.	Supply voltage (50 Hz AC)	220 ± 10 V
6.	Electric power of the device, not more	150 W
7.	Setting the exposure time	(1 ÷ 10) min
8.	Overall dimensions of cooling device	(160 × 235 × 50) mm
9.	Overall dimensions of electronic control and power supply unit	(100 × 240 × 250) mm
10.	The ability to cool each eye separately at a common set temperature	+
11.	Availability of protection against mains voltage	+
12.	Length of hoses for liquid cooling of TE cooling modules	3 m
13.	Device weight	1.5 kg
14.	Time of reaching temperature mode by the device	10 min
15.	Time of continuous operation of the device	48 h

Electronic unit 2 provides power and control of thermoelectric modules in order to maintain the temperature values set by the operator, forms the necessary time intervals for temperature exposure, selects the temperature effect on the patient's eyes (right eye, left eye, both eyes), and also protects the patient from being damaged by the mains voltage in an emergency.

On the front panel of the electronic unit 2 there are "ON", "RIGHT EYE", "LEFT EYE" toggle switches, a programmable microprocessor thermostat with an electronic display for setting and visualizing temperature values, a "HOLD TIME" switch, a "START" button.

On the rear panel of the electronic unit 2 there is a protective cut-out device, a connector for connecting a cooling device, a cord for connecting to a 220 V mains, a fuse 5 A.

In addition, the design of the device provides for the mounting of the cooling device on the ophthalmological table. After connecting water from the water supply network to the cooling device and connecting the electronic unit 2 to a 220 V mains, the device is ready for operation.

In an emergency, if mains voltage appears on the metal parts of the device, the protective cut-out device will operate and the device will be completely disconnected from the voltage. After eliminating the emergency, the protective cut-out device on the rear panel of the electronic unit 2 must be switched on again.

Block-diagram of the device
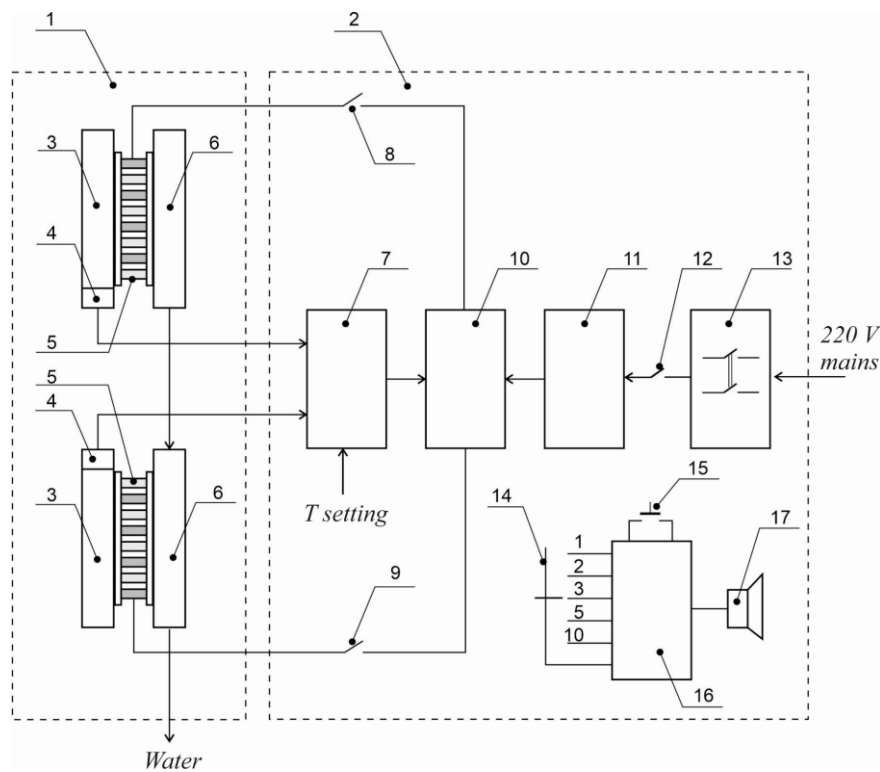
Fig.2. Block-diagram of thermoelectric device for non-contact cooling of the human eyes:
1 – cooling device, 2 – electronic control and power supply unit, 3 – cooling surface, 4 – temperature sensor, 5 – thermoelectric cooling module, 6 – liquid heat exchanger, 7 – programmable microprocessor thermostat, 8 – "LEFT EYE" toggle switch, 9 – "RIGHT EYE" toggle switch, 10 – power control unit of TE cooling module, 11 – power supply unit, 12 – "MAINS" toggle switch– switching of device to a 220 V mains, 13 – protective cut-out device,14 – "HOLD TIME" switch, 15 – "START" button, 16 – timer, 17 – buzzer.

The block-diagram of thermoelectric device for non-contact cooling of the human eyes is given in Fig.2, where 1 is a cooling device, 2 is an electronic control and power supply unit, 3 is a cooling surface, 4 is a temperature sensor, 5 is a thermoelectric cooling module, 6 is a liquid heat exchanger, 7 is a programmable microprocessor thermostat, 8 is a "LEFT EYE" toggle switch, 9 is a "RIGHT EYE" toggle switch, 10 is power control unit of TE cooling module, 11 is power

supply unit, 12 is a "MAINS" toggle switch– switching of the device to a 220 V mains, 13 is a protective cut-out device, 14 is a "HOLD TIME" switch, 15 is a "START" button, 16 is a timer, 17 is a buzzer.

The principle of operation of the device

The principle of operation of the device consists in non-contact cooling of the human eyes in order to treat acute and chronic eye diseases, reduce intraocular pressure, alleviate pain and inflammation.

The proposed device works as follows (Fig. 2). The operator connects the liquid heat exchangers 6 with the help of hoses to the water supply network, opens the water tap and controls the flow of water through the corresponding heat exchangers. Connects the electronic unit 2 to a grounded outlet and turns it on. Then turns on the "MAINS" toggle switch 12. On the digital indicator of the programmable microprocessor temperature controller 7, the current temperature of the cooling surfaces 3 will be displayed in red, and the value of the set temperature will be displayed in blue. Using the buttons on the thermostat, the operator sets the required cooling temperature (the value is selected experimentally). Then the operator turns on cooling the right eye with the "RIGHT EYE" toggle switch 8, or cooling the left eye with the "LEFT EYE" toggle switch 9, or selects the cooling both eyes together. Only after choosing the appropriate toggle switches 8, 9 will the cooling surfaces 3 begin to cool down. After 5 - 10 minutes, the temperature of surfaces 3 stabilizes and equals the set temperature. After that, the patient is placed in front of the cooling device 1 so that his eyes were at a distance of 1-5 cm from the cooling surfaces 3. Then the operator selects the required exposure time (temperature exposure time) with the "HOLD TIME" switch 14 and presses the "START" button 15. After the expiry of the holding time, an audible signal sounds from the buzzer 17. The procedure can be ended at this point or extended by pressing the START button again. On the case of the cooling device 1, on top for clarity, there are LED indicators of the operation of the cooling surfaces 3.

The specified device is simple, compact and reliable in operation, which allows a doctor or medical worker to use it without special training, having previously read the instructions. Thus, the technical advantages of such a device include: non-contact cooling of the surface of the human eye in real time, the ability to set and maintain the required temperature with a resolution of ±1 °C and the safety of the device.

The introduction of such a device into medical practice will be of great social and economic importance, as it will reduce the risk of ophthalmic complications, preserve the viability of patients' eye structures and ensure the provision of highly qualified care in specialized medical institutions and in extreme conditions. This, in turn, will provide appropriate conditions for preserving people's health, increase the efficiency and quality of medical care in the health care system and will become a significant contribution to the development of new domestic medical thermoelectric equipment.

It should be noted that to confirm the efficiency of the device, develop the method for treatment and clinical trials, the developed experimental prototype of device for non-contact cooling of the human eyes was transferred to the State Institution "The Filatov Institute of Eye Diseases and Tissue Therapy of the NAMS of Ukraine" within cooperation agreement. The results of clinical trials of the device will be the subject of subsequent publications on this topic.

The device is designed to treat acute and chronic eye diseases, reduce intraocular pressure, alleviate pain and inflammation of the eye. The developed thermoelectric medical device makes it possible to cool the eye structures without contact, which will allow developing and implementing the technology of controlled local therapeutic hypothermia in ophthalmology.

Conclusions

1. For the first time, a design was developed and an experimental prototype of a thermoelectric device for non-contact cooling of the human eyes was manufactured. The device is designed to treat acute and chronic eye diseases, reduce intraocular pressure, alleviate pain and inflammatory processes in the human eye. The proposed device has no analogues in the world.

2. The developed thermoelectric medical device makes it possible to carry out non-contact controlled cooling of the human eye surface in the temperature range (-25 ÷ +10) °C and in the future will allow the development and implementation of the technology of artificial non-contact controlled local therapeutic hypothermia in ophthalmology.

References

1. Fisk R.L., Gelfand E.T., Callaghan J.C. (1977). Hypothermic coronary perfusion for intraoperative cardioplegia. *Ann Thorac Surg*, 23, 58-61.

2. McDowall D.G. (1971). The current usage of hypothermia in British neurosurgery. *Br J Anaesth*, 43, 1084 – 1087.

3. Wickham J.E., Hanley H.G., Joekes A.M. (1967). Regional renal hypothermia. *Br J Urol*, 39, 727 – 743.

4. Katsimpris J. M., Xirou T., Paraskevopoulos K., et al. (2003). Effect of local hypothermia on the anterior chamber and vitreous cavity temperature: in vivo study in rabbits. *Klin. Monbl. Augenheilkd*, 220 (3), 148-151.

5. Chanchikov G.F., Zavolskaya Z.P., Bereznikova V.I. (1978. Vliianiie umerennoi lokalnoi hipotermii na ophtalmotonus, zritelnyie funktsii i gidrodinamiku glaz bolnykh glaukomoi [Influence of moderate local hypothermia on intralocular tension, visual functions and hydrodynamics of patients ill with glaucoma]. *Oftalmologicheskii Zhurnal - J. Ophthalmology*, 8, 594-597 [in Russian].

6. Lazarenko V.I., Chanchikov G.F., Kornilovskii I.M., Gaidabura V.G. (1976). Vliianiie umerennoi

lokalnoi hipotermii na hemo- i hidrodinamicheskiie pokazateli zdorovykh glaz [Influence of moderate local hypothermia on the hemo-and hydrodynamic parameters of healthy eyes]. *Oftalmologicheskii Zhurnal - J. Ophthalmology*, 6, 419-422 [in Russian].

7. Jabbour N.M., Schepens C.L., Buzney S.M. (1988). Local ocular hypothermia in experimental intraocular surgery. *Ophthalmology*, 95, 1685-1690.

8. Anatychuk L., Pasechnikova N., Naumenko V., Kobylianskyi R., Nazaretyan R., Zadorozhnyy O. (2020). Prospects of temperature management in vitreoretinal surgery.*Ther. Hypothermia Temp. Manag*. https://doi.org/10.1089/ther.2020.0019

9. Shif L.V., Taratynova A.V., Neiman V.A., Angelova N.V. (1981). Primeneniie lokalnoi gipotermii pri ostrom pristupe glaukomy i glaukome v terminalnoi stadii, oslozhnivsheisia bolevym sindromom [The use of local hypothermia in an acute attack of glaucoma and glaucoma in the terminal stage, complicated by pain]. *Oftalmologicheskii Zhurnal - J. Ophthalmology,* 3, 187-188 [in Russian].

10. Anatychuk L.I., Pasechnikova N.V., Naumenko V.O., Zadorozhnyi O.S., Nazaretian R.E., Havryliuk M.V., Tiumentsev V.A., Kobylianskyi R.R. (2019). Thermoelectric device for hyperthermia of the human eye. *J.Thermoelectricity*, 3, 64-73.

11. Anatychuk L. I., Pasechnikova N. V., Naumenko V. O., Zadorozhnyi O. S., Danyliuk S. L., Havryliuk M. V., Tiumentsev V. A., & Kobylianskyi R. R. (2020). Thermoelectric device for contact cooling of the human eye. *Physics and Chemistry of Solid State*, 21(1), 140-145.

12. Vail Yu.S., Varanovskii Ya.M. (1969). *Infrakrasnyie luchi v klinicheskoi diagnostike i mediko-biologicheskikh issledovaniiakh [Infrared rays in clinical diagnostics and biomedical research].* Leningrad: Meditsina [in Russian].

13. Avetisov S.E., Novikov I.A., Lutsevich Ye.E., Reyn E.S. (2017). Primeneniie termografii v oftalmologii [The use of thermography in ophthalmology]. *Vestnik oftalmologii – Bulletin of Ophtalmology*, 6, 99-104 [in Russian].

14. Anatychuk L.I., Pasechnikova N.V., Zadorozhnyi O.S., Kobylianskyi R.R., Havryliuk M.V., Nazaretian R.E., Mirnenko V.V. (2015). Thermoelectric device for measurement of intraocular temperature. *J.Thermoelectricity*, 3, 31-40.

15. Anatychuk L.I., Pasechnikova N.V., Zadorozhnyi O.S., Nazaretian R.E., Mirnenko V.V., Kobylianskyi R.R., Havryliuk N.V. (2015). Originalnoie ustroistvo i podkhody k izucheniiu raspredeleniia temperatury v razlichnykh otdelakh glaza [Original device and approaches to studying the temperature distribution in different parts of the eye]. *Oftalmologicheskii Zhurnal - J. Ophthalmology,* 6, 50-53 [in Russian].

16. Anatychuk L.I., Pasechnikova N.V., Kobylianskyi R.R., Havryliuk N.V., Naumenko V.A., Mirnenko V.V. Nazaretian R.E., Zadorozhnyi O.S. (2016). Termoelektricheskiie datchiki dlia registratsii vnutriglaznoi temperatury [Thermoelectric sensors for registration of intraocular temperature]. *Sensorna elektronika i mikrosystemni tekhnologii - Sensor Electronics and Microsystem Technologies*, 13(3), 30-38 [in Russian].

17. Anatychuk L.I., Pasechnikova N.V., Zadorozhnyi O.S., Kobylianskyi R.R., Nazaretian R.E., Mirnenko V.V., Havryliuk N.V. (2016). Ustroistvo dlia intraokuliarnoi termometrii i osobennosti raspredeleniia temperatury v razlichnykh otdelakh glaza krolika [A device for intraocular thermometry and features of temperature distribution in various chambers of the rabbit's eye]. *Zhurnal Natsionalnoi Akademii Medychnykh Nauk Ukrainy - J. of the National Academy of Medical Sciences of Ukraine*, 22(1), 103-108 (in Russian).

18. Anatychuk L.I.., Pasechnikova N.V., Kobylianskyi R.R., Prybyla A.V., Naumenko V.O., Zadorozhnyi O.S., Nazaretian R.E., Mirnenko V.V. (2017). Computer simulation of thermal processes in human eye. *J.Thermoelectricity*, 5, 41-58.

19. Anatychuk L.I., Pasechnikova N.V., Naumenko V.O., Zadorozhnyi O.S., Havryliuk M.V., Kobylianskyi R.R. (2018). Thermoelctric device for determination of heat flux from the surface of eyes. *J.Thermoelectricity*, 5, 52-67.

20. Anatychuk L.I., Pasechnikova N.V., Naumenko V.A., Zadorozhnyi O.S., Kobylianskyi R.R., Havryliuk N.V. (2019). Termoelektricheskoie ustroistvo dlia oftalmoteplometrii i osobennosti registratsii plotnosti teplovogo potoka glaza cheloveka [Thermoelectric device for ophthalmothermometry and features of registration of heat flux density of the human eye]. *Oftalmologicheskii Zhurnal - J. Ophthalmology,* 3, 45-51 [in Russian]. http://doi.org/10.31288/oftalmolzh201934551

21. Anatychuk L.I. (1979). *Termoelementy i termoelektricheskiie ustroistva. Spravochnik (Thermoelements and thermoelectric devices. Handbook).* Kyiv: Naukova Dumka [in Russian].

22. Anatychuk L.I. (2003). *Termoelektrichestvo. T.2. Termoelektricheskiie prepbrazovateli energii [Thermoelectricity. Vol.2. Thermoelectric power converters].* Kyiv-Chernivtsi: Institute of Thermoelectricity [in Russian].

Submitted 30.07.2020

Анатичук Л.І., *акад. НАН України*[1,2]
Пасєчнікова Н.В., *докт. мед. наук,*
член-кореспондент НАМН України [3]
Науменко В.О., *докт. мед. наук*[3]
Задорожний О.С., *докт. мед наук*[3]
Назаретян Р.Е.[3]**, Гаврилюк М.В.**[1,2]
Тюменцев В.А.[1]**, Кобилянський Р.Р.**, *канд. фіз.-мат. наук* [1,2]

[1]Інститут термоелектрики НАН і МОН України,

вул. Науки, 1, Чернівці, 58029, Україна;

e–mail: anatych@gmail.com

[2]Чернівецький національний університет

ім. Юрія Федьковича, вул. Коцюбинського 2,

Чернівці, 58012, Україна;

[3]ДУ «Інститут очних хвороб і тканинної терапії

імені В.П. Філатова НАМН України», Одеса, Україна

ТЕРМОЕЛЕКТРИЧНИЙ ПРИЛАД
ДЛЯ БЕЗКОНТАКТНОГО ОХОЛОДЖЕННЯ ОЧЕЙ ЛЮДИНИ

У роботі наведено результати розробки термоелектричного приладу для безконтактного охолодження очей людини. Прилад призначений для лікування гострих і хронічних захворювань ока, зниження внутрішньоочного тиску, зменшення больового синдрому та запальних процесів ока. Розроблений термоелектричний медичний прилад дає можливість безконтактно охолоджувати структури ока, що дозволить розробити та впровадити технологію контрольованої локальної терапевтичної гіпотермії в офтальмології. Наведено особливості конструкції приладу, принцип роботи та його технічні характеристики. Бібл. 22, рис. 2, табл. 1.

Ключові слова: термоелектричний прилад, безконтактне охолодження, гіпотермія ока людини.

Анатычук Л.И., *акад. НАН Украины*[1,2]

Пасечникова Н.В., *докт. мед. наук,*

член-корреспондент НАМН Украины [3]

Науменко В.А., *докт. мед. наук*[3]

Задорожный А.С., *докт. мед наук*[3]

Назаретян Р.Э.[3]**, Гаврилюк Н.В.**[1,2]

Тюменцев В.А.[1]**, Кобылянский Р.Р.,** *канд. физ.-мат. наук* [1,2]

[1]Институт термоэлектричества НАН и МОН Украины, ул. Науки, 1,

Черновцы, 58029, Украина, *e–mail: anatych@gmail.com;*

[2]Черновицкий национальный университет

им. Юрия Федьковича, ул. Коцюбинского, 2,

Черновцы, 58012, Украина;

[3]ГУ «Институт глазных болезней и тканевой терапии

имени В.П. Филатова АМН Украины », Одесса, Украина

ТЕРМОЭЛЕКТРИЧЕСКИЙ ПРИБОР ДЛЯ БЕСКОНТАКТНОГО ОХЛАЖДЕНИЯ ГЛАЗ ЧЕЛОВЕКА

В работе приведены результаты разработки термоэлектрического прибора для бесконтактного охлаждения глаз человека. Прибор предназначен для лечения острых и хронических заболеваний глаза, снижение внутриглазного давления, уменьшение болевого синдрома и воспалительных процессов глаза. Разработанный термоэлектрический медицинский прибор дает возможность бесконтактно охлаждать структуры глаза, что позволит разработать и внедрить технологию контролируемой локальной терапевтической гипотермии в офтальмологии. Приведены особенности конструкции прибора, принцип работы и его технические характеристики. Библ. 22, рис. 2, табл. 1.

Ключевые слова: термоэлектрический прибор, бесконтактное охлаждение, гипотермия глаза человека.

References

1. Fisk R.L., Gelfand E.T., Callaghan J.C. (1977). Hypothermic coronary perfusion for intraoperative cardioplegia. *Ann Thorac Surg*, 23, 58-61.

2. McDowall D.G. (1971). The current usage of hypothermia in British neurosurgery. *Br J Anaesth*, 43, 1084 – 1087.

3. Wickham J.E., Hanley H.G., Joekes A.M. (1967). Regional renal hypothermia. *Br J Urol*, 39, 727 – 743.

4. Katsimpris J. M., Xirou T., Paraskevopoulos K., et al. (2003). Effect of local hypothermia on the anterior chamber and vitreous cavity temperature: in vivo study in rabbits. *Klin. Monbl. Augenheilkd*, 220 (3), 148-151.

5. Chanchikov G.F., Zavolskaya Z.P., Bereznikova V.I. (1978. Vliianiie umerennoi lokalnoi hipotermii na ophtalmotonus, zritelnyie funktsii i gidrodinamiku glaz bolnykh glaukomoi [Influence of moderate local hypothermia on intralocular tension, visual functions and hydrodynamics of patients ill with glaucoma]. *Oftalmologicheskii Zhurnal - J. Ophthalmology*, 8, 594-597 [in Russian].

6. Lazarenko V.I., Chanchikov G.F., Kornilovskii I.M., Gaidabura V.G. (1976). Vliianiie umerennoi lokalnoi hipotermii na hemo- i hidrodinamicheskiie pokazateli zdorovykh glaz [Influence of moderate local hypothermia on the hemo-and hydrodynamic parameters of healthy eyes]. *Oftalmologicheskii Zhurnal - J. Ophthalmology*, 6, 419-422 [in Russian].

7. Jabbour N.M., Schepens C.L., Buzney S.M. (1988). Local ocular hypothermia in experimental intraocular surgery. *Ophthalmology*, 95, 1685-1690.

8. Anatychuk L., Pasechnikova N., Naumenko V., Kobylianskyi R., Nazaretyan R., Zadorozhnyy O. (2020). Prospects of temperature management in vitreoretinal surgery.*Ther. Hypothermia Temp. Manag*. https://doi.org/10.1089/ther.2020.0019

9. Shif L.V., Taratynova A.V., Neiman V.A., Angelova N.V. (1981). Primeneniie lokalnoi gipotermii pri ostrom pristupe glaukomy i glaukome v terminalnoi stadii, oslozhnivsheisia bolevym sindromom [The use of local hypothermia in an acute attack of glaucoma and glaucoma in the terminal stage, complicated by pain]. *Oftalmologicheskii Zhurnal - J. Ophthalmology,* 3, 187-188 [in Russian].

10. Anatychuk L.I., Pasechnikova N.V., Naumenko V.O., Zadorozhnyi O.S., Nazaretian R.E., Havryliuk M.V., Tiumentsev V.A., Kobylianskyi R.R. (2019). Thermoelectric device for hyperthermia of the human eye. *J.Thermoelectricity*, 3, 64-73.

11. Anatychuk L. I., Pasechnikova N. V., Naumenko V. O., Zadorozhnyi O. S., Danyliuk S. L., Havryliuk M. V., Tiumentsev V. A., & Kobylianskyi R. R. (2020). Thermoelectric device for contact cooling of the human eye. *Physics and Chemistry of Solid State*, 21(1), 140-145.

12. Vail Yu.S., Varanovskii Ya.M. (1969). *Infrakrasnyie luchi v klinicheskoi diagnostike i mediko-biologicheskikh issledovaniiakh [Infrared rays in clinical diagnostics and biomedical research].* Leningrad: Meditsina [in Russian].

13. Avetisov S.E., Novikov I.A., Lutsevich Ye.E., Reyn E.S. (2017). Primeneniie termografii v oftalmologii [The use of thermography in ophthalmology]. *Vestnik oftalmologii – Bulletin of Ophtalmology*, 6, 99-104 [in Russian].

14. Anatychuk L.I., Pasechnikova N.V., Zadorozhnyi O.S., Kobylianskyi R.R., Havryliuk M.V., Nazaretian R.E., Mirnenko V.V. (2015). Thermoelectric device for measurement of intraocular temperature. *J.Thermoelectricity*, 3, 31-40.

15. Anatychuk L.I., Pasechnikova N.V., Zadorozhnyi O.S., Nazaretian R.E., Mirnenko V.V., Kobylianskyi R.R., Havryliuk N.V. (2015). Originalnoie ustroistvo i podkhody k izucheniiu raspredeleniia temperatury v razlichnykh otdelakh glaza [Original device and approaches to studying the temperature distribution in different parts of the eye]. *Oftalmologicheskii Zhurnal - J. Ophthalmology,* 6, 50-53 [in Russian].

16. Anatychuk L.I., Pasechnikova N.V., Kobylianskyi R.R., Havryliuk N.V., Naumenko V.A., Mirnenko V.V. Nazaretian R.E., Zadorozhnyi O.S. (2016). Termoelektricheskiie datchiki dlia registratsii vnutriglaznoi temperatury [Thermoelectric sensors for registration of intraocular temperature]. *Sensorna elektronika i mikrosystemni tekhnologii - Sensor Electronics and Microsystem Technologies*, 13(3), 30-38 [in Russian].

17. Anatychuk L.I., Pasechnikova N.V., Zadorozhnyi O.S., Kobylianskyi R.R., Nazaretian R.E., Mirnenko V.V., Havryliuk N.V. (2016). Ustroistvo dlia intraokuliarnoi termometrii i osobennosti raspredeleniia temperatury v razlichnykh otdelakh glaza krolika [A device for intraocular thermometry and features of temperature distribution in various chambers of the

rabbit's eye]. *Zhurnal Natsionalnoi Akademii Medychnykh Nauk Ukrainy - J. of the National Academy of Medical Sciences of Ukraine*, 22(1), 103-108 (in Russian].

18. Anatychuk L.I.., Pasechnikova N.V., Kobylianskyi R.R., Prybyla A.V., Naumenko V.O., Zadorozhnyi O.S., Nazaretian R.E., Mirnenko V.V. (2017). Computer simulation of thermal processes in human eye. *J.Thermoelectricity*, 5, 41-58.

19. Anatychuk L.I., Pasechnikova N.V., Naumenko V.O., Zadorozhnyi O.S., Havryliuk M.V., Kobylianskyi R.R. (2018). Thermoelctric device for determination of heat flux from the surface of eyes. *J.Thermoelectricity*, 5, 52-67.

20. Anatychuk L.I., Pasechnikova N.V., Naumenko V.A., Zadorozhnyi O.S., Kobylianskyi R.R., Havryliuk N.V. (2019). Termoelektricheskoie ustroistvo dlia oftalmoteplometrii i osobennosti registratsii plotnosti teplovogo potoka glaza cheloveka [Thermoelectric device for ophthalmothermometry and features of registration of heat flux density of the human eye]. *Oftalmologicheskii Zhurnal - J. Ophthalmology,* 3, 45-51 [in Russian]. http://doi.org/10.31288/oftalmolzh201934551

21. Anatychuk L.I. (1979). *Termoelementy i termoelektricheskiie ustroistva. Spravochnik (Thermoelements and thermoelectric devices. Handbook).* Kyiv: Naukova Dumka [in Russian].

22. Anatychuk L.I. (2003). *Termoelektrichestvo. T.2. Termoelektricheskiie prepbrazovateli energii [Thermoelectricity. Vol.2. Thermoelectric power converters].* Kyiv-Chernivtsi: Institute of Thermoelectricity [in Russian].

L.I.Anatychuk *acad. National Academy*
of sciences of Ukraine[1,2]
A.V. Prybyla, *cand. phys.- math. Sciences*[1,2]
Kibak A.M.[1]

[1]Institute of Thermoelectricity
of the NAS and MES of Ukraine,
1, Nauky str., Chernivtsi, 58029, Ukraine;
e-mail: anatych@gmail.com
[2]Yu.Fedkovych Chernivtsi National University,
2, Kotsiubynskyi str., Chernivtsi, 58000, Ukraine

THERMOELECTRIC AIR CONDITIONERS FOR VEHICLE SEATS

The paper discusses the prospects of thermoelectric air conditioning of vehicle seats, which can be used to save energy resources and improve the temperature conditions of a person's stay in a vehicle. To determine the most rational options for using these air conditioners, their classification was carried out depending on the method of thermoelectric air conditioning. Bibl. 30, Fig. 4.
Key words: thermoelectric air conditioner, thermoelectric heat pump, air conditioning, thermal conditions.

Introduction

General characterization of the problem. In recent decades, the number of vehicles is growing rapidly. According to the analytical company Navigant Research, today their number has exceeded 1.2 billion units, and by the end of 2035 the figure could reach 2 billion [1]. At the same time, due to the intensity of traffic, people spend more and more of their time in it. For this reason, there is a need to ensure optimal thermal comfort of the person while in the vehicle, and hence the need to create air conditioners.

In [2-8], various methods of air conditioning in vehicles are considered, each of which has its own advantages and disadvantages. Thus, in [8], a comparison was made between the use of compression and thermoelectric air conditioners and the advantages of each were shown depending on climatic conditions. Despite the different methods of air conditioning, it is common that air conditioning occurs for the entire volume of transport. This leads to increased electricity costs and the problem of airflow distribution, as drivers or passengers feel comfortable for those parts of the body that are directly facing the air outlet. In so doing, ordinary seats will act as an insulator, reducing the cooling of the body, preventing the evaporation of sweat and raising the skin temperature in contact with the seat surface [9].

To solve these problems, it is advisable to use local air conditioning, namely air conditioning of the vehicle seat. This option will provide a comfortable environment with lower energy costs and solve the problem associated with the distribution of airflow.

In the literature, there are various options for air conditioning of vehicle seats [10 - 15], among which air conditioning with the use of thermoelectric converters has become widespread. This is due to the presence in such converters of a number of advantages, namely: high reliability, the ability to provide cooling and heating, the absence of harmful refrigerants, low maintenance cost, possibility of temperature control in a wide range [16]. In so doing, of particular interest is the possibility of using thermoelectric air conditioning for operators of armored vehicles, including tanks, which will optimize the thermal conditions for the stay of tankers during combat operations.

Based on the foregoing, it seems important to consider the known methods of thermoelectric conditioning of transport seats in order to highlight the most rational options. The latter is reduced to the study and analysis of the known options of thermoelectric air conditioners for vehicle seats and their classification according to the thermal scheme.

Analysis of the literature. Active work is underway to create thermoelectric air conditioners for car seats in many countries around the world. Thus, in [17] a temperature controlled seat was developed, powered by an exhaust thermoelectric heat recovery system. A series of experiments, including bench and real vehicle tests, showed that the thermoelectric system was able to reduce the temperature of the seat surface by 14.59% after the temperature controlled seat was operated for 10 minutes.

In [18], a thermoelectric system was created, which was used for climate control of car seats. Experimental results showed that the system reduces the temperature of the air pumped to the seat by about 9 ° C at a performance factor of about $\varepsilon = 0.41$, while the results of the heating mode showed that the device can increase the air temperature by about 34 °C at $\varepsilon = 1.34$.

In [19], a thermoelectric device for regulating the temperature of the surface of a car seat was modeled and designed. The test results showed that at a voltage of 12 V, the thermoelectric system can reduce the seat temperature by about 18 °C in cooling mode and increase it by 22 °C in heating mode.

In [20], an automated seat cooling system for cars using a thermoelectric device was developed, which is aimed at preventing the death and injury of young children left unattended in parked cars at high ambient temperatures. An experimental series of tests has shown the high efficiency of the system.

In [21], a seat with variable temperature was developed and tested using a thermoelectric cooler to increase thermal comfort and reduce fuel consumption. Experimental results have shown that at an ambient temperature of 27 °C, such a system can remove approximately 33.3 watts of power from the conditioned air pumped to the seat.

In [22], the authors applied an optimal design method to develop thermoelectric air-liquid conditioning and managed to obtain a performance factor of 1.68 at the same input power. This optimal design method used dimensional analysis to optimize the applied current and the geometric

ratio of the thermocouple (or the number of pairs of thermocouples) simultaneously for a given set of fixed parameters.

In [23], a thermoelectric system for regulating the temperature of a car seat was developed and tested to provide rapid cooling and heating. Experimental tests have shown that the thermoelectric system has the advantage of accelerating the cooling of the car seat from 50 °C to about 6 °C with a significant response time.

All of the above listed thermoelectric options for air conditioning of vehicle seats have their own strengths and weaknesses. Considering that the need for further research related to the use of thermoelectric air conditioning will only grow, it is necessary to classify and systematize the known options of such air conditioning with the subsequent determination of more rational ones.

The purpose of the proposed work is to analyze the known options of thermoelectric air conditioners for vehicle seats and determine the most rational ones.

Companies engaged in the production of serial samples of air conditioners for car seats

One of the leaders in the field of thermoelectric air conditioning of transport seats is the American company *Gentherm Incorporated*, formerly *Amerigon*. The company has created the world's first system of seats with thermoelectric heating and cooling for the automotive industry. The developed system was named "Seat Climate Control" and was first adopted by the *Ford Motor Company* as an option for the *Lincoln Navigato 2000*. Today this system is available in more than 50 vehicles, such as Ford, General Motors, Toyota (Lexus), Kia, Hyundai, Nissan (Infinity), Range Rover, Jaguar, Land Rover, etc.

In one of the company's patented technology, the climate control system includes a thermoelectric device based on a metal plate that heats up on one side and cools down on the other [14]. The heat exchange between the heat generated or absorbed by the Peltier element and the air transferred from the fan is due to the heat exchangers. The housing, which accommodates the Peltier elements and the heat exchanger, includes special parts that are connected to a tube for supplying air from the fan to the seat temperature controller and for connection to the exhaust pipe.

Today, *Gentherm Incorporated* is not only the world's leading company in thermoelectric cooling and heating of car seats, but also one of the best among its competitors that use other ways of air conditioning. The company cooperates with almost all well-known automotive manufacturers, therefore, as the case requires, it has a variety of options for its products. The company currently owns many patents for thermoelectric cooling / heating of car seats.

The Indian company *Dhama Innovations* has developed a thermoelectric temperature control system for car seats [25]. The product is called *Dhama Comfort* and is a temperature-controlled seat that connects to the car's battery. The user can adjust the temperature level in any mode. *Dhama Comfort* is based on *Climacon* technology, which is a small unit consisting of a thermoelectric module and specially designed heat sinks. These units are placed in the seat to provide thermal

comfort anywhere. Today, *Dhama Innovations* seats are installed in many cars and trucks. Studies have shown that the use of such seats creates optimal temperature conditions. Moreover, drivers feel less tired, which allows them to drive longer.

The use of special covers (cushions) for car seats has become widespread. Such products do not require significant costs and are suitable for all types of car seats.   The products of the Beijing company *Huimao Cooling Equipment Co., Ltd* are in the greatest demand among cushions [26]. The company has been working in the global market since 1996. It specializes in the research, development and manufacture of thermoelectric cooling modules and components.

The American company Arizon Line-X is also developing seat cushions for drivers [27]. Their developments allow reducing fuel consumption. The companies estimate that such savings in the future may even offset the cost of purchasing a seat cushion. There is also an AC power adapter included so that you can use it in the office or at home.

Another American company, *Tempronics*, was founded with the invention of the **Climate Ribbon** [28]**.** Initially, it focused on the development and patenting of technology, and then moved to the market. The main product is the Tempronics personal climate system, PCS 200. This thermoelectric technology allows one to maintain a comfortable temperature in the form of a personal cover used in the cars for cooling or heating.

Classification of thermoelectric air conditioners for vehicle seats

In the proposed work, the classification of thermoelectric air conditioners for vehicle seats is based on two main features: the method of cooling or heating (air or liquid) and the method of removing unwanted waste heat (in the car or outside the vehicle).

Scheme A. The first classification option is shown in Fig. 1. Considered is thermoelectric seat conditioning using air cooling while removing unwanted waste heat into the car cabin.

Fig.1. Option of thermoelectric air conditioning of a seat with the use of air cooling when removing heat to a car cabin: 1 – schematic image of a passenger, 2 – cold loop radiator, |3 – hot loop radiator, 4 – thermoelectric modules, 5 – air fans, 6 – air radiators, 7 – schematic image of a transport seat, 8 – schematic image of a car cabin.

Scheme A works in cooling mode. To switch to heating mode, you only need to change the direction of electric current supply to the thermoelectric modules. In this mode, the fans 5 inject air through the radiators 2 and 3, which dissipate the cold and hot heat flow from the thermoelectric modules 4. The cooled air passes through a system of air ducts to the seat 7, where it exits via the radiators 6 through the seat surface thus cooling the passenger. The heated air is discharged through a special duct system directly into the cabin. In this case, the temperature inside the cabin will not change significantly, and the cooling or heating effect will only take place for the people who are on the seat.

In [13 – 15], the described method of seat conditioning was used, but with certain variations in the very design of the thermoelectric system. Thus, for instance, [11] describes a scheme consisting of a rear seat heat pump that regulates the temperature of the air passing through the seat back and a lower seat heat pump for air conditioning passing through the lower part of the seat. These two pumps contain a thermoelectric device, a main heat exchanger and heat exchangers for waste heat. Attached to one end of each main heat exchanger is an outlet from the main fan, which is used to transfer conditioned air to the back or lower part of the seat. The outlet end of each main heat exchanger is connected to an air duct, which in turn is connected to the corresponding air inlet in the rear seat or the air inlet in the lower part of the seat. Attached to one end of each waste heat exchanger is an outlet from a fan that serves to transfer unwanted waste heat to the outside. Temperature sensors are attached to the side of the main heat exchanger in each heat pump. Each temperature sensor can contain an electric thermocouple.

Scheme B. Another classification option is shown in Fig. 2. Thermoelectric air conditioning of the seat with the use of air cooling during the removal of unwanted waste heat to the environment outside the vehicle is considered.

The operating principle of scheme B is similar to scheme A and differs only in that the unwanted waste heat is not removed in the middle, but outside the car. Also, on the inlet side of the air duct for unwanted heat it is possible to place the inlet for air supply outside the vehicle. The advantage of this method is that the temperature inside the vehicle can change, as unwanted heat will be released into the environment. Despite this, in the literature reviewed, very few works use this conditioning scheme. This is mainly due to the complexity of the implementation of additional holes.

In [29], a thermoelectric air conditioner for a vehicle seat using circuit B is described. One of the main parts of such an air conditioner includes an electric fan and a thermoelectric unit. An air duct and a fan are provided. On the inlet side of the air duct there are inlets for air supply outside the vehicle and internal inlets for air supply inside the vehicle. The ratio of mixing the external and internal air is switched by the corresponding dampers. The described air conditioner is controlled by a control unit, which receives signals from temperature sensors. In one aspect of the invention, the removal of unwanted waste heat outside the vehicle is provided.
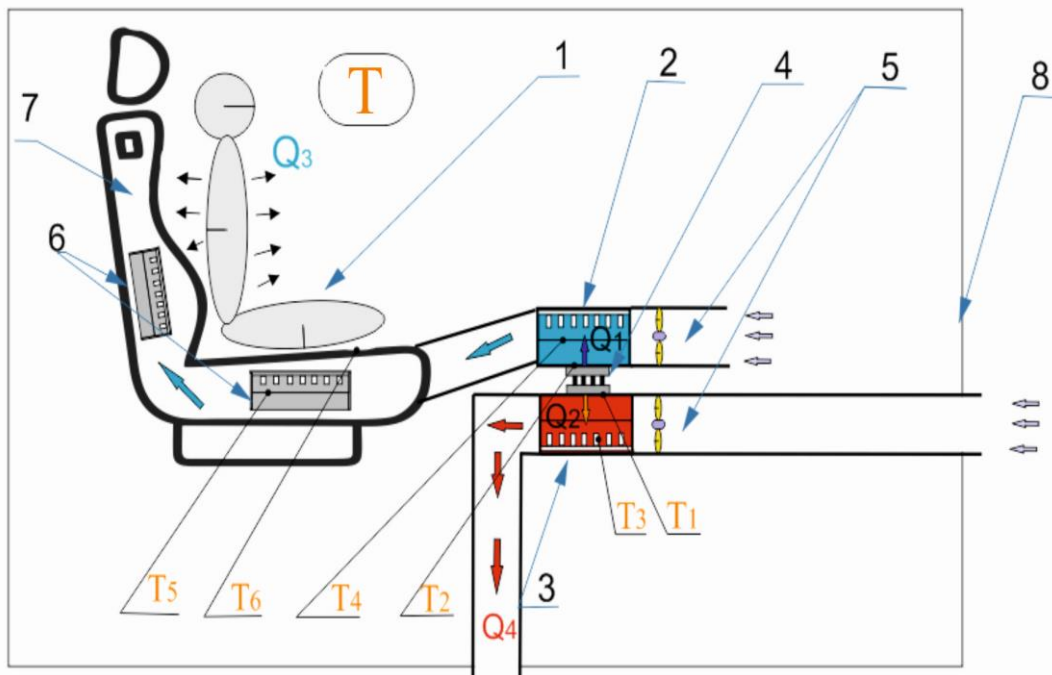
Fig.2. Option of thermoelectric air conditioning of a seat with the use of air
cooling when removing heat to environment outside the vehicle;
1 – schematic image of a passenger; 2 – cold loop radiator;
3 – hot loop radiator; 4 – thermoelectric modules;
5 – air fans; 6 – air radiators; 7 – schematic image of
a transport seat; 8 – schematic image of a car cabin

Scheme C. The next classification option is shown in Fig. 3. The paper considers thermoelectric seat conditioning using liquid cooling while dissipating unwanted waste heat into the vehicle cabin.

The difference between the operating principle of such air conditioning and those discussed earlier, is the presence of a liquid cooling system. Thermoelectric modules cool (or heat) the liquid, which circulates through a closed system by means of a liquid pump. The cooled (or heated) liquid passes through the seats creating the necessary temperature conditions for drivers or passengers. Unwanted heat is dissipated in the cabin of the car.

Ref. [30] describes a special heating and cooling system for the seat, which works in a similar way. The system consists of a thermoelectric device that selectively cools or heats a liquid-filled heat exchanger. The liquid is sucked in by the pump through the reel on a seat. The coil transfers heat by passing it through the seat to the passenger. The controller allows one to select the heating or cooling temperature. The switch determines the polarity of the voltage applied to the thermoelectric device.

Scheme D. The last classification option is shown in Fig. 4. Considered is thermoelectric seat conditioning using liquid cooling while dissipating unwanted waste heat to the environment outside the vehicle.
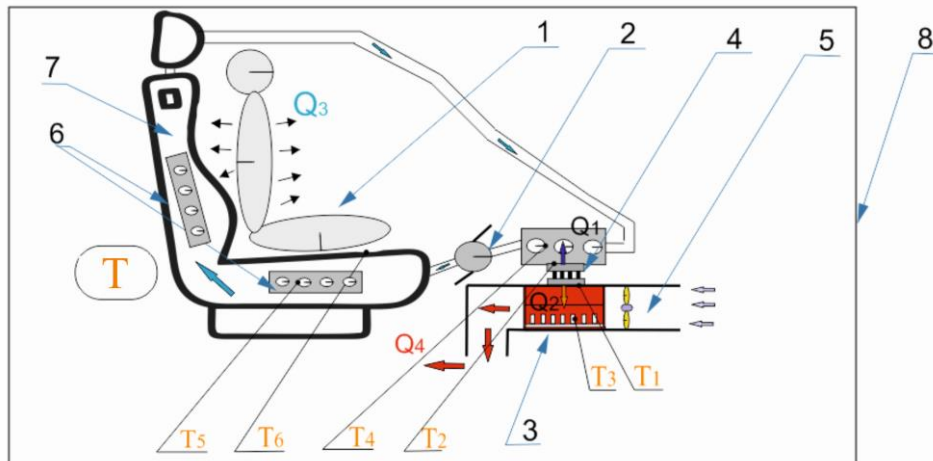
Fig.3. Option of thermoelectric air conditioning of a seat with the use of liquid cooling when removing heat to a car cabin: 1 – schematic image of a passenger, 2 – liquid pump, 3 – hot loop radiaty, 4 – thermoelectric modules, 5 – air fan, 6 – cooling system elements, 7 – schematic image of a transport seat, 8 – schematic image of a car cabin.

The operating principle of scheme D is similar to that of scheme C and differs only in that the unwanted waste heat is removed outside the car. Also, on the inlet side of the air duct for unwanted heat it is possible to place the inlet for suction of air outside the vehicle. This option of air conditioning is hardly considered in the scientific literature, despite the fact that it is the most effective in air conditioning. This is mainly due to the complexity of the implementation process.
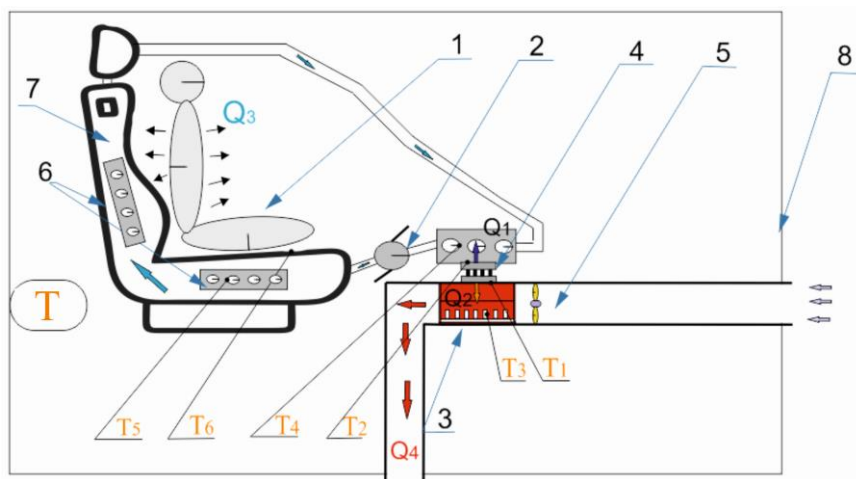

Fig.4. Option of thermoelectric air conditioning of a seat with the use of liquid cooling when removing heat to environment outside the vehicle: 1 – schematic image of a passenger, 2 – liquid pump, 3 – hot loop radiator, 4 – thermoelectric modules, 5 – air fan, 6 – cooling system elements, 7 – schematic image of a transport seat, 8 – schematic image of a car cabin.

Analysis of the most rational options of thermoelectric air conditioners for vehicle seats

A number of important conclusions can be drawn from the literature analysis and classification of thermoelectric air conditioning schemes described in the previous section. The most widespread is

the option of scheme *A* – thermoelectric air conditioning of the seat using air cooling with heat dissipation in the car cabin. This is due to the simplicity of this scheme, as such a thermoelectric air conditioner is universal and autonomous and does not require additional changes in the design of the car. However, this scheme has its drawbacks. The largest of these is that the overall cooling efficiency will be lower than in the options of schemes *B* and *D*, because the waste heat will not be dissipated into the environment, but will lead to a small increase in the overall temperature inside the car.

The air conditioner which works according to the option of scheme *D*, has the highest efficiency. Its advantage over the option of scheme B is the removal of waste heat outside the vehicle, and the advantages over the options of scheme **A** and *B* is the greater efficiency of the selected method of cooling. Moreover, this option is the most difficult to implement, since special holes for waste heat must be provided in addition to the overall liquid cooling system. Therefore, today such a method of conditioning has not been implemented commercially, although research is underway to introduce it into production.

Depending on the process of implementing thermoelectric air conditioning for car seats, there are two most appropriate options. If the priority in the production of such an air conditioner is its autonomy and lack of binding to a particular vehicle design, then scheme *A* is the best option. In this case, it is necessary to understand the losses in the efficiency of such an air conditioner.

The most appropriate in terms of energy efficiency is the option of scheme *D*, but in this case it is necessary to design and optimize the thermoelectric air conditioner in conjunction with the development of the vehicle itself.

Conclusions

1. The most rational options of thermoelectric air conditioners for vehicle seats are determined.
2. Using the option of scheme A is the most rational in the development of autonomous and universal air conditioning system, which can be used for any seat of an existing car. This will ensure the mass use of such air conditioners.
3. The most appropriate in terms of energy efficiency is the option of scheme D, but in this case it is necessary to design and optimize the thermoelectric air conditioner in conjunction with the development of the vehicle itself.

References

1. https://www.autonews.ru/news/5c9114d69a7947491f827c6e
2. Lee M.Y., Lee D.Y. (2013). Review on conventional air conditioning, alternative refrigerants and CO2 heat pumps for vehicles. *Adv. Mech. Eng*., 5, 713924
3. Lee H.S., Lee M.Y. (2013). Cooling performance characteristics on mobile air-conditioning system for hybrid electric vehicles. *Adv. Mech. Eng*., 5, 282313.
4. Ma G.Y. (1998). Study on thermoelectric air conditioning for electric vehicles. *Refrig. Air Cond*., 14, 5 – 10

5. Qi Z.G. (2014). Advances on air conditioning and heat pump system in electric vehicles – A review. *Renew. Sustain. Energy Rev.*, 38, 754–764.

6. Qinghong Peng and Qungui Du. (2016). Progress in heat pump air conditioning systems for electric vehicles – A Review. *Open Access Energies*, 9(4), 240; doi: 10.3390/en9040240.

7. Rozver Yu.Yu. (2003). Thermoelectric air conditioner for vehicles. *J.Thermoelectricity*, 2, 52 – 56.

8. Anatychuk L.I., Prybyla A.V. (2019). On the efficiency of thermoelectric air conditioners for vehicles. *J. Thermoelectricity*, 1, 86 – 94.

9. Chuqi Su, Wenbin Dong, Yadong Deng, Yiping Wang. (2017). Numerical and experimental investigation on the performance of a thermoelectric cooling automotive seat. *Journal of Electronic Materials*; DOI: 10.1007/s11664-017-5960-4

10. *Pat US6119463A* (2001). Lon Bell. Thermoelectric heat exchanger.

11. *Pat US5524439A* (1993). David F. Gallup, David R. Noles, Richard R. Willis. Variable temperature seat climate control system

12. *Pat US20050161193A1* (2004). Chris McKenzie, Danny Bates. Seat heating and cooling system.

13. *Pat US7827805B2* (1998). Brian Comiskey, John Terech. Seat climate control system.

14. *Pat US5924766A* (1998). Hidenori Esaki, Tomohide Kudo, Takeshi Shiba. Temperature conditioner for vehicle seat.

15. *Pat US4923248A* (1998). Steve Feher. Cooling and heating seat pad construction.

16. *Pat US5921314A* (1996). Ferdinand Schuller, Hans-Georg Rauh, Gunter Lorenzen, Michael Weiss. Conditioned seat.

17. Du H., Wang Y.P., Yuan X.H., Deng Y.D., Su C.Q. (2016). Experimental investigation of a temperature-controlled car seat powered by an exhaust thermoelectric generator. *Journal of Electronic Materials*, 45(3).

18. Elarysi Abdulmunaem, Attar Alaa, Lee Hosung. (2017). Analysis and experimental investigation of optimum design of thermoelectric cooling/heating system for car seat climate control (CSCC). *Journal of Electronic Materials*; DOI: 10.1007/s11664-017-5854-5

19. Choi H.S., Yun S., and Whang K.I. (2007). *Appl. Therm. Eng.* 27, 2841.

20. Vinoth M. and Prema D. (2014). *2014 International Conference on Computation of Power, Energy, Information and Communication (ICCPEIC),* vol. 188.

21. Feher Steve (1993). Thermoelectric air conditioned variable temperature seat (VTS) and effect upon vehicle occupant comfort, vehicle energy efficiency, and vehicle environmental compatibility. *SAE Technical Paper*, 931111.

22. Attar Alaa, Lee Hosung, Weera Sean (2015). Experimental validation of the optimum design of an automotive air-to-air thermoelectric air conditioner (TEAC). *Journal of Electronic Materials*; DOI: 10.1007/s11664-015-3750-4

23. Menon M., Asada H. Harry. (2006). Iterative learning control of shape memory alloy actuators with thermoelectric temperature regulation for a multifunctional car seat. *Proceedings of the 2006 American Control Conference Minneapolis* (Minnesota, USA, June 14-16, 2006).

24. https://www.gentherm.com/en/home

25. https://www.dhamainnovations.com/seating
26. http://www.huimao.com/about/show.php?lang=en&id=2
27. http://arizonaline-x.com/about.html
28. https://tempronics-pcs.com/
29. *Pat JP3637395B2* (1997). David Knolls, Yoshihiko Hotta .Vehicle air conditioner and seat heating / cooling device.
30. *Pat US5117638A* (1991). Steve Feher. Selectively cooled or heated seat construction and apparatus for providing temperature conditioned fluid and method therefor.

Анатичук Л.І., *акад. НАН України*[1,2]
Прибила А.В. *канд. фіз.-мат. наук*[1,2], **Кібак А.М.**[1]

[1]Інститут термоелектрики НАН і МОН України,
вул. Науки, 1, Чернівці, 58029, Україна;
e-mail: anatych@gmail.com;
[2]Чернівецький національний університет
ім. Юрія Федьковича, вул. Коцюбинського 2,
Чернівці, 58000, Україна

ТЕРМОЕЛЕКТРИЧНІ КОНДИЦІОНЕРИ ДЛЯ СИДІНЬ АВТОТРАНСПОРТУ

У роботі розглядаються перспективи використання термоелектричного кондиціонування сидінь автотранспорту, якими може бути здійснена економія енергетичних ресурсів та покращення температурних умов перебування людини у транспортному засобі. Для визначення найбільш раціональних варіантів використання даних кондиціонерів здійснено їх класифікацію в залежності від способу термоелектричного кондиціонування. Бібл. 30, рис. 4.

Ключові слова: термоелектричний кондиціонер, термоелектричний тепловий насос, кондиціонування, теплові умови.

Анатычук Л.И., *акад. НАН Украины*[1,2]
Прибыла А.В., *канд. физ.-мат. наук*[1,2]
Кибак А.М.[1]

[1]Институт термоэлектричества НАН и МОН Украины,
ул. Науки, 1, Черновцы, 58029, Украина,
e–mail: anatych@gmail.com;
[2]Черновицкий национальный университет
им. Юрия Федьковича, ул. Коцюбинского, 2,
Черновцы, 58012, Украина

ТЕРМОЭЛЕКТРИЧЕСКИЕ КОНДИЦИОНЕРЫ ДЛЯ СИДЕНИЙ АВТОТРАНСПОРТА

В работе рассматриваются перспективы использования термоэлектрического кондиционирования сидений автотранспорта, при помощи которого могут быть осуществлены экономия энергетических ресурсов и улучшение температурных условий пребывания человека в транспортном средстве. Для определения наиболее рациональных вариантов использования данных кондиционеров осуществлена их классификация в зависимости от способа термоэлектрического кондиционирования. Библ. 30, рис. 4.

Ключевые слова: термоэлектрический кондиционер, термоэлектрический тепловой насос, кондиционирование, тепловые условия.

References

1. https://www.autonews.ru/news/5c9114d69a7947491f827c6e

2. Lee M.Y., Lee D.Y. (2013). Review on conventional air conditioning, alternative refrigerants and CO2 heat pumps for vehicles. *Adv. Mech. Eng.*, 5, 713924

3. Lee H.S., Lee M.Y. (2013). Cooling performance characteristics on mobile air-conditioning system for hybrid electric vehicles. *Adv. Mech. Eng.*, 5, 282313.

4. Ma G.Y. (1998). Study on thermoelectric air conditioning for electric vehicles. *Refrig. Air Cond.*, 14, 5 – 10

5. Qi Z.G. (2014). Advances on air conditioning and heat pump system in electric vehicles – A review. *Renew. Sustain. Energy Rev.*, 38, 754–764.

6. Qinghong Peng and Qungui Du. (2016). Progress in heat pump air conditioning systems for electric vehicles – A Review. *Open Access Energies*, 9(4), 240; doi: 10.3390/en9040240.

7. Rozver Yu.Yu. (2003). Thermoelectric air conditioner for vehicles. *J.Thermoelectricity*, 2, 52 – 56.

8. Anatychuk L.I., Prybyla A.V. (2019). On the efficiency of thermoelectric air conditioners for vehicles. *J. Thermoelectricity*, 1, 86 – 94.

9. Chuqi Su, Wenbin Dong, Yadong Deng, Yiping Wang. (2017). Numerical and experimental investigation on the performance of a thermoelectric cooling automotive seat. *Journal of Electronic Materials*; DOI: 10.1007/s11664-017-5960-4

10. *Pat US6119463A* (2001). Lon Bell. Thermoelectric heat exchanger.

11. *Pat US5524439A* (1993). David F. Gallup, David R. Noles, Richard R. Willis. Variable

temperature seat climate control system

12. *Pat US20050161193A1* (2004). Chris McKenzie, Danny Bates. Seat heating and cooling system.

13. *Pat US7827805B2* (1998). Brian Comiskey, John Terech. Seat climate control system.

14. *Pat US5924766A* (1998). Hidenori Esaki, Tomohide Kudo, Takeshi Shiba. Temperature conditioner for vehicle seat.

15. *Pat US4923248A* (1998). Steve Feher. Cooling and heating seat pad construction.

16. *Pat US5921314A* (1996). Ferdinand Schuller, Hans-Georg Rauh, Gunter Lorenzen, Michael Weiss. Conditioned seat.

17. Du H., Wang Y.P., Yuan X.H., Deng Y.D., Su C.Q. (2016). Experimental investigation of a temperature-controlled car seat powered by an exhaust thermoelectric generator. *Journal of Electronic Materials*, 45(3).

18. Elarysi Abdulmunaem, Attar Alaa, Lee Hosung. (2017). Analysis and experimental investigation of optimum design of thermoelectric cooling/heating system for car seat climate control (CSCC). *Journal of Electronic Materials*; DOI: 10.1007/s11664-017-5854-5

19. Choi H.S., Yun S., and Whang K.I. (2007). *Appl. Therm. Eng.* 27, 2841.

20. Vinoth M. and Prema D. (2014). *2014 International Conference on Computation of Power, Energy, Information and Communication (ICCPEIC),* vol. 188.

21. Feher Steve (1993). Thermoelectric air conditioned variable temperature seat (VTS) and effect upon vehicle occupant comfort, vehicle energy efficiency, and vehicle environmental compatibility. *SAE Technical Paper*, 931111.

22. Attar Alaa, Lee Hosung, Weera Sean (2015). Experimental validation of the optimum design of an automotive air-to-air thermoelectric air conditioner (TEAC). *Journal of Electronic Materials*; DOI: 10.1007/s11664-015-3750-4

23. Menon M., Asada H. Harry. (2006). Iterative learning control of shape memory alloy actuators with thermoelectric temperature regulation for a multifunctional car seat. *Proceedings of the 2006 American Control Conference Minneapolis* (Minnesota, USA, June 14-16, 2006).

24. https://www.gentherm.com/en/home

25. https://www.dhamainnovations.com/seating

26. http://www.huimao.com/about/show.php?lang=en&id=2

27. http://arizonaline-x.com/about.html

28. https://tempronics-pcs.com/

29. *Pat JP3637395B2* (1997). David Knolls, Yoshihiko Hotta .Vehicle air conditioner and seat heating / cooling device.

30. *Pat US5117638A* (1991). Steve Feher. Selectively cooled or heated seat construction and apparatus for providing temperature conditioned fluid and method therefor.

ARTICLE SUBMISSION GUIDELINES

For publication in a specialized journal, scientific works are accepted that have never been printed before. The article should be written on an actual topic, contain the results of an in-depth scientific study, the novelty and justification of scientific conclusions for the purpose of the article (the task in view).

The materials published in the journal are subject to internal and external review which is carried out by members of the editorial board and international editorial board of the journal or experts of the relevant field. Reviewing is done on the basis of confidentiality. In the event of a negative review or substantial remarks, the article may be rejected or returned to the author(s) for revision. In the case when the author(s) disagrees with the opinion of the reviewer, an additional independent review may be done by the editorial board. After the author makes changes in accordance with the comments of the reviewer, the article is signed to print.

The editorial board has the right to refuse to publish manuscripts containing previously published data, as well as materials that do not fit the profile of the journal or materials of research pursued in violation of ethical norms (for instance, conflicts between authors or between authors and organization, plagiarism, etc.). The editorial board of the journal reserves the right to edit and reduce the manuscripts without violating the author's content. Rejected manuscripts are not returned to the authors.

Submission of manuscript to the journal

The manuscript is submitted to the editorial office of the journal in paper form in duplicate and in electronic form on an electronic medium (disc, memory stick). The electronic version of the article shall fully correspond to the paper version. The manuscript must be signed by all co-authors or a responsible representative.

In some cases it is allowed to send an article by e-mail instead of an electronic medium (disc, memory stick).

English-speaking authors submit their manuscripts in English. Russian-speaking and Ukrainian-speaking authors submit their manuscripts in English and in Russian or Ukrainian, respectively. Page format is A4. The number of pages shall not exceed 15 (together with References and extended abstracts). By agreement with the editorial board, the number of pages can be increased.

To the manuscript is added:

1. Official recommendation letter, signed by the head of the institution where the work was carried out.

2. License agreement on the transfer of copyright (the form of the agreement can be obtained from the editorial office of the journal or downloaded from the journal website – Dohovir.pdf). The license agreement comes into force after the acceptance of the article for publication. Signing of the license agreement by the author(s) means that they are acquainted and agree with the terms of the agreement.

3. Information about each of the authors – full name, position, place of work, academic title, academic degree, contact information (phone number, e-mail address), ORCID code (if available). Information about the authors is submitted as follows:

authors from Ukraine - in three languages, namely Ukrainian, Russian and English;
authors from the CIS countries - in two languages, namely Russian and English;
authors from foreign countries – in English.

4. Medium with the text of the article, figures, tables, information about the authors in electronic form.

5. Colored photo of the author(s). Black-and-white photos are not accepted by the editorial staff. With the number of authors more than two, their photos are not shown.

Requirements for article design

The article should be structured according to the following sections:

- *Introduction*. Contains the problem statement, relevance of the chosen topic, analysis of recent research and publications, purpose and objectives.
- *Presentation of the main research material* and the results obtained.
- *Conclusions* summing up the work and the prospects for further research in this direction.
- *References*.

The first page of the article contains information:

1) in the upper left corner – UDC identifier (for authors from Ukraine and the CIS countries);
2) surname(s) and initials, academic degree and scientific title of the author(s);
3) the name of the institution where the author(s) work, the postal address, telephone number, e-mail address of the author(s);
4) article title;
5) abstract to the article – not more than 1 800 characters. The abstract should reflect the consistent logic of describing the results and describe the main objectives of the study, summarize the most significant results;
6) key words – not more than 8 words.

The text of the article is printed in Times New Roman, font size 11 pt, line spacing 1.2 on A4 size paper, justified alignment. There should be no hyphenation in the article.

Page setup: "mirror margins" – top margin – 2.5 cm, bottom margin – 2.0 cm, inside – 2.0 cm, outside – 3.0 cm, from the edge to page header and page footer – 1.27 cm.

Graphic materials, pictures shall be submitted in color or, as an exception, black and white, in .opj or .cdr formats, .jpg or .tif formats being also permissible. According to author's choice, the tables and partially the text can be also in color.

Figures are printed on separate pages. The text in the figures must be in the font size 10 pt. On the charts, the units of measure are separated by commas. Figures are numbered in the order of their arrangement in the text, parts of the figures are numbered with letters – a, b, .. On the back of the figure, the title of the article, the author (authors) and the figure number are written in pencil. Scanned images and graphs are not allowed to be inserted.

Tables are provided on separate pages and must be executed using the MSWord table editor. Using pseudo-graph characters to design tables is inadmissible.

Formulae shall be typed in Equation or MatType formula editors. Articles with formulae written by hand are not accepted for printing. It is necessary to give definitions of quantities that are first used in the text, and then use the appropriate term.

Captions to figures and tables are printed in the manuscript after the references.

Reference list shall appear at the end of the article. References are numbered consecutively in the order in which they are quoted in the text of the article. References to unpublished and unfinished works are inadmissible.

Attention! In connection with the inclusion of the journal in the international bibliographic abstract database, the reference list should consist of two blocks: CITED LITERATURE and REFERENCES (this requirement also applies to English articles):

CITED LITERATURE – sources in the original language, executed in accordance with the

Ukrainian standard of bibliographic description DSTU 8302:2015. With the aid of VAK.in.ua (http://vak.in.ua) you can automatically, quickly and easily execute your "Cited literature" list in conformity with the requirements of State Certification Commission of Ukraine and prepare references to scientific sources in Ukraine in understandable and unified manner. This portal facilitates the processing of scientific sources when writing your publications, dissertations and other scientific papers.

REFERENCES – the same cited literature list transliterated in Roman alphabet (recommendations according to international bibliographic standard APA-2010, guidelines for drawing up a transliterated reference list "References" are on the site http//www.dse.org.ua, section for authors).

To speed up the publication of the article, please adhere to the following rules:

- in the upper left corner of the first page of the article – the UDC identifier;

- family name and initials of the author(s);

- academic degree, scientific title;

begin a new line, Times New Roman font, size 12 pt, line spacing 1.2, center alignment;

- name of organization, address (street, city, zip code, country), e-mail of the author(s);

begin a new line 1 cm below the name and initials of the author(s), Times New Roman font, size 11 pt, line spacing 1.2, center alignment;

- the title of the article is arranged 1 cm below the name of organization, in capital letters, semi-bold, font Times New Roman, size 12 pt, line spacing 1.2, center alignment. The title of the article shall be concrete and possibly concise;

- the abstract is arranged 1 cm below the title of the article, font Times New Roman, size 10 pt, in italics, line spacing 1.2, justified alignment in Ukrainian or Russian (for Ukrainian-speaking and Russian-speaking authors, respectively);

- key words are arranged below the abstract, font Times New Roman, size 10 pt, line spacing 1.2, justified alignment. The language of the key words corresponds to that of the abstract. Heading "Key words" - font Times New Roman, size 10 pt, semi-bold;

- the main text of the article is arranged 1 cm below the abstract, indent 1 cm, font Times New Roman, size 11 pt, line space spacing 1.2, justified alignment;

- formulae are typed in formula editor, fonts Symbol, Times New Roman. Font size is "normal" – 12 pt, "large index" – 7 pt, "small index" – 5 pt, "large symbol" – 18 pt, "small symbol" – 12 pt. The formula is arranged in the text, center aligned and shall not occupy more than 5/6 of the line width, formulae are numbered in parentheses on the right;

- dimensions of all quantities used in the article are represented in the International System of Units (SI) with the explication of the symbols employed;

- figures are arranged in the text. The figures and pictures shall be clear and contrast; the plot axes – parallel to sheet edges, thus eliminating possible displacement of angles in scaling; figures are submitted in color, black-and-white figures are not accepted by the editorial staff of the journal;

- tables are arranged in the text. The width of the table shall be 1 cm less than the line width. Above the table its ordinary number is indicated, right alignment. Continuous table numbering throughout the text. The title of the table is arranged below its number, center alignment;

● references should appear at the end of the article. References within the text should be enclosed in square brackets behind the text. References should be numbered in order of first appearance in the text. Examples of various reference types are given below.

Examples of LITERATURE CITED

Journal articles

Anatychuk L.I., Mykhailovsky V.Ya., Maksymuk M.V., Andrusiak I.S. Experimental research on thermoelectric automobile starting pre-heater operated with diesel fuel. *J.Thermoelectricity*. 2016. №4. P.84–94.

Books

Anatychuk L.I. *Thermoelements and thermoelectric devices. Handbook.* Kyiv, Naukova dumka, 1979. 768 p.

Patents

Patent of Ukraine № 85293. Anatychuk L.I., Luste O.J., Nitsovych O.V. Thermoelement.

Conference proceedings

Lysko V.V. *State of the art and expected progress in metrology of thermoelectric materials.* Proceedings of the XVII International Forum on Thermoelectricity (May 14-18, 2017, Belfast). Chernivtsi, 2017. 64 p.

Authors' abstracts

Kobylianskyi R.R. *Thermoelectric devices for treatment of skin diseases*: extended abstract of candidate's thesis. Chernivtsi, 2011. 20 p.

Examples of REFERENCES

Journal articles

Gorskiy P.V. (2015). Ob usloviakh vysokoi dobrotnosti i metodikakh poiska perspektivnykh sverhreshetochnykh termoelektricheskikh materialov [On the conditions of high figure of merit and methods of search for promising superlattice thermoelectric materials]. *Termoelektrichestvo - J.Thermoelectricity,* 3, 5 – 14 [in Russian].

Books

Anatychuk L.I. (2003). *Thermoelectricity. Vol.2. Thermoelectric power converters*. Kyiv, Chernivtsi: Institute of Thermoelectricity.

Patents

Patent of Ukraine № 85293. Anatychuk L. I., Luste O.Ya., Nitsovych O.V. Thermoelements [In Ukrainian].

Conference proceedings

Rifert V.G. Intensification of heat exchange at condensation and evaporation of liquid in 5 flowing-down films. In: *Proc. of the 9th International Conference Heat Transfer.* May 20-25, 1990, Israel.

Authors'abstracts

Mashukov A.O. *Efficiency hospital state of rehabilitation of patients with color carcer.* PhD (Med.) Odesa, 2011 [In Ukrainian].